

ความเข้ากันได้ของพอลิเมอร์ผสมของพอลิสไตรีนทนแรงกระแทกสูงกับพอลิเอทิลีนความหนาแน่นสูง
โดยใช้โคพอลิเมอร์แบบบล็อกของสไตรีน/เอทิลีน-บิวทิลีน/สไตรีน



นาย อาศิร จิระวิทยานุกูญ

สถาบันวิทยบริการ

จุฬาลงกรณ์มหาวิทยาลัย

วิทยานิพนธ์นี้เป็นส่วนหนึ่งของการศึกษาตามหลักสูตรปริญญาวิทยาศาสตรมหาบัณฑิต
สาขาวิชาปิโตรเคมีและวิทยาศาสตร์พอลิเมอร์ หลักสูตรปิโตรเคมีและวิทยาศาสตร์พอลิเมอร์


คณะวิทยาศาสตร์ จุฬาลงกรณ์มหาวิทยาลัย

ปีการศึกษา 2544

ISBN 974-03-1364-7

ลิขสิทธิ์ของจุฬาลงกรณ์มหาวิทยาลัย

COMPATIBILIZATION OF HIGH IMPACT POLYSTYRENE/HIGH DENSITY POLYETHYLENE BLENDS
BY STYRENE/ETHYLENE-BUTYLENE/STYRENE BLOCK COPOLYMER



Mr. Asira Chirawithayaboon

สถาบันวิทยบริการ
จุฬาลงกรณ์มหาวิทยาลัย

A Thesis Submitted in Partial Fulfillment of the Requirements
for the Degree of Master of Science in Petrochemistry and Polymer Science

Program of Petrochemistry and Polymer Science

Faculty of Science

Chulalongkorn University

Academic Year 2001

ISBN 974-03-1364-7

อาศิริ จิระวิทยาบุญ : ความเข้ากันได้ของพอลิเมอร์ผสมของพอลิสไตรีนทนแรงกระแทกสูงกับพอลิเอทิลีนความหนาแน่นสูงโดยใช้โคพอลิเมอร์แบบบล็อกของสไตรีน/เอทิลีน-บิวทิลีน/สไตรีน (COMPATIBILIZATION OF HIGH IMPACT POLYSTYRENE/HIGH DENSITY POLYETHYLENE BLENDS BY STYRENE/ETHYLENE-BUTYLENE/STYRENE BLOCK COPOLYMER) อ. ที่ปรึกษา : ศ.ดร. สุดา เกียรติกำจรวงศ์, 102 หน้า. ISBN 974-03-1364-7.

ในงานวิจัยนี้ได้ศึกษาความเข้ากันได้ของพอลิเมอร์ผสมระหว่างพอลิสไตรีนทนแรงกระแทกสูง (เอชไอพีเอส) กับพอลิเอทิลีนความหนาแน่นสูง (เอชดีพีอี) โดยใช้โคพอลิเมอร์แบบบล็อกของสไตรีน/เอทิลีน-บิวทิลีน/สไตรีน (เอชอีบีเอส) โดยการเตรียมพอลิเมอร์ผสมทั้งสองด้วยสัดส่วนต่าง ๆ ผสมด้วยเอชอีบีเอสปริมาณต่าง ๆ เมื่อพิจารณาจากสมบัติเชิงกลของพอลิเมอร์ผสม พบว่าแรงกระแทกแบบ Izod และระยะยืดที่จุดขาดเพิ่มขึ้นเมื่อปริมาณของเอชอีบีเอสในพอลิเมอร์ผสมเพิ่มขึ้นและเพิ่มขึ้นอย่างสูงเมื่อสัดส่วนของเอชดีพีอีมากกว่าร้อยละ 50 โดยน้ำหนัก ส่วนความทนแรงดึงยืดเพิ่มขึ้นเมื่อปริมาณเอชอีบีเอสไม่เกิน 5 ส่วนต่อพอลิเมอร์ผสมร้อยละ 50 (พีพีเอชอาร์) และเมื่อปริมาณเอชอีบีเอสมากกว่า 5 พีพีเอชอาร์ พบว่าความทนแรงดึงยืดลดลงและลดลงมากขึ้นเมื่อสัดส่วนของเอชดีพีอีมากกว่าร้อยละ 50 โดยน้ำหนัก ในงานวิจัยนี้ศึกษาความเข้ากันได้ของพอลิเมอร์ผสมโดยใช้แบบจำลอง log additivity rule พบว่าพอลิเมอร์ผสมที่มีสัดส่วนของเอชไอพีเอสเป็นวัฏภาคหลักมีความเข้ากันได้ดีที่อัตราเงื่อนไขมีค่าสูง ในทางกลับกันพอลิเมอร์ผสมที่มีสัดส่วนของเอชดีพีอีเป็นวัฏภาคหลักมีความเข้ากันได้ดีที่อัตราเงื่อนไขมีค่าต่ำ สมบัติทางสัณฐานวิทยาแสดงว่าเอชอีบีเอสช่วยให้พอลิเมอร์ผสมมีความเข้ากันได้ดี จากอุณหภูมิเปลี่ยนสถานะคล้ายแก้วและอุณหภูมิหลอมเหลวของพอลิเมอร์ผสมแสดงให้เห็นว่า พอลิเมอร์ผสมที่มีสัดส่วนของเอชดีพีอีในระหว่างร้อยละ 90 ถึงร้อยละ 50 โดยน้ำหนัก จะมีความเข้ากันได้บางส่วนเมื่อมีปริมาณของเอชอีบีเอสสูงขึ้น และค่าเวลาการผ่อนคลาย (T_2) จากการวัดโดย pulsed NMR พบว่าพอลิเมอร์ผสมมีความเข้ากันได้มากขึ้นเมื่อปริมาณเอชอีบีเอสเพิ่มขึ้น เมื่อประมวลผลจากการทดสอบความเข้ากันได้แบบต่าง ๆ เปรียบเทียบกับผลของสมบัติเชิงกล สามารถสรุปได้ว่าเอชอีบีเอสช่วยให้พอลิเมอร์ผสมของเอชไอพีเอสและเอชดีพีอีมีความเข้ากันได้ดีขึ้นที่สัดส่วนต่าง ๆ หลายค่า

หลักสูตร ปิโตรเคมีและวิทยาศาสตร์พอลิเมอร์
 สาขาวิชา ปิโตรเคมีและวิทยาศาสตร์พอลิเมอร์
 ปีการศึกษา 2544

ลายมือชื่อนิสิต
 ลายมือชื่ออาจารย์ที่ปรึกษา
 ลายมือชื่ออาจารย์ที่ปรึกษาร่วม -

4373417523 : MAJOR PETROCHEMISTRY AND POLYMER SCIENCE

KEY WORD: HIGH IMPACT POLYSTYRENE/ HIGH DENSITY POLYETHYLENE/
SEBS/ COMPATIBILIZATION / LOG ADDITIVITY RULE/ RELAXATION TIME

ASIRA CHIRAWITHAYABOON: COMPATIBILIZATION OF HIGH IMPACT
POLYSTYRENE/ HIGH DENSITY POLYETHYLENE BLENDS BY STYRENE/
ETHYLENE-BUTYLENE/STYRENE BLOCK COPOLYMER. THESIS ADVISOR:
PROF. SUDA KIATKAMJORNWONG, Ph.D. 102 pp. ISBN 974-03-1364-7.

In this research, compatibilization of polymer blends of high impact polystyrene (HIPS) and high-density polyethylene (HDPE) by a triblock polymer of styrene/ethylene-butylene/styrene (SEBS) was elucidated. The polymer blends from many ratios of HIPS and HDPE with various concentrations of SEBS was prepared. Upon the mechanical property studies, Izod impact strength and elongation at break of the blends increased with increases in SEBS contents. They increased markedly when the HDPE contents were higher than 50 wt%. Tensile strength of blends increased when the SEBS concentrations were not higher than 5 pphr. Whenever the SEBS loading were higher than 5 pphr, tensile strength decreased and the greater increment of decrease were found in blends wherein the HDPE concentrations were more than 50 wt%. The log additivity rule model was applied to these blends. The blends containing the HIPS-rich phase showed the higher compatibility at the higher shear rates. Unlikewise, the blends containing the HDPE-rich phase yielded the greater compatibility at the lower shear rates. Morphology observations of the blends indicated the better compatibility of the blends with increasing SEBS concentrations. Glass transition temperature and melting temperature of the blends showed some miscibility at the HDPE contents between 90 to 50 wt% especially in the presence of high loading of SEBS. The relaxation time (T_2) values from the pulsed NMR measurements revealed that both polymer blends became more compatible when the SEBS concentrations were increased. When integrating all the investigations of compatibility in comparison with the mechanical properties, it is possible to conclude that SEBS promotes a certain level of compatibilization for several ratios of HIPS/HDPE blends.

Program Petrochemistry and Polymer Science

Field of study Petrochemistry and Polymer Science

Academic year 2001

Student's signature

Advisor's signature

Co-advisor's signature -

ACKNOWLEDGEMENTS

The author is grateful to Professor Dr. Suda Kiatkamjornwong, the thesis advisor, for her guidance, suggestions, reviewing the experimental work and thesis content, as well as encouragement during the research work and the thesis preparation.

He thanks Professor Dr. Pattarapan Prasassarakich, Associate Professor Dr. Wimonrat Trakarnpruk, and Assistant Professor Dr. Nuanphun Chantarasiri for serving as chairperson and member of thesis committee, respectively.

In addition, he would like to acknowledge the Research and Development Department, Thai Petrochemical Industry (Public) Co., Ltd., for permission to use the equipment and instruments during the courses of research. Moreover, deep gratitude is also due to the Department of Rubber Technology and Polymer Science, Faculty of Science and Technology, Prince of Songkla University, Pattani for permission to use the facilities of capillary rheometer as well as many assistances from Assistant Professor Dr. Charoen Nakason and his students for the rheology measurement. Without this support this thesis has not been completed.

He is obliged to Professor Toshio Nishi and his Ph.D. course student at the Department of Applied Physics, Faculty of Engineering, the University of Tokyo for the measurement of spin-spin relaxation time T_2 at room temperature of HIPS/HDPE + SEBS. This information gives additional facet conclusions of the work.

Finally, he is grateful to his parents for their love, encouragement, and support. Many thanks are going to his friends and everyone, whose names are not mentioned here, who contribute suggestions and supports during the course of research.

CONTENTS

	PAGE
ABSTRACT (IN THAI)	iv
ABSTRACT (IN ENGLISH)	v
ACKNOWLEDGEMENTS	vi
CONTENTS	vii
LIST OF TABLES	x
LIST OF FIGURES	xi
ABBREVIATIONS	xiv
 CHAPTER I INTRODUCTION	
1.1 Introduction.....	1
1.2 Research objective.....	2
1.3 Scope of the research.....	4
 CHAPTER II THEORY AND LITERATURE REVIEW	
2.1 Theoretical Background.....	5
2.1.1 Polymer-polymer compatibility.....	5
2.1.2 Log additivity rule model.....	7
2.1.3 Phase morphology of immiscible polymer blends.....	9
2.1.4 T_g -composition analysis of polymer blends.....	10
2.1.5 High-impact polystyrene.....	11
2.1.6 High-density polyethylene.....	12
2.1.7 Styrene/ethylene-butylene/styrene block copolymer.....	12
2.2 Literature Review	14

CHAPTER III EXPERIMENTAL

3.1 Materials.....	21
3.2 Instruments.....	21
3.3 Blends preparation.....	22
3.4 Rheological properties.....	25
3.5 Thermal analysis.....	26
3.6 Morphological observation.....	26
3.7 Mechanical properties.....	26
3.7.1 Izod impact strength testing.....	26
3.7.2 Tensile property measurement.....	27
3.7.3 Flexural strength testing.....	28
3.8 Relaxation time by pulsed nuclear magnetic resonance.....	28

CHAPTER IV RESULTS AND DISCUSSION

4.1 Rheological properties of HIPS/HDPE blends.....	30
4.2 Morphological observation of HIPS/HDPE blends.....	41
4.3 Thermal analysis of HIPS/HDPE blends.....	50
4.4 Mechanical properties of HIPS/HDPE blends.....	56
4.4.1 Impact strength of HIPS/HDPE blends.....	56
4.4.2 Tensile strength of HIPS/HDPE blends.....	57
4.4.3 Flexural strength of HIPS/HDPE blends.....	58
4.5 Relaxation time by pulsed NMR.....	62

CHAPTER V CONCLUSIONS AND SUGGESTION FOR FURTHER WORK

5.1 Conclusions.....	65
5.2 Suggestion for further work.....	67

LIST OF TABLES

TABLE	PAGE
3.1	Composition of HIPS/HDPE/SEBS blends..... 24
4.1	Shear viscosity of HIPS/HDPE blends compatibilized with SEBS from experimental data versus log additivity rule model.....38
4.2	T_g and T_m of HIPS/HDPE blends with various SEBS concentrations..... 52
4.3	Mechanical properties of HIPS/HDPE blends with various SEBS block copolymer concentrations..... 59
4.4	The results of T_2 and the fractional amount of HIPS/HDPE blends..... 62



สถาบันวิทยบริการ
จุฬาลงกรณ์มหาวิทยาลัย

LIST OF FIGURES

FIGURE	PAGE
2.1 Classification of polymer blends.....	4
2.2 Location of block and graft copolymers at phase interfaces.....	5
2.3 Phase morphology of immiscible polymer blends.....	7
3.1 Izod impact strength apparatus and test specimen.....	20
3.2 Tensile testing apparatus and test specimen.....	21
3.3 Flexural strength testing.....	21
3.4 Pulsed ¹ H-NMR analyzer – minispec (Bruker) model PC-20.....	29
3.5 Pulsed NMR diagram.....	29
3.6 Block diagram of real time pulsed NMR measurement system.....	29
4.1 Flow curve of uncompatibilized HIPS/HDPE blends.....	31
4.2 Flow curve of HIPS/HDPE (90/10) blends with various SEBS concentrations.....	32
4.3 Flow curve of HIPS/HDPE (70/30) blends with various SEBS concentrations.....	32
4.4 Flow curve of HIPS/HDPE (50/50) blends with various SEBS concentrations.....	33
4.5 Flow curve of HIPS/HDPE (30/70) blends with various SEBS concentrations.....	33
4.6 Flow curve of HIPS/HDPE (10/90) blends with various SEBS concentrations.....	34
4.7 Flow curve of HIPS, HDPE and SEBS pure component at 473 K.....	34

4.8	Variation of viscosity with SEBS concentrations in HIPS/HDPE (90/10) blends.....	39
4.9	Variation of viscosity with SEBS concentrations in HIPS/HDPE (70/30) blends.....	39
4.10	Variation of viscosity with SEBS concentrations in HIPS/HDPE (50/50) blends.....	40
4.11	Variation of viscosity with SEBS concentrations in HIPS/HDPE (30/70) blends.....	40
4.12	Variation of viscosity with SEBS concentrations in HIPS/HDPE (10/90) blends.....	41
4.13	Scanning electron micrographs showing unetched fracture surface of HIPS/ HDPE (90/10) blends compatibilized with SEBS as compatibilizer..	42
4.14	Scanning electron micrographs showing etched fracture surface of HIPS/ HDPE (70/30) blends compatibilized with SEBS as compatibilizer.....	43
4.15	Scanning electron micrographs showing etched fracture surface of HIPS/ HDPE (50/50) blends compatibilized with SEBS as compatibilizer.....	44
4.16	Scanning electron micrographs showing etched fracture surface of HIPS/ HDPE (30/70) blends compatibilized with SEBS as compatibilizer.....	45
4.17	Scanning electron micrographs showing etched fracture surface of HIPS/ HDPE (10/90) blends compatibilized with SEBS as compatibilizer.....	46
4.18	Scanning electron micrographs showing unetched cryogenic fracture surface of HIPS/HDPE (90/10) blends compatibilized with SEBS as compatibilizer which prepared by internal mixer.....	49

4.19	Scanning electron micrographs showing unetched cryogenic fracture surface of HIPS/HDPE (10/90) blends compatibilized with SEBS as compatibilizer which prepared by internal mixer.....	49
4.20	DSC thermograms of HIPS/HDPE (90/10) blends uncompatibilized and compatibilized with SEBS as compatibilizer.....	53
4.21	DSC thermograms of HIPS/HDPE (70/30) blends uncompatibilized and compatibilized with SEBS as compatibilizer.....	53
4.22	DSC thermograms of HIPS/HDPE (50/50) blends uncompatibilized and compatibilized with SEBS as compatibilizer.....	54
4.23	DSC thermograms of HIPS/HDPE (30/70) blends uncompatibilized and compatibilized with SEBS as compatibilizer.....	54
4.24	DSC thermograms of HIPS/HDPE (10/90) blends uncompatibilized and compatibilized with SEBS as compatibilizer.....	55
4.25	Izod impact strength of HIPS/HDPE blends with various SEBS concentrations.....	60
4.26	Tensile strength of HIPS/HDPE blends with various SEBS concentrations..	60
4.27	Elongation at break of HIPS/HDPE blends with various SEBS concentrations.....	61
4.28	Flexural strength of HIPS/HDPE blends with various SEBS concentrations.....	61
4.29	Dependence of T_2 of HIPS/HDPE phase in the blends.....	63
4.30	Dependence of fractional amount of HIPS and HDPE phase in the blends..	64

ABBREVIATIONS

DMTA	dynamic mechanical thermal analysis
DSC	differential scanning calorimetry
EB	poly(ethylene- <i>b</i> -butylene) or hydrogenated polybutadiene
FID	free induction decay
HDPE	high-density polyethylene
HIPS	high impact polystyrene
HPB-<i>b</i>-PS	hydrogenated polybutadiene-polystyrene tapered diblock copolymer
LDPE	low-density polyethylene
LLDPE	linear low-density polyethylene
L/D	extruder length per diameter ratio (aspect ratio)
MFI	melt flow index
NDB	negative deviation behavior
NMR	nuclear magnetic resonance
PDB	positive deviation behavior
PE	polyethylene
PNDB	positive-negative deviation behavior
pphr	parts per hundred resin
PS	polystyrene
aPS	atactic polystyrene
sPS	syndiotactic polystyrene
rpm	revolution per minute
SBS	styrene/butadiene/styrene block copolymer
S-E	poly(styrene- <i>b</i> -ethylene) block copolymer
SEB	styrene/ethylene-butylene diblock copolymer
SEBS	styrene/ethylene-butylene/styrene block copolymer
SEM	scanning electron microscopy
T_2	spin-spin relaxation time
T_g	glass-transition temperature
T_m	melting temperature
wt%	weight percentage

CHAPTER I

INTRODUCTION

1.1 Introduction

Polymer blends have gained an increasing popularity in the field of polymer science and industry during the last few decades. The blending of polymers provides an efficient way of developing new materials with tailored properties, which is often faster and more cost-effective means of achieving a desired set of properties than synthesizing new polymers. The growth in the use of polymer blends is mainly due to their ability to combine the properties of their phases in a unique product. The final properties of polymer blends are directly related to the quality of their morphology, which in turn depends on rheological properties of the phases of the blend, on the composition of the blend, and on compatibility between the polymers forming the blend. Immiscible polymer blends are preferable over miscible blends since in immiscible blends a combination of properties of individual components is obtained, while in miscible blends an average of the individual properties is obtained [1]. However, most of polymer blends are immiscible or incompatible at the molecular level, because the combinatorial entropy of mixing of two polymers is drastically smaller than that of low molecular weight mixtures, whereas the enthalpy of mixing is often positive or near zero. The incompatibility of polymeric blends are responsible for poor mechanical properties because of a lack of physical and chemical interactions across the phase boundaries and poor interfacial adhesion. Therefore,

compatibilization is demanded to obtain a blend with desired properties. A common way to improve the compatibility and interfacial adhesion of polymer blends is to add compatibilizers or interfacial agents [2]. One of the most frequently used methods to increase compatibility of immiscible blends is to add a third component which is totally or partially miscible (or at least compatible) with both phases. The component may be a homopolymer or suitable block or graft copolymer. It is well known that a block copolymer is an efficient compatibilizer for immiscible polymer blends. Here each block of diblock or triblock copolymer is usually either miscible, or has strong affinities, with one of the two homopolymer phases. Therefore, the block copolymer will preferentially locate at the interface between the two phases, thus reducing the interfacial tension and enhancing adhesion between phases [3].

Compatibilization of polystyrene and polyethylene blends has been the considerable research and development in recent decades. Both of polyethylene and polystyrene are two of the most widely used plastics in the world as structural material for engineering applications. As it is well known, polystyrene and rubber modified polystyrene are very easily thermoformed and exhibit good impact strength and low temperature properties when thermoformed, however, they are known to have poor solvent resistance. Polyethylene has relatively good solvent resistance but it is very difficult to thermoform due to its low glass transition temperature and relatively sharp melting point at elevated temperature. When polystyrene is blended with polyethylene so as to combine the toughness and solvent resistance of polyethylene with the high modulus and thermoformability of polystyrene, however, the blending is rather complicated by the incompatibility of these two polymers [4].

In this study, the compatibilization effect of styrene/ethylene-butylene/styrene (SEBS) triblock copolymer is employed as compatibilizer of high-impact polystyrene (HIPS) and high-density polyethylene (HDPE) blends as a function of the blend ratio and compatibilizer concentration.

1.2 Research objective

The main purpose of this study is focused on the compatibilizing effect of SEBS triblock copolymer in HIPS/HDPE blends. Morphology, impact strength, thermal and rheological properties of the resulting HIPS/HDPE blends are measured to investigate the compatibilization effects of the SEBS triblock copolymer. In addition, the relaxation time by pulsed NMR to observe microphase separation and phase separated structure are carried out in order to conclude the compatibility.

1.3 Scope of the research

The scope of this research work includes:

1. Literature survey and in-depth study of this research work.
2. Preparation of HIPS/HDPE blends with and without SEBS as compatibilizer at various blend ratios (90/10, 70/30, 50/50, 30/70 and 10/90) and compatibilizer concentrations (5, 10, 15 and 20 pphr for each HIPS/HDPE weight ratio) using a twin-screw extruder.
3. Preparation of HIPS/HDPE blends with SEBS compatibilizer at HIPS/HDPE blend ratios of 90/10 and 10/90 and compatibilizer concentrations 15 and 20 pphr using an internal mixer.

4. Measurement of rheological behavior of the blends using a capillary rheometer to study the compatibility of the blends based on a log additivity rule model.
5. Observation of the morphological structures using scanning electron microscopy (SEM) technique.
6. Evaluation of the thermal properties of blend samples using differential scanning calorimetry (DSC).
7. Determination of some mechanical properties of the blends to evaluate the blend compatibility.
8. Summarizing the results, writing the thesis.



สถาบันวิทยบริการ
จุฬาลงกรณ์มหาวิทยาลัย

CHAPTER II

THEORY AND LITERATURE REVIEW

2.1 Theoretical background

2.1.1 Polymer-polymer compatibility

Mixing two or more polymers together may be miscible, partially miscible, or completely immiscible. The general relation between blends and alloys is shown in Figure 2.1

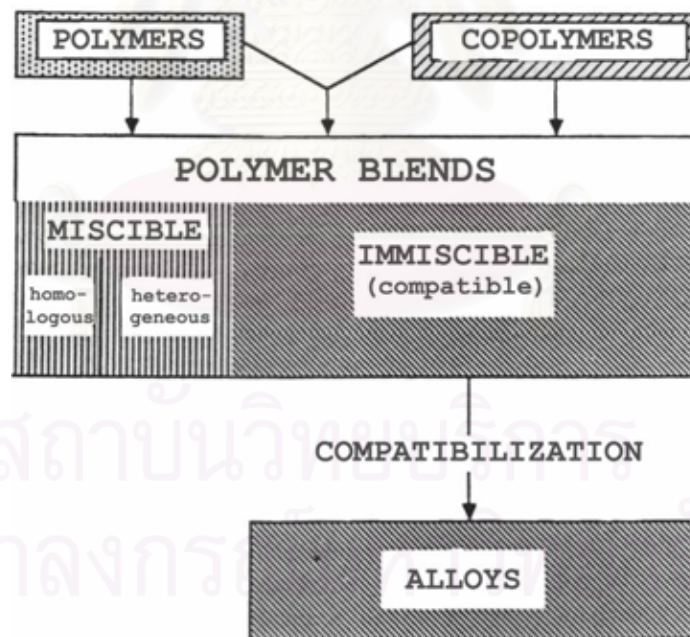


Figure 2.1 Classification of polymer blends.

The miscibility between polymers is determined by a balance of enthalpic and entropic contributions to the free energy of mixing. While for small molecules, the entropy is high enough to ensure miscibility; for polymers the entropy is almost zero,

causing enthalpy to be decisive in determining miscibility. The change in free energy in mixing (ΔG_{mix}) is written as

$$\Delta G_{\text{mix}} = \Delta H_{\text{mix}} - T\Delta S_{\text{mix}}, \quad (2.1)$$

where H_{mix} is enthalpy of mixing, S_{mix} is entropy of mixing and T is temperature. For spontaneous mixing, ΔG_{mix} must be negative.

It is known that simple blends of two immiscible polymers usually have large discrete dispersed phases and weak interfacial adhesion, resulting in poor mechanical properties coupling between phases. Therefore, a compatibilizer is required to enhance interfacial adhesion between the phases of immiscible polymers. Generally, an effective compatibilizer should reduce the interfacial tension between the two phases leading to a finer dispersion of one phase to another, enhance adhesion by coupling the phases together, and stabilizing the dispersed the dispersed phase against coalescence [2]. Block and graft copolymers represent the most extensive use as a compatibilizer for the stabilization of phase structures. Compatibilizers are usually in the form of block or graft copolymers. They may be added separately or formed during compounding, mastication or polymerization of a monomer in the presence of another polymer. The copolymer compatibilizers often contain segments, which are either chemically similar to those in blend components (non-reactive compatibilizer) or miscible or adhered to one of the components in the blend (reactive compatibilizer). In the case of a reactive copolymer compatibilizer, the segments of the copolymer are capable of forming strong bonds (covalent or ionic) with at least one of components in the blend. In the non-reactive copolymer compatibilizer, the segments of the copolymer are miscible with each of blend components. The classical

view of how such copolymers locate at interfaces is shown in Figure 2.2. Copolymer structure and molecular weight impose important influences on their effectiveness [3].

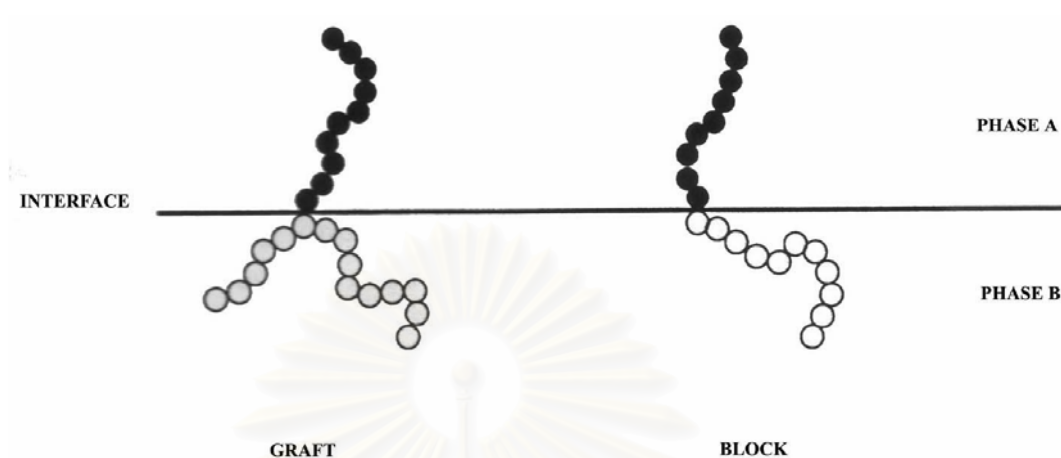


Figure 2.2 Location of block and graft copolymers at phase interfaces.

The behavior of small amounts of copolymer-compatibilizer in an immiscible blend has been described as a classical emulsifying agent, similar to the soap molecules at an oil-water interface that have on the ability to mix oil and water [2,3].

The addition of the block copolymer to improve the phase separation of polymer blend, which can divide in two generalizations. If the two homopolymers are very nearly miscible, addition of their block copolymer to the blend may result in a one-phase system. This would be favored by a low molecular weight for the block copolymer. If the two polymers are far from being miscible, then no block copolymer is likely to cause one-phase mixture. In this case the role of block copolymer is to be an interfacial agent and this is only possible if the block copolymer phase segregates readily. The latter is favored by the high molecular weight copolymer.

2.1.2 Log additivity rule model

Generally, the flow behavior of a homopolymer depends on the flow geometry and processing conditions such as the temperature, shear rate, time of flow, etc.

Contrary to the polymer blends which the flow behavior become more complex and is influenced by additional factor like the miscibility of the system, the morphology, interfacial adhesion and interfacial thickness. The melt viscosity of polymer blends shows three types of behavior as the following.

- (1) Positive deviation behavior (PDB) where blend viscosities show a higher value than the log additivity value (see Equation 2.2).
- (2) Negative deviation behavior (NDB) where blend viscosities show a lower value than the log additivity value.
- (3) Positive-negative deviation behavior (PNDB) where the same blend exhibits both positive and negative deviation behavior, depending on the composition, morphology and processing conditions.

$$\log (\eta_{blend}) = \sum_i x_i \log (\eta_i), \quad (2.2)$$

where η_{blend} and η_i are the shear viscosity of the blend and that of the phase i and x_i is the weight fraction of the phase i .

The log additivity rule is an indication of strong or weak interactions between the phases of the blend. The immiscible blends show negative deviation behavior due to the heterogeneous nature of components. Thus, the observed negative deviation is due to the incompatibility between the phases and interlayer slip as a result of the decreasing viscosity of the system. Also, the compatible blends lead to a positive deviation in rheological properties, such as the increasing viscosity [5].

2.1.3 Phase morphology of immiscible polymer blends

Most immiscible polymers form coarse mixtures with comparatively large domain sizes and sharp interface, as a result of the high interfacial tension between the components, which further leads to poor interfacial adhesion. The properties of a blend not only depend on the mechanical behavior of the interface, but also on the size of the respective polymer phases. The phase morphology of immiscible blend from two polymers, for example, when polymer A and polymer B are blended together. In case of there is a lot more of polymer A than polymer B, polymer B separates into little spherical globs. The spheres of polymer B will be separated from each other by the matrix of polymer A, as shown in Figure 2.3. In this case, polymer A is called the major component and polymer B is the minor component. When more polymer B is put into the immiscible blend system, the spheres will get bigger until they become joined together and are the domains of polymer A. In this case, polymer B is called a co-continuous phase (the middle picture in Figure 2.3) or a region of phase inversion. Moreover, the polymer B is put more over than the co-continuous phase until the polymer B becomes the major phase or the matrix phase, and polymer A becomes the minor phase or the disperse phase [6].

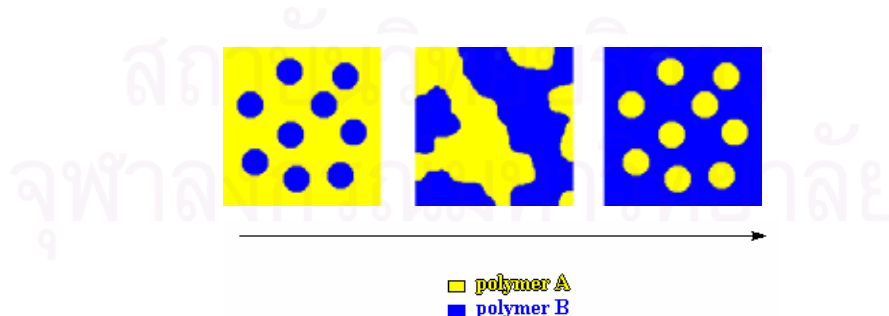


Figure 2.3 Phase morphology of immiscible polymer blends

The addition of the block copolymer is for emulsification and enhancement of mechanical properties of immiscible polymer blends. In order for the block copolymer

to be effective in these roles, it must first of all be interfacial active. Indeed, a block copolymer adsorbs onto the interface if its segment selectively mixes with the immiscible polymers. The principal effects of interfacial modification on the morphology in an immiscible blend are to reduce the particle size and to narrow the particle-size distribution. This reduction in particle size is related to both a decrease in interfacial tension and reduced coalescence. The molecular characteristics of each block determine the structure, composition, and performance of the interfacial layer. At the interface between the two polymer phases, the block copolymer can promote stress transfer across the interface, thereby preventing facile fracture along the interface [7].

2.1.4 T_g -composition analysis of polymer blends

The glass transition temperature (T_g) of a polymer is the temperature at which the molecular chains have sufficient energy to overcome attractive forces and move vibrationally and translationally. The number and locations of the T_g provide much insight into the nature of a polymer blend. For example, a miscible one-phase blend should have only one T_g , whereas an immiscible two-phase blend should have two glass transitions, that closely approximate for the individual polymers are expected.

For ideal systems, which are miscible and amorphous over the entire composition range, the T_g can often be predicted by using simple equations. A linear relationship has been noted in some miscible systems and the T_g can be calculated with the Gordon-Taylor expression,

$$T_g = W_a T_{ga} + W_b T_{gb}, \quad (2.3)$$

and the Fox equation,

$$(1/T_g) = (W_a/T_{ga}) + (W_b/T_{gb}), \quad (2.4)$$

where T_g is the glass transition temperature of the blend, T_{ga} and T_{gb} are the glass transition temperatures of polymers A and B, respectively, and W_a and W_b are the corresponding weight fractions of polymers A and B in the blend. The above equations, commonly expressed the T_g -composition relationships for copolymers and plasticizer-polymer compositions, are quite useful for miscible blends [8].

2.1.5 High impact polystyrene

High impact polystyrenes (HIPS) are considered to be styrene polymers modified by the incorporation of a rubber component to give impact-resistant materials with only minor sacrifices in hardness and strength. The rubber component is usually a diene polymer or copolymer, most often 5 to 10% polybutadiene, which is added to crystalline polystyrene to increase energy absorbed ability, that is to reduce its tendency to fracture when subjected to impact.

Commercial high impact polystyrene products are made by polymerization of unsaturated rubber dissolved in styrene in a solution or mass-suspension process, together with various optional additives such as catalyst, chain transfer agent, and mineral oil designed to produce an appropriate balance between production economics and desired end product properties. The rubber, generally polybutadiene, is dispersed throughout the polystyrene matrix in the form of discrete particles.

Standard HIPS materials are used in both injection molding ($MFI_{5, 473 K}$ is greater than $3 \text{ g } 10^{-1} \text{ min}^{-1}$) and extrusion application ($MFI_{5, 473 K}$ is less than $3 \text{ g } 10^{-1} \text{ min}^{-1}$). HIPS has low post-molding shrinkage, good melt strength, and a wide melt processing window, making the ideal for many sheet and thermoforming applications,

injection molding applications include cutlery, appliance parts, and furniture components. Typical end uses are toys, appliance parts, packaging and furniture. These applications require property improvements over polystyrene, such as increased impact strength and ductility [9].

The practical developments of HIPS to improve more impact strength at room temperature, environmental stress-crack resistance are compatibilized blend with polyolefin such as polyethylene.

2.1.6 High-density polyethylene

High-density polyethylene is the product of ethylene polymerization with a density range of 940 - 960 kg m⁻³. That can be produced by suspension polymerization technique using Ziegler-Natta catalyst. High-density polyethylene is a moderate stiffness material that retains excellent toughness.

HDPE has crystallinity of 75-95%, higher strength and modulus and better creep properties than LDPE. The unbranched chains or linear chains of HDPE can pack side by side much more efficiently and optimize the van der Waals intermolecular forces, higher resistance to environmental stress cracking than LDPE, better chemical resistance because the denser packing of the molecules makes solvent penetration more difficult [10].

High-density polyethylene has a relatively sharp melting point and low glass transition temperature, which becomes difficult for thermoforming. This problem can be improved by compatibilizing with polystyrene that eases thermoforming.

2.1.7 Styrene/ethylene-butylene/styrene block copolymer

The styrene/ethylene-butylene/styrene (SEBS) block copolymer consists three discrete polymer blocks of the A-B-A type from which the endblocks (A) are a hard

thermoplastic (polystyrene), while the midblocks (B) are elastomers (poly(ethylene-butylene)). The SEBS might be expected to adhere or wet both components of the present system owing to the identity of the endblocks with the PS component and the expected affinity of the poly(ethylene-butylene) midblock with HDPE. At room temperature, the polystyrene endblocks are hard and strong, and lock the elastomer blocks in place to give a physically cross-link network, which gives their elastomeric properties, comparable to those of conventional vulcanized rubbers. The physical cross-link can be defined as a non-covalent bond that is stable under one condition but not under another. On heating, the polystyrene softens and the polymer is able to flow and be molded. When the molded product is cooled, the polystyrene becomes hard again, and the network regains its strength. These block copolymers have midblocks of a saturated elastomer, poly(ethylene-butylene), that lead to the advantages of increased oxidation and weather resistance, improved solvent resistance, higher upper service temperature, and better processing stability. The normal processing temperature range is from 463 K to 533 K and often processed at higher shear rates [11,12].

2.2 Literature reviews

Blending of immiscible polymers for the development of new materials with good performance is often used as an alternative to the synthesis of new properties or for the preparation of new materials or for the modification of specific properties of some polymers. Blends of polyethylene (PE) with polystyrene (PS) are appropriate for various applications as materials with high oil resistance and advantageous barrier properties. A large number of studies have been devoted to PE and PS blends. Fayt and Teyssié [13] investigated the interfacial activity of a hydrogenated polybutadiene-polystyrene tapered diblock copolymer, (HPB-*b*-PS) in the blends of a low-density

polyethylene (LDPE) with a high impact polystyrene (HIPS) prepared in the melt state on a two-roll mill. Optical and scanning electron microscopic examinations of smoothed or fracture surfaces and also surfaces obtained after THF-extraction of PS phases demonstrate that the copolymer promotes the dispersion and interfacial adhesion of the components, whatever the composition and is able to create and stabilize particular dispersions of the rubber particles in these blends. Tensile and Charpy impact properties are also very significantly improved. All these features demonstrate that the ductility and toughness of PS and LDPE/PS blends can be closely controlled by adequate combination of rubber particles and a HPB-*b*-PS copolymer. Guo et al. [14] determined the phase and mechanical properties of a low-density polyethylene/polystyrene (LDPE/PS) 70/30 blend after compatibilization with various styrene-ethylene, styrene-ethylene/butene and styrene-ethylene/propylene block copolymers. It is shown that high interfacial activity, as reflected in the reduction of the dispersed phase size, does not necessarily bring about an improvement in the mechanical properties of the blend. Although the diblock copolymers were more efficient in reducing the phase size, the triblock copolymers were even more effective in improving the mechanical properties. The effect of a poly(styrene-*b*-ethylene) (S-E) block copolymer on the particle coalescence and rheological properties of the LDPE/PS 70/30 blend has been investigated. It is shown that small amounts of the block copolymer can significantly retard or actually suppress the coalescence of the dispersed phases, and thus stabilize the morphology of the blend. The addition of the S-E copolymer increases the elastic modulus and dynamic viscosity of the blend, and the samples become more non-Newtonian as the block copolymer concentration increases. Taha and Frerejean [15] studied the compatibilization of LDPE-PS blends using three PS-hydrogenated polybutadiene-PS

and one PS-hydrogenated polybutadiene block copolymers. The blends were prepared by co-rotating twin screw extrusion, then they were injection-modeled. During processing, the morphology evolution of the blends was studied using SEM and image-analyzing techniques. Different screw profiles were used for the extrusion. Under the extrusion conditions and when all the blend constituents had melted, the use of one kneading-disc section resulted in a high mixing effect. The addition of other kneading-disc sections did not increase the dispersion. The flow of the blend, through the extruder die or in the injection mold, induced heterogeneous skin-core structures. The analysis of the evolution of the structure of these blends during processing showed that the addition of a compatibilizer increased their stability. Going from LDPE-rich to PS-rich blends, the morphology evolves from a nodular dispersion of PS in LDPE to a co-continuous phase structure. With the addition of a copolymer to a 25-75 wt% LDPE-PS blend, the structure changes from a co-continuous to a nodular one. Comparing the effect of the different copolymers on the blend morphology, the diblock copolymer results in the most homogeneous and finest dispersions. The stabilization of increasing potential values of the interface surface of these blends requires increasing concentrations of the copolymers. Fortelný et al. [16] studied the effect of a styrene-butadiene block copolymer on the phase structure and impact strength of HDPE and LDPE/HIPS blends with various compositions. For both blends, the type of the phase structure was not affected by addition of a styrene-butadiene compatibilizer. The localization and structure of the compatibilizer in the blends were dependent on their composition. Addition of the compatibilizer improved impact strength of the blends in the whole concentration range. The improvement was the largest for blends with a low amount of the minor phase.

A significant part of this problem is poor stress transfer between component phases owing to a lack of adhesion or wetting. An approach to this situation has been to employing additives, which might be expected to improve adhesion between the phases by an interfacial mechanism, and beneficial results have been obtained using these so-called compatibilizers. Li et al. [17] studied compatibilization of blends of LDPE and PS with block copolymers of styrene (S) and butadiene (B) or hydrogenated butadiene (EB). The morphology of the LLDPE/PS (50/50) composition typically with 5% copolymer was characterized primarily by SEM. The SEB and SEBS copolymer were effective in reducing the PS domain size, while the SB and SBS copolymers were less effective. The non-crystalline copolymers lowered the tensile modulus of the blend by as much as 50%. Modulus calculations based on a core-shell model, with the rubbery copolymer coating the PS particle, predicted that 50% of the rubbery SEBS copolymer was located at the interface compared to only 5-15% of the SB and SBS copolymers. The modulus of blends compatibilized with crystalline, non-rubbery SEB and SEBS copolymers approached Hashin's upper modulus bound. An interconnected interface model was proposed in which the blocks selectively penetrated the LLDPE and PS phases to provide good adhesion and improved stress and strain transfer between the phases. Harrats et al. [18] studied the emulsification efficiency of low-density polyethylene/polystyrene (LDPE/PS) blends in LDPE-rich blends with different block copolymers consist of hydrogenated polybutadiene and polystyrene (pure diblock, tapered diblock and triblock copolymer) on the phase morphology, the ultimate tensile properties and the dynamic viscosity of the modified blends. They found the tapered diblock copolymer is the most efficient emulsifier in LDPE/PS (80/20) blend. For instance, a plateau is observed in the property-copolymer content dependence when 2 wt% tapered diblock are used

compared to 5 wt% in case of the pure diblock and no visible plateau is observed when a triblock is used. This is assumed to result from the less quantitative localization of these two copolymers (pure diblock or the triblock) at the LDPE/PS surface. Bourry and Favis [19] studied the level of continuity and co-continuity for blends of HDPE/PS prepared on a twin-screw extruder by both morphology and dissolution studies. Addition of SEBS as an interfacial modifier results in a shift of the percolation threshold for dispersed PS to higher concentrations. The region of phase inversion, however, is maintained at 70% PS. The shift in the percolation threshold to higher values is related to reduce elongation of the PS dispersed phase after interfacial compatibilization. These results indicate that an interfacial modifier significantly influences percolation phenomena without shifting the region of phase inversion. Models based on viscosity ratio have failed to predict the region of phase inversion in this study. Elastic effects are shown to be able to describe the basic tendencies. However, little information is available on impact behavior of the SEBS-compatible HDPE/HIPS blends.

The purpose of this article is to report on some very encouraging results that have been developed in relation to improving the properties of immiscible blends. The effect of the addition of SEBS triblock copolymer on morphology, rheology, thermal properties, and mechanical properties of HDPE/HIPS has been investigated. A commercially available Kraton™ G1652 (SEBS) triblock copolymer, a type mentioned by Lindsey et al. [20], and Tjong and Xu [21] was used as an additive to this system. Lindsey et al. studied the blends of HDPE, PS and SEBS triblock copolymer. The blends were extruded, palletized and injection molded. The binary HDPE-PS blends exhibit very poor ductibility; however, addition of the SEBS block copolymer greatly improves this characteristics, but with an accompanying loss in

strength and modulus. The modified blends are very tough and have mechanical properties suitable for many end use applications. However, weld lines pose a problem and should be avoided with this blend. Tjong and Xu also studied the effect of SEBS triblock copolymer as a compatibilizer for the blends of PS and HDPE. The morphology and static mechanical and impact properties of the blends were investigated by means of SEM, uniaxial tension, and instrumented falling-weight impact measurements. Tensile tests showed that the yield strength of the PS/HDPE/SEBS blends decreases considerably with increasing HDPE content. However, the elongation at break of the blends tended to increase significantly with increasing HDPE content. The excellent tensile ductility of the HDPE-rich blends resulted from shear yielding of the matrix. Charpy impact measurement indicated that the impact strength of the blends increases slowly with HDPE content up to 50 wt%; thereafter, it increases sharply with increasing HDPE content. The impact energy of the HDPE-rich blends exceeded that of pure HDPE, implying that the HDPE polymer can be further toughened by the incorporation of brittle PS minor phase in the presence of SEBS compatibilizer. Bureau et al. [22] investigated the processing and compatibilization effects on the phase morphology and the tensile behavior of blends of polystyrene and high-density polyethylene. As predicted by theory that high shear rates encountered during extrusion blending led to efficient minor phase emulsification in immiscible PS/HDPE blends for which the viscosity ratio approaches unity. Consequently, the emulsifying effect of an SEBS compatibilizer was found to be negligible. In the subsequent molding process, disintegration, shape relaxation and coarsening of the minor phase domains were found to be responsible for the morphological evolution. In the compression molding process, morphological observations showed that the rate of minor phase coarsening followed the predictions

of the Ostwald ripening theory, in agreement with the rheological analysis. In the injection molding process, minor phase coarsening was attributed to shear coalescence. Tensile test performed on compression molded and injection molded blends showed that the mechanical behavior of PS/HDPE blends depend strongly upon the matrix orientation as well as the dispersed phase morphology and orientation. In both post-forming operations, compatibilization effects on the morphological stability and the tensile behavior of PS/HDPE blends were found to be dependent upon the composition and the rheological behavior of the blend. Evidence of adhesion between the PS and HDPE phases was observed in the presence of SEBS in HDPE-rich blends.

In recent years, the sPS blends with PE has been also attractive. Chen et al. [23] studied the effectiveness of the compatibilizer between three triblock copolymer of SEBS of different molecular weights and SEB diblock copolymer for high density polyethylene/syndiotactic polystyrene (80/20) blend. Morphology observation showed that phase size of dispersed sPS particles was significantly reduced on addition of all the four copolymers and interfacial adhesion between the two phases was enhanced. Tensile strength of the blends increased at the lower copolymer content, but decreased with increasing copolymer content. The elongation at break of the blends improved and sharply increased with increments of the copolymers. The modulus of the blend suffered a decrease on addition of the rubbery copolymer. The mechanical properties of the blends depend not only on size of the dispersed sPS and interfacial adhesion between the two phases but also on the compatibilizer content and mechanical properties of compatibilizers. Addition of the compatibilizer to the HDPE/sPS blends has little influence on the crystallization temperature of the HDPE but resulted in reduction in crystallinity of both HDPE and sPS. Vicat softening temperatures of the

blends show that heat resistance of HDPE has been improved by incorporation of 20 wt% sPS.



สถาบันวิทยบริการ
จุฬาลงกรณ์มหาวิทยาลัย

CHAPTER III

EXPERIMENTAL

3.1 Materials

The materials used in this study were commercial grade. The high impact polystyrene (HIPS) *Porene*® *HI650* ($MFI_{5, 473\text{ K}} = 8.0\text{ g } 10^{-1}\text{ min}^{-1}$) having 7.0-8.0% polybutadiene content (particle size between 3-4 micrometers) and commercial injection grade high-density polyethylene (HPDE) *Polene*® *R1760* ($MFI_{2.16, 463\text{ K}} = 9.0\text{ g } 10^{-1}\text{ min}^{-1}$, 75% crystallinity) were supplied by Thai Petrochemical Industry Public Company Limited, Rayong, Thailand. The compatibilizer used in this study was a styrene/ethylene-butylene/styrene triblock copolymer (SEBS), *Kraton*™ *G1652* ($MFI_{5, 473\text{ K}} = 1.0\text{ g } 10^{-1}\text{ min}^{-1}$, Block EB $M_w = 35,000$, Block PS $M_w = 7500$), from Shell Chemicals, United States of America (USA), containing 70 wt% of a random copolymer of ethylene-butylene, and 30 wt% of styrene.

3.2 Instruments

Followings are the list of major instruments used in this research

1. PL-2000 Brabender Plasti-Corder (BPC), Germany, with other compartments such as a DSK 42/7 twin-screw extruder, internal mixer and 881201 Brabender pelletizer. The twin screw configuration was of intermeshing counter-rotating type with 41.8 mm screw diameter, 7D screw length, 6.45 mm depth of thread and 10 mm pitch.

2. IS100G 100MT Toshiba injection molding machine, Japan
3. LR10K Lloyd universal testing machine, USA
4. 258D Pendulum impact tester, USA
5. DSC-200 NETZSCH Differential Scanning Calorimeter, Germany
6. JSM-5800LV JEOL Scanning Electron Microscope, Japan
7. RH-7 Rosand Single Bore Capillary Rheometer, United Kingdom
8. Bruker PC-20 ¹H-pulsed NMR (20 MHz), USA

3.3 Blends Preparation

The blends were prepared in a twin screw Brabender extruder model 42/7 (D = 42 mm, L/D = 7) attached to a Brabender Plasti-Corder PL2000. The twin screw extruder is an intermeshing counter-rotating twin screw extruder. The weight ratios of HIPS and HDPE were 90/10, 70/30, 50/50, 30/70 and 10/90. The compatibilizer concentrations used were 5, 10, 15 and 20 pphr for each HIPS/HDPE weight ratio. The various blend compositions prepared are given in Table 3.1.

All materials for each blend were dry mixed in an LMX 5W Lab Tech mechanical mixer for 10 minutes. The mixed materials were then introduced into a hopper of the twin-screw extruder, with the controlled temperatures at all three heating zones and die zone at 473 K; the speed was fixed at 40 rpm. The long strand extrudates were chopped into granules using the pelletizer and subsequently dried at 343 K for 6 hours.

In addition to the morphological study, HIPS/HDPE blend ratios of 90/10 and 10/90 with the compatibilizer concentrations of 15 and 20 pphr were also prepared in an internal mixer attached to a Brabender Plasti-Corder PL2000. All materials in these blend ratios were hand tumbled for 10 minutes before being put into the mixing bowl, which had been heated and controlled at 473 K, at a speed 40 rpm and the mixing time for 10 minutes. About 70% of the total available volume (~50 grams) was filled with the materials. The mixing time was counted from the time of sample loading into the mixing bowl. After melt mixing, the blends were quenched in cold tap water and dried overnight at 343 K. The blended samples were compression molded by preheating the blend in the press at 443 K for about 15 minutes, then applying a pressure of 3.85 MPa was applied for 6 minutes. The presses were then water-cooled to room temperature with the plaque under pressure.



สถาบันวิทยบริการ
จุฬาลงกรณ์มหาวิทยาลัย

Table 3.1 Composition of HIPS/HDPE/SEBS blends

No.	HIPS/HDPE/SEBS (wt%/wt%/pphr)	Weight fraction		
		x_{HIPS}	x_{HDPE}	x_{SEBS}
1	90/10/0	0.9	0.1	0
2	70/30/0	0.7	0.3	0
3	50/50/0	0.5	0.5	0
4	30/70/0	0.3	0.7	0
5	10/90/0	0.1	0.9	0
6	90/10/5	0.8572	0.0952	0.0476
7	70/30/5	0.6667	0.2857	0.0476
8	50/50/5	0.4762	0.4762	0.0476
9	30/70/5	0.2857	0.6667	0.0476
10	10/90/5	0.0952	0.8572	0.0476
11	90/10/10	0.8182	0.0909	0.0909
12	70/30/10	0.6364	0.2727	0.0909
13	50/50/10	0.4546	0.4546	0.0909
14	30/70/10	0.2727	0.6364	0.0909
15	10/90/10	0.0909	0.8182	0.0909
16	90/10/15	0.7826	0.0870	0.1304
17	70/30/15	0.6087	0.2609	0.1304
18	50/50/15	0.4348	0.4348	0.1304
19	30/70/15	0.2609	0.6087	0.1304
20	10/90/15	0.0870	0.7826	0.1304
21	90/10/20	0.7500	0.0833	0.1667
22	70/30/20	0.5833	0.2500	0.1667
23	50/50/20	0.4167	0.4167	0.1667
24	30/70/20	0.2500	0.5833	0.1667
25	10/90/20	0.0833	0.7500	0.1667

3.4 Rheological properties

An RH7 Rosand single bore capillary rheometer was used to characterize shear flow properties in terms of shear stress and shear viscosity. The tests were carried out at a wide range of shear rate (20 to 9000 s⁻¹) at a test temperature of 473 K. Dimensions of the capillary die used were 1 mm diameter, 16 mm length and 180° entry angle with an aspect ratio (L/D) of 16:1. The material was first preheated in a barrel for 5 minutes under a pressure of approximately 3-5 MPa to get a compact mass. The excess material was then automatically purged until no bubbles were observed. The test was then carried out at a set shear rate in a program via a microprocessor. During the test, the pressure drop across capillary channel and melt temperature was captured via a data acquisition system. The apparent values of shear stress, shear rate and shear viscosity were calculated using the derivation of the Poiseuille law for capillary flow:

$$\text{Apparent wall shear stress (Pa); } \tau = \frac{R\Delta P}{2L}, \quad (3.1)$$

$$\text{Apparent wall shear rate (s}^{-1}\text{); } \dot{\gamma}_{app} = \frac{4Q}{\pi R^3}, \quad (3.2)$$

$$\text{Apparent shear viscosity (Pa s); } \eta_s = \frac{\tau}{\dot{\gamma}_{app}}, \quad (3.3)$$

where ΔP is a pressure drop across the channel (Pa), Q is volumetric flow rate (m³s⁻¹), R is the capillary radius (m), and L is the length of the capillary (m). The values of R and L used in this work were 1 mm and 16 mm, respectively.

3.5 Thermal analysis

The melting and glass transition temperatures of the blend were studied using DSC200 under a nitrogen atmosphere with a heating and cooling rate of 10 K min^{-1} . The temperature cycle consisted of an initial heating from 303 K to 473 K, followed by cooling to 303 K and a second heating to 473 K. Data were collected during the second heating thermogram.

3.6 Morphological observation

The SEM samples for morphology studies were directly taken from the broken pieces after the impact test. HIPS and SEBS were etched off from the sample surfaces with toluene to better reveal the microstructure. Etching was performed at room temperature for 2 hours, after which the surfaces were rinsed, dried at 343 K for 6 hours, the sample was immersed in 2% OsO_4 aqueous solution for staining the unsaturated components at room temperature for 12 hours. After removal from the staining solution, the samples were carefully washed to remove the unreacted osmium tetroxide, then the samples were coated with gold to prevent charging before they were examined under SEM observation.

3.7 Mechanical properties

3.7.1 Izod impact strength testing

Testing specimens of 64 mm x 12.7 mm x 3.2 mm for the measurement of Izod impact strength were prepared by following ASTM D4101. They were tested according to the standard method of ASTM D256. A pendulum swung on its track and struck a notched, cantilevered plastic sample. The energy lost

(required to break the sample) as the pendulum continued on its path was measured from the distance of its follow through.

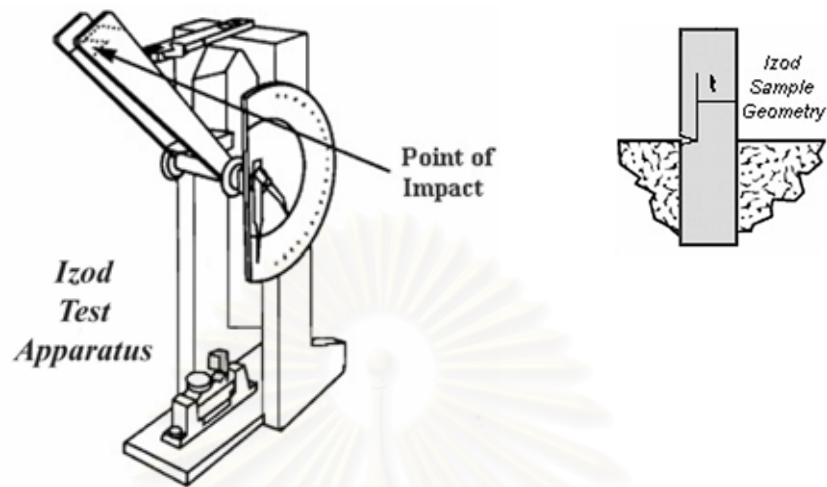


Figure 3.1 Izod impact strength apparatus and test specimen.

3.7.2 Tensile property measurement

The dumbbell specimens for the tensile property measurement were prepared according to ASTM D4101. They were tested in accordance with ASTM D638. The sample was pulled, by the tensile testing machine, from both ends. The force required to pull the specimen apart, and how much the sample was stretched before its breaking, was measured.

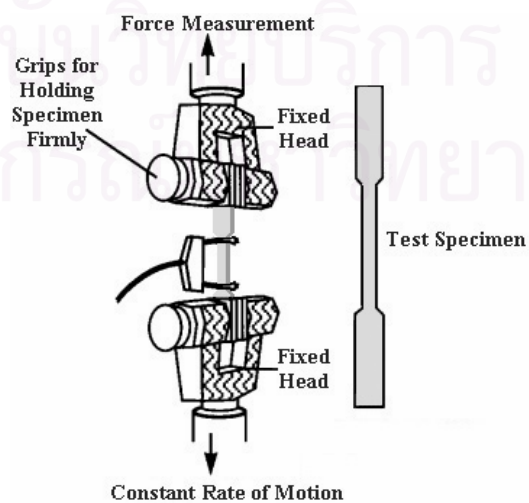


Figure 3.2 Tensile testing apparatus and test specimen.

3.7.3 Flexural strength testing

The flexural test measures the force required to bend a beam under 3-point loading conditions. Test specimens of 3.2 mm x 12.7 mm x 128 mm for the measurement of flexural strength were prepared following ASTM D4101. They were tested according to the standard method of ASTM D790. Specimen was placed on two supports and a load was applied at the center. The load at yield measured at 5% deformation/strain of the outer surface is flexural strength. The test beam is under compressive stress at the concave surface and tensile stress at the convex surface.



Figure 3.3 Flexural strength testing.

3.5 Relaxation Time by Pulsed Nuclear Magnetic Resonance

In addition, investigation of the phase separation or compatibility of the polymer blends can be observed by ^1H -pulsed NMR technique. The ^1H -pulsed NMR equipment is the Bruker PC-20 (resonance frequency of proton at 20 MHz) as shown in Figure 3.4. The pulsed NMR diagram is shown in Figure 3.5. Measurements were carried out under the control of a microcomputer. The PC-20 operates by beaming one or more radio-frequency (RF) pulses into a sample of the material to be analyzed, examining the resulting NMR signals from protons in the sample and extracting certain data from that signal to calculate the quantity of interest. The real time pulsed NMR measurements is presented in Figure 3.6.

The spin-spin relaxation time (T_2) measurement (see Appendix D) is made by both solid-echo ($90^\circ_x \tau 90^\circ_y$) and the spin-echo [Carr-Purcell-Meiboom-Gill (CPMG)]

method ($90^\circ_x \tau (180^\circ_y 2\tau_n)$). The T_2 in this experiment was measured at room temperature and the related signal intensity is analyzed.



Figure 3.4 Pulsed ^1H -NMR analyzer – minispec (Bruker) model PC-20

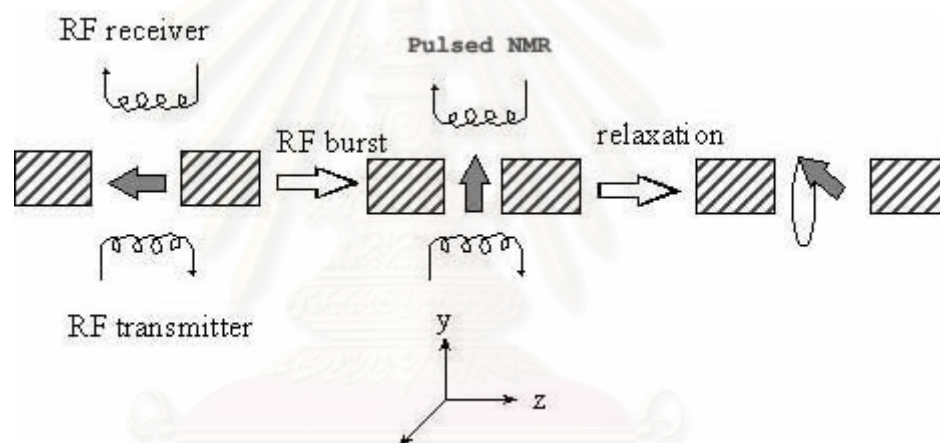


Figure 3.5 Pulsed NMR diagram

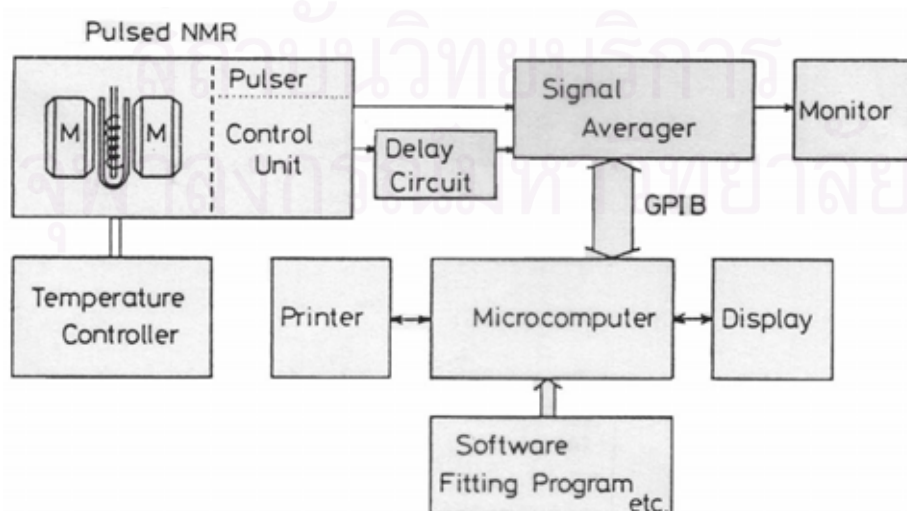


Figure 3.6 Block diagram of real time pulsed NMR measurement system

CHAPTER IV

RESULTS AND DISCUSSION

4.1 Rheological properties of HIPS/HDPE blends

The effects of blend ratio and shear rate on the shear viscosity of uncompatibilized HIPS/HDPE blends, which were prepared by melt mixing in a counter-rotation twin screw extruder at the temperature 473 K are shown in Figure 4.1. It can be seen that the viscosity of all the blends decreased with increases in shear rate, indicating pseudoplastic (shear-thinning) behavior of the blends. The pseudoplasticity is due to the random orientation and high entanglement of molecules. Under a high shear rate, the molecules became disentangled and oriented, resulting in a reduction of viscosity. In polymer blends, the viscosity depends on the interfacial thickness and interfacial adhesion in addition to the characteristics of the components in the polymer.

In polymer blends, an interlayer slip along with the orientation and disentanglement takes place when increasing more shear rate or shear stress. The blend undergoes further the elongational flow. If the interfacial bonding is strong, deformation of the dispersed phase is effectively transferred to the continuous phase. When the interfacial bonding is weak, the interlayer slip takes place easily to reduce the blend viscosity. The greater decrease in viscosity at the higher shear rate in the uncompatibilized blends occurs because the dispersed phase of the incompatible blend

(either HIPS or HDPE) loses its structure in the solid phase to become a liquid-like phase.

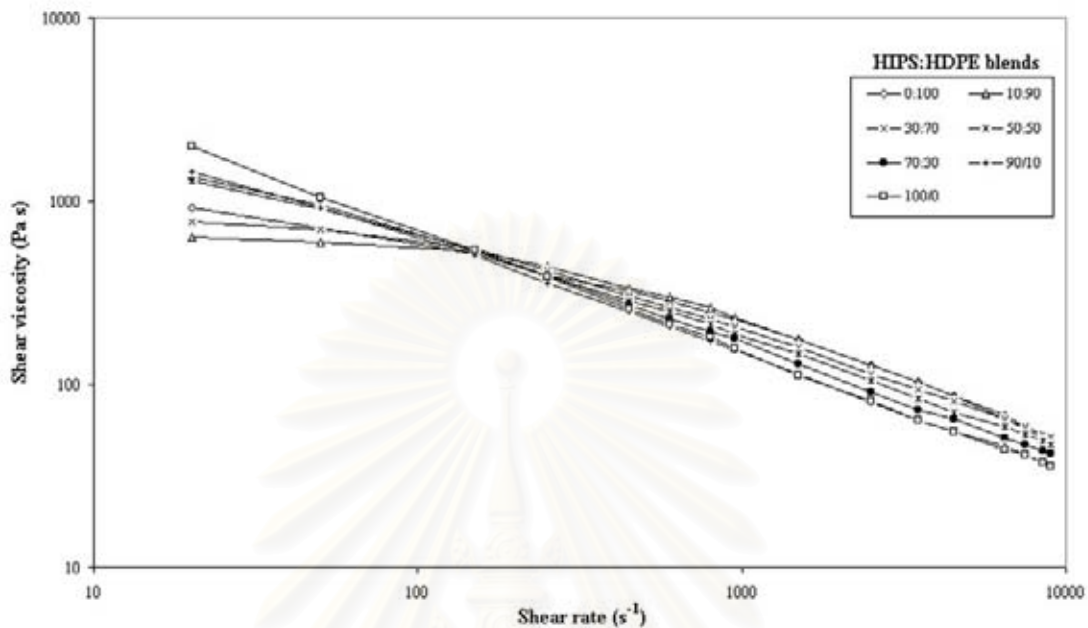


Figure 4.1 Flow curve of uncompatibilized HIPS/HDPE blends

The effects of SEBS block copolymer loading (5, 10, 15 and 20 pphr) and shear rate on the melt viscosities of HIPS/HDPE blends in each ratio (90/10, 70/30, 50/50, 30/70 and 10/90) prepared by the same condition of the uncompatibilized blends and melt mixed at 473 K in the counter-rotation twin screw extruder are shown in Figures 4.2 – 4.6, respectively. In the compatibilized blends, all the blend compositions gave the pseudoplastic flow under various shear rates. The shear viscosity of the compatibilized blends is higher than that of the uncompatibilized one.

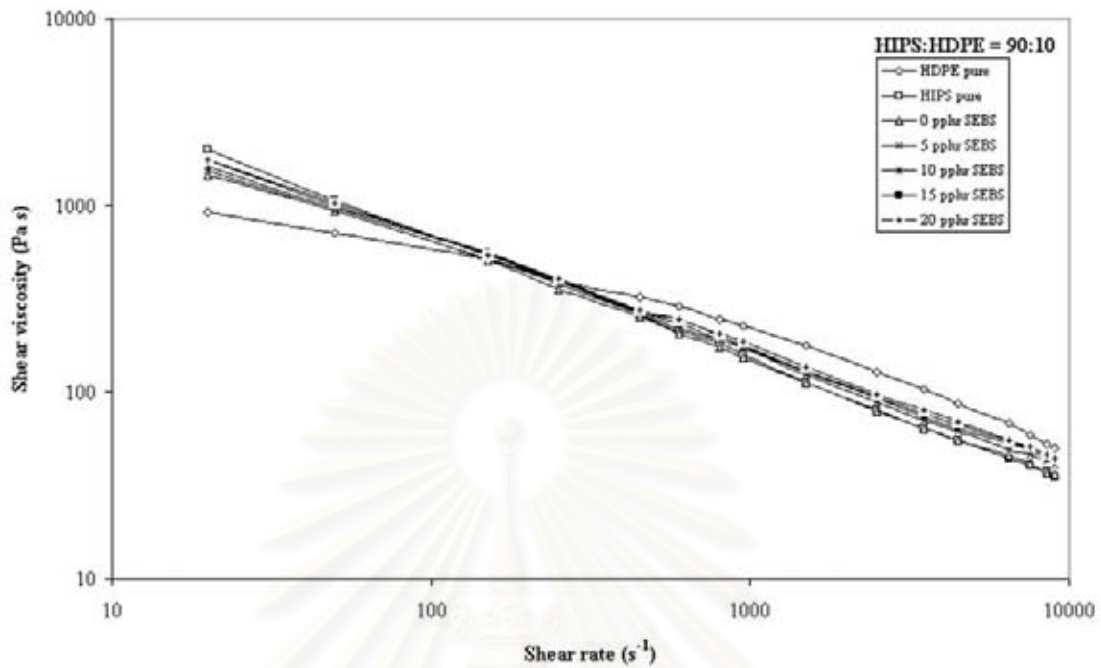


Figure 4.2 Flow curve of HIPS/HDPE (90/10) blends with various SEBS concentrations

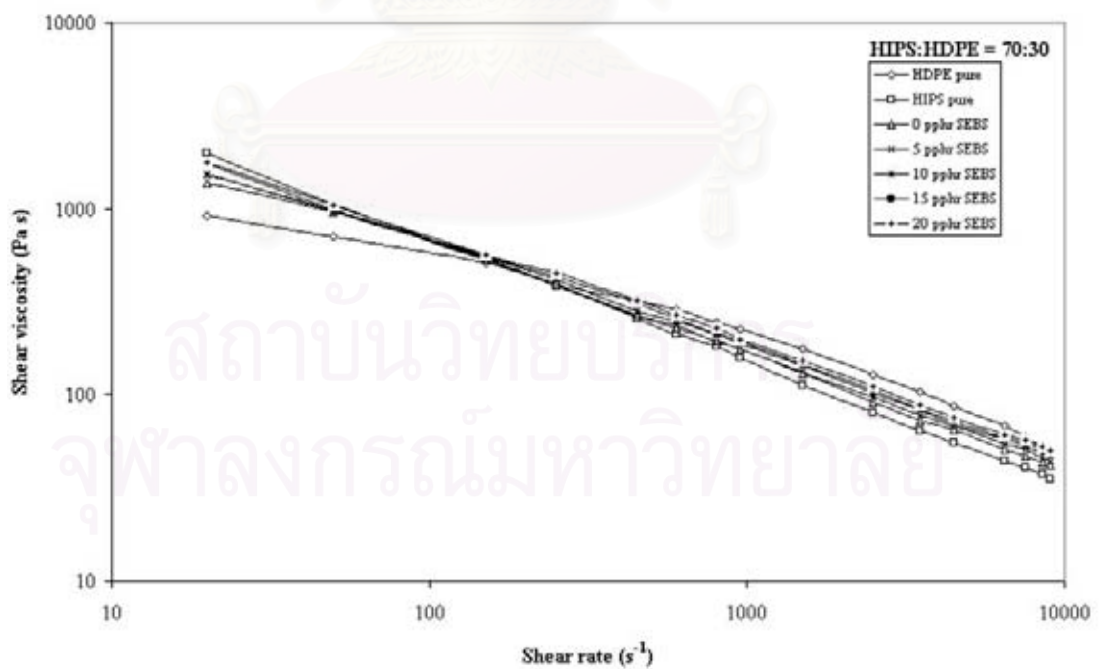


Figure 4.3 Flow curve of HIPS/HDPE (70/30) blends with various SEBS concentrations

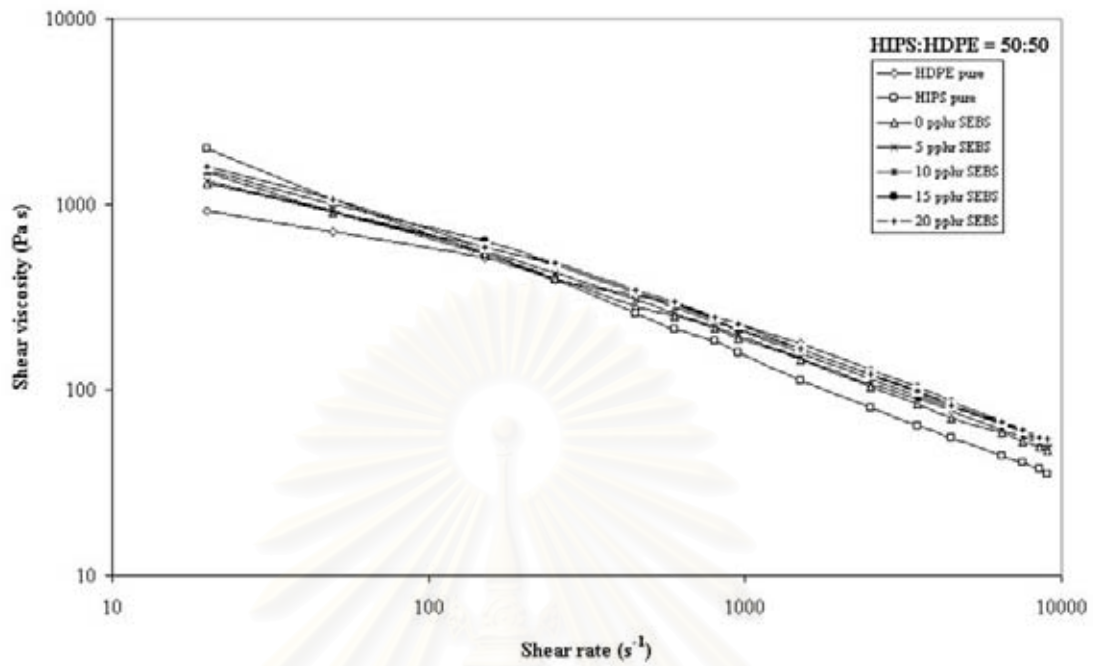


Figure 4.4 Flow curve of HIPS/HDPE (50/50) blends with various SEBS concentrations

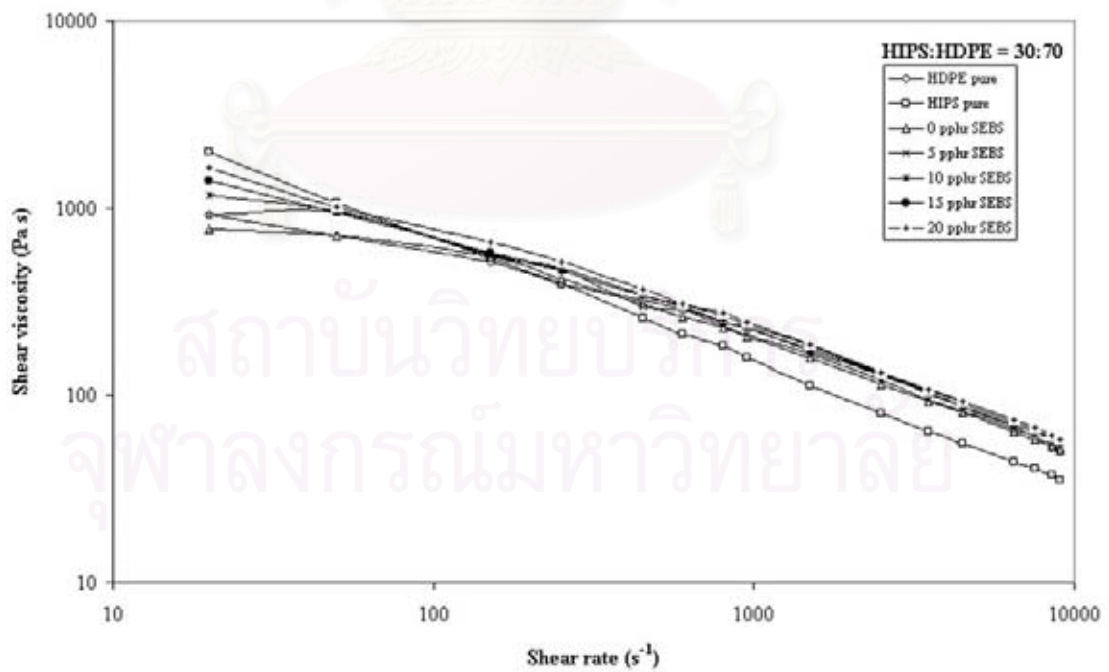


Figure 4.5 Flow curve of HIPS/HDPE (30/70) blends with various SEBS concentrations

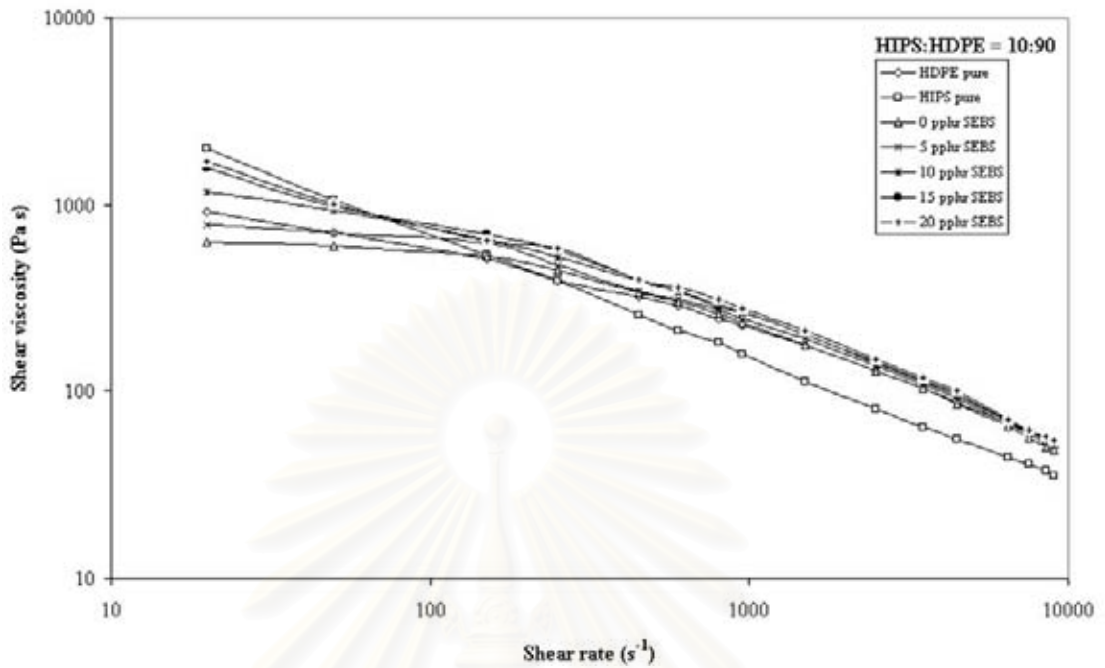


Figure 4.6 Flow curve of HIPS/HDPE (10/90) blends with various SEBS concentrations

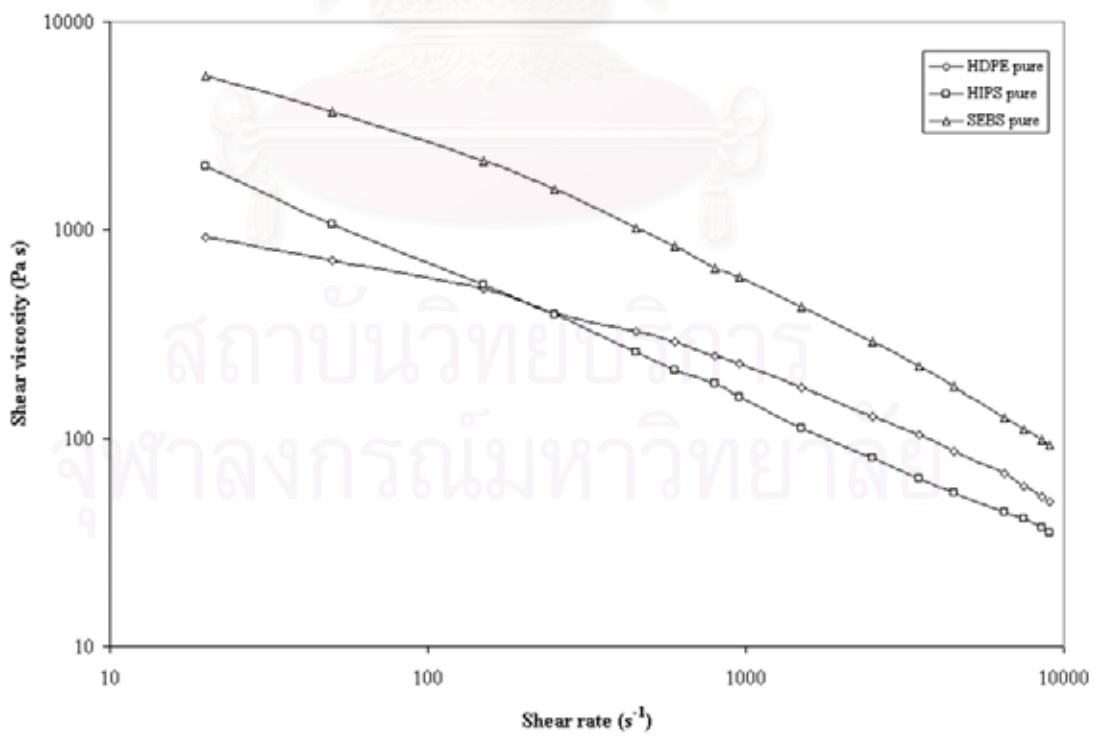


Figure 4.7 Flow curve of HIPS, HDPE and SEBS pure component at 473 K

One can observe from Figures 4.2 to 4.6 that the shear viscosity of compatibilized HIPS/HDPE blends increases with increasing the amount of SEBS in the blends. The addition of compatibilizers to polymer blends affects their flow behavior. Chemical reactions occurring between the components of a blend upon compatibilization generally increase the viscosity of the system. These are probably because of a coupling effect of the block copolymer when loading the SEBS into the blends. It introduces the better interfacial adhesion between the HIPS and HDPE phases as the polystyrene and poly(ethylene-*b*-butylene) blocks in SEBS are penetrated into HIPS and HDPE phases, respectively. In addition, the SEBS block copolymer has the higher viscosity than those of HIPS and HDPE at 473 K at all shear rates as shown in Figure 4.7. The higher viscosities of polystyrene block and poly(ethylene-*b*-butylene) block contribute to the higher viscosities of the blends. At this point, we anticipate that the triblock copolymer can combine the phases of HIPS and HDPE. However, it is not conclusive, further studies on log additivity rule model are carried out.

The indication of strong or weak interactions between phases of the blends can be determined by a positive or negative deviation of measured viscosity from that calculated by the log additivity rule model (Equation 2.2). It is used for the evaluation of the thermodynamic compatible of the polymer blend for the deviations of the blend viscosities from the ideal behavior [24-27]. According to the following equation:

$$\log (\eta_{blend}) = \sum_i x_i \log (\eta_i), \quad (2.2)$$

where η_{blend} and η_i are the shear viscosity of the blend and that of the phase i and x_i is the weight fraction of the phase i .

The melt viscosity of polymer blends shows three types of behavior as the following [25]:

- (1) Positive deviation behavior (PDB) where blend viscosities show a higher value than the log additivity value.
- (2) Negative deviation behavior (NDB) where blend viscosities show a lower value than the log additivity value.
- (3) Positive-negative deviation behavior (PNDB) where the same blend exhibits both positive and negative deviation behavior, depending on the composition, morphology and processing conditions.

The results of compatibility analysis by log additivity rule model are shown in Table 4.1 and Figures 4.8 to 4.12 for the uncompatibilized and compatibilized blends in 90/10, 70/30, 50/50, 30/70 and 10/90 blend ratio of HIPS/HDPE, respectively.

In relation to log additivity rule model, the HIPS/HDPE blend ratios from 90/10 to 30/70 (Figures 4.8 – 4.11) are shown the slightly negative deviation behavior (NDB) at low shear rates, and a positive deviation behavior (PDB) at high shear rates. This indicates the incompatibility at low shear rates, and it becomes more compatible at the higher shear rates. In contrast, the 10/90 HIPS/HDPE blend ratio (Figure 4.12) gives a PDB with an NDB at very high shear rates. This 10/90 blend ratio provides a compatibility at low shear rate. This may give some indication that the overall morphological dispersion of the small component of HIPS functions as a disperse phase in the HDPE matrix phase for HIPS/HDPE (10/90) blend. We anticipate that the 10/90 ratio of HIPS/HDPE has a different morphology from other blends. In Figure 4.7, the shear viscosity of HDPE at low shear rate is higher than that of HIPS.

At the high shear rate, the shear viscosity of HIPS become higher than that of HDPE. This result can be explained as follows: the compatibility of these blends is considered in terms of the viscosity ratio of the blends. If the minor component has a lower viscosity than that of the major one, the minor component will then be finely and uniform dispersed in the major component. Reversely, the minor component will be coarsely dispersed if its viscosity is higher than that of the major component [28]. In the case of the HIPS matrix phase and HDPE dispersed phase, the higher shear rate is required to impose HDPE dispersed phase to give the lower viscosity. The HDPE can, therefore, become finely and uniformly dispersed into the HIPS matrix. Through this behavior, HDPE can be compatible with HIPS matrix. Likewise, the HDPE matrix phase and HIPS dispersed phase can be compatible via this technique.

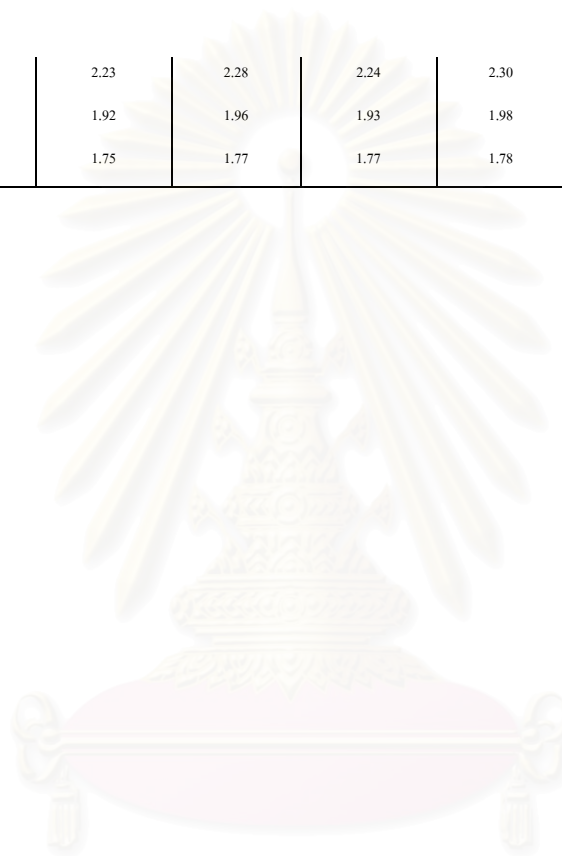


สถาบันวิทยบริการ
จุฬาลงกรณ์มหาวิทยาลัย

Table 4.1 Shear viscosity of HIPS/HDPE blends compatibilized with SEBS from experimental data versus log additivity rule model

HIPS/HDPE	Shear rate (s ⁻¹)	η HDPE Pa s	η HIPS Pa s	η SEBS Pa s	SEBS (pphr)									
					0		5		10		15		20	
					Log η blend	Log η Eq 2.2	Log η blend	Log η Eq 2.2	Log η blend	Log η Eq 2.2	Log η blend	Log η Eq 2.2	Log η blend	Log η Eq 2.2
90/10	150	515.114	542.662	2128.700	2.7	2.73	2.71	2.76	2.74	2.79	2.75	2.81	2.73	2.83
	600	286.906	211.954	831.970	2.31	2.34	2.34	2.37	2.37	2.39	2.39	2.41	2.39	2.44
	1500	175.632	112.753	424.637	2.05	2.07	2.09	2.1	2.11	2.12	2.12	2.14	2.13	2.16
	4500	86.917	55.201	176.542	1.74	1.76	1.79	1.78	1.80	1.81	1.83	1.82	1.84	1.84
	7500	58.627	40.931	110.904	1.62	1.63	1.67	1.65	1.69	1.67	1.70	1.68	1.71	1.70
70/30	150	515.114	542.662	2128.700	2.73	2.73	2.73	2.76	2.74	2.78	2.74	2.81	2.75	2.83
	600	286.906	211.954	831.970	2.36	2.37	2.38	2.39	2.40	2.42	2.41	2.44	2.43	2.46
	1500	175.632	112.753	424.637	2.12	2.11	2.12	2.13	2.15	2.16	2.17	2.18	2.18	2.20
	4500	86.917	55.201	176.542	1.81	1.80	1.83	1.82	1.84	1.84	1.85	1.86	1.88	1.88
	7500	58.627	40.931	110.904	1.67	1.66	1.71	1.68	1.73	1.69	1.75	1.71	1.76	1.72
50/50	150	515.114	542.662	2128.700	2.73	2.72	2.75	2.75	2.77	2.78	2.80	2.80	2.77	2.82
	600	286.906	211.954	831.970	2.40	2.39	2.41	2.42	2.45	2.44	2.46	2.46	2.47	2.48
	1500	175.632	112.753	424.637	2.17	2.15	2.17	2.17	2.20	2.19	2.22	2.21	2.22	2.23
	4500	86.917	55.201	176.542	1.85	1.84	1.89	1.86	1.91	1.88	1.92	1.89	1.92	1.91
	7500	58.627	40.931	110.904	1.72	1.69	1.75	1.71	1.77	1.72	1.78	1.74	1.78	1.75
30/70	150	515.114	542.662	2128.700	2.74	2.72	2.74	2.75	2.75	2.77	2.76	2.80	2.82	2.82
	600	286.906	211.954	831.970	2.42	2.42	2.45	2.44	2.47	2.46	2.48	2.48	2.49	2.50
	1500	175.632	112.753	424.637	2.20	2.19	2.22	2.21	2.23	2.23	2.26	2.24	2.27	2.26
	4500	86.917	55.201	176.542	1.91	1.88	1.92	1.90	1.94	1.91	1.96	1.93	1.97	1.94
	7500	58.627	40.931	110.904	1.77	1.72	1.78	1.74	1.80	1.75	1.82	1.76	1.83	1.78
	150	515.114	542.662	2128.700	2.72	2.71	2.80	2.74	2.82	2.77	2.84	2.79	2.81	2.82
	600	286.906	211.954	831.970	2.48	2.44	2.49	2.47	2.54	2.49	2.53	2.51	2.56	2.52

10/90	1500	175.632	112.753	424.637	2.25	2.23	2.28	2.24	2.30	2.26	2.30	2.28	2.32	2.29
	4500	86.917	55.201	176.542	1.94	1.92	1.96	1.93	1.98	1.95	1.99	1.96	2.00	1.97
	7500	58.627	40.931	110.904	1.75	1.75	1.77	1.77	1.78	1.78	1.78	1.79	1.80	1.80



สถาบันวิทยบริการ
จุฬาลงกรณ์มหาวิทยาลัย

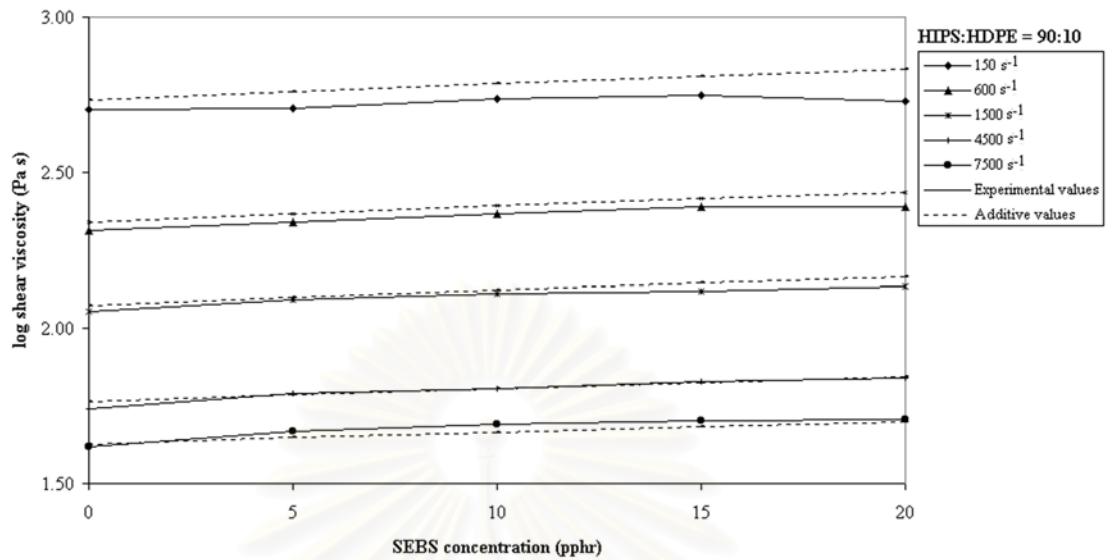


Figure 4.8 Variation of viscosity with SEBS concentrations in HIPS/HDPE (90/10) blends

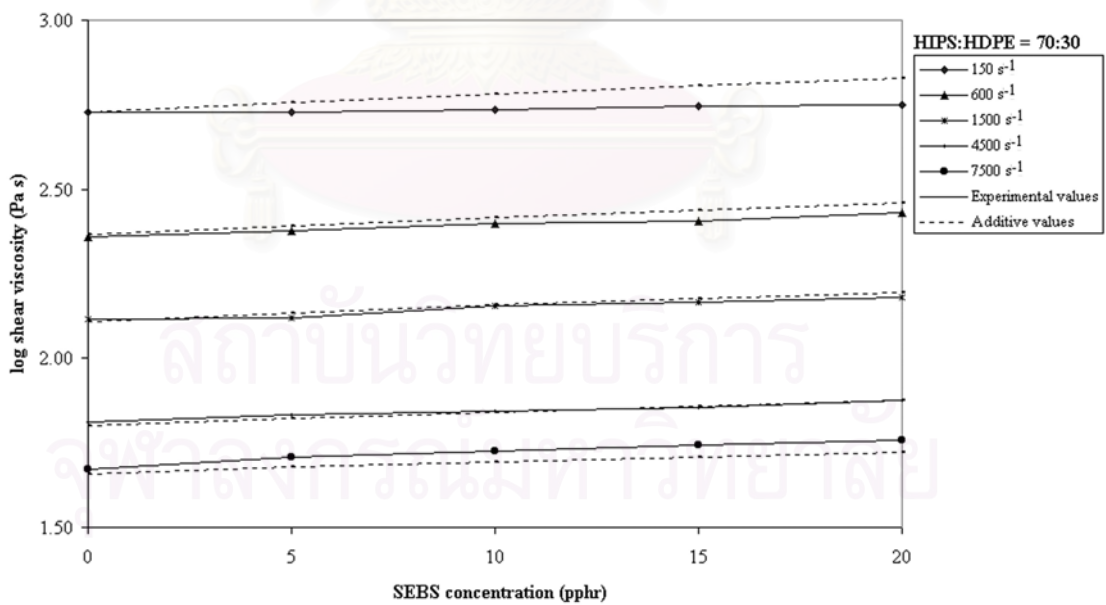


Figure 4.9 Variation of viscosity with SEBS concentrations in HIPS/HDPE (70/30) blends

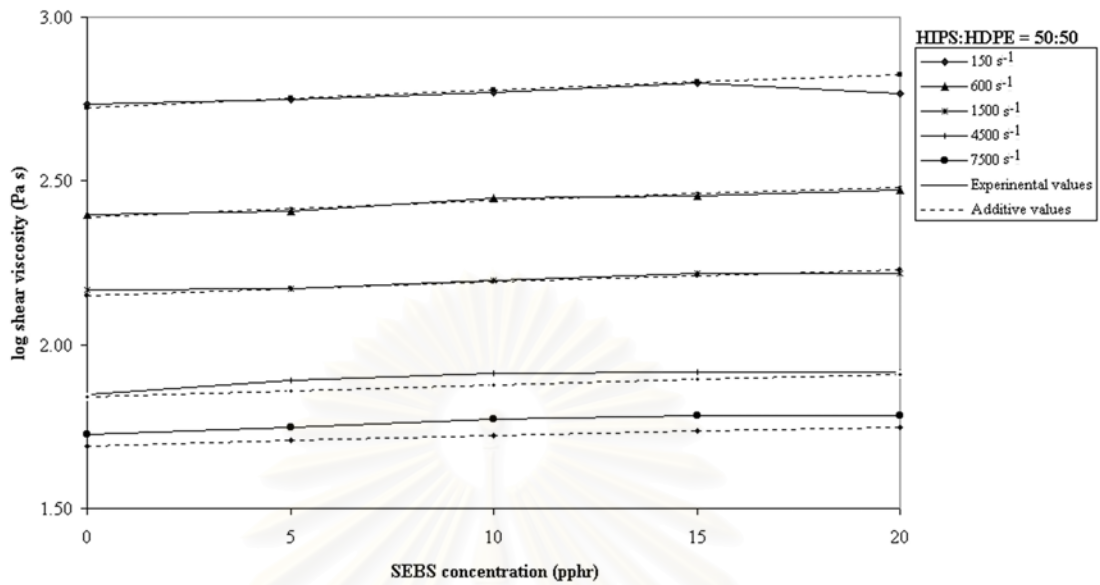


Figure 4.10 Variation of viscosity with SEBS concentrations in HIPS/HDPE (50/50) blends

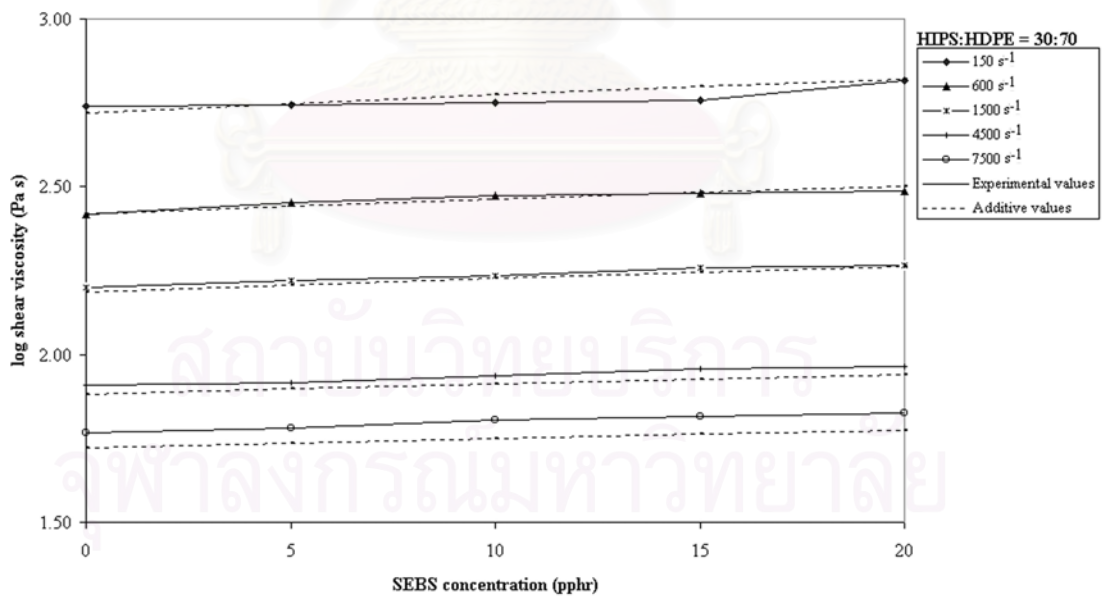


Figure 4.11 Variation of viscosity with SEBS concentrations in HIPS/HDPE (30/70) blends

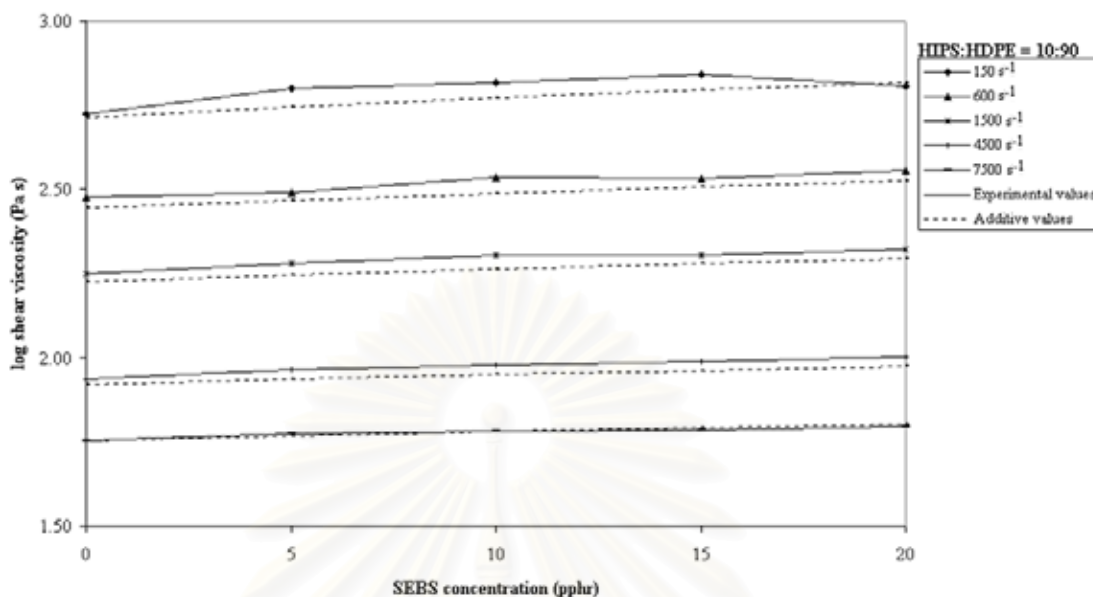


Figure 4.12 Variation of viscosity with SEBS concentrations in HIPS/HDPE (10/90) blends

4.2 Morphological observation of HIPS/HDPE blends

The morphology of uncompatibilized and compatibilized blends of HIPS and HDPE (90/10, 70/30, 50/50, 30/70 and 10/90) with SEBS block copolymer as compatibilizer prepared in a counter-rotation twin screw extruder is shown in Figures 4.13 to 4.17, respectively. Because of the inherent incompatibility of PE with PS, their blends produce two-phase materials, indicating immiscibility of the blend components. The blend volume ratio plays a predominant role in determining which of the two component forms the dispersed phase and which the matrix phase. Based on the blend volume, it indicates that, in the HIPS-rich blend, HDPE forms the dispersed phase in the HIPS matrix, and the reverse is true in the HDPE-rich blends. The SEM micrographs of the uncompatibilized blends, as shown in Figures 4.13A to 4.17A exhibited coarse and heterogeneous dispersions of the phases.

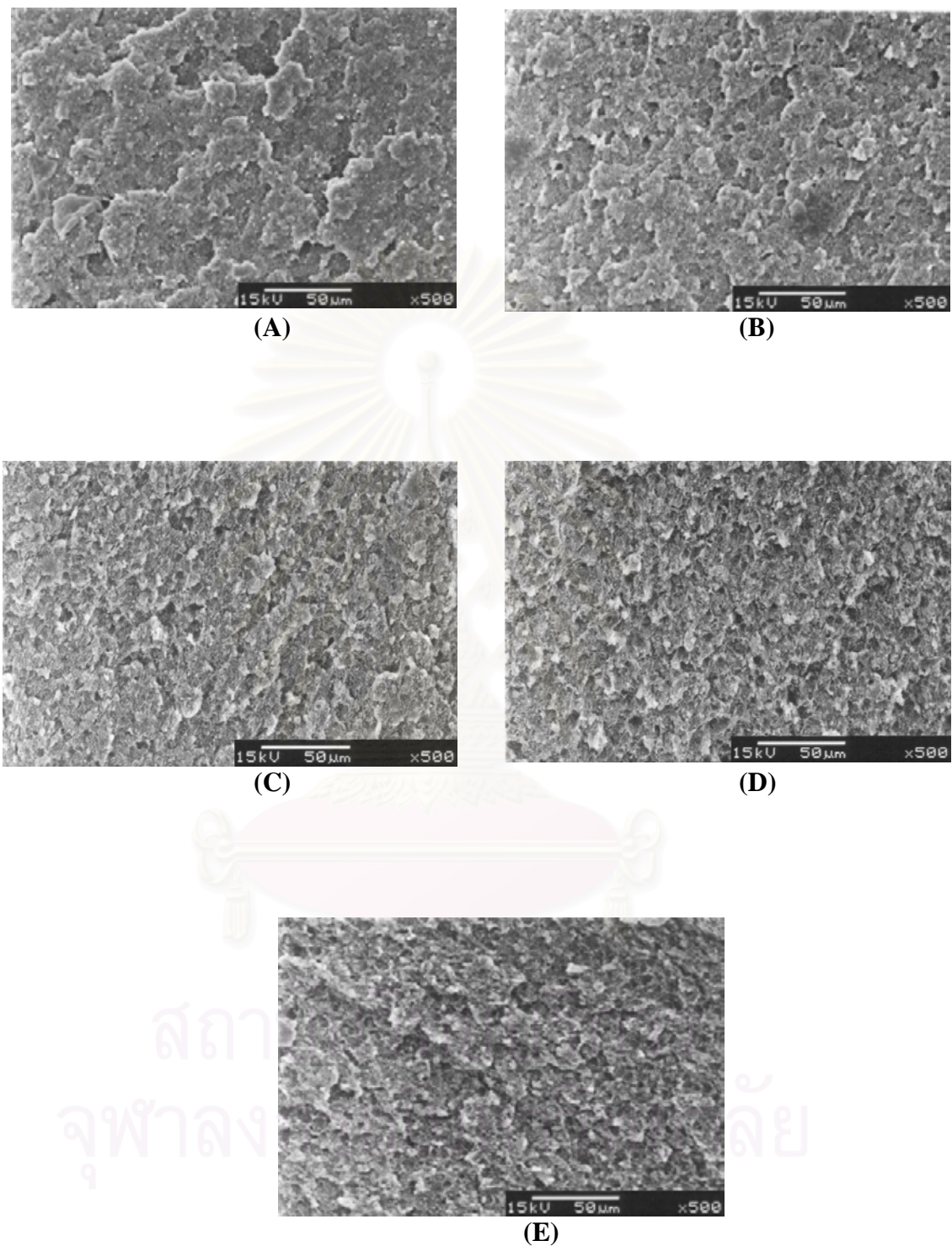


Figure 4.13 Scanning electron micrographs showing unetched impact fracture surfaces of HIPS/HDPE (90/10) blends compatibilized with SEBS as compatibilizer; (A) without SEBS; (B) 5 pphr; (C) 10 pphr; (D) 15 pphr and (E) 20 pphr

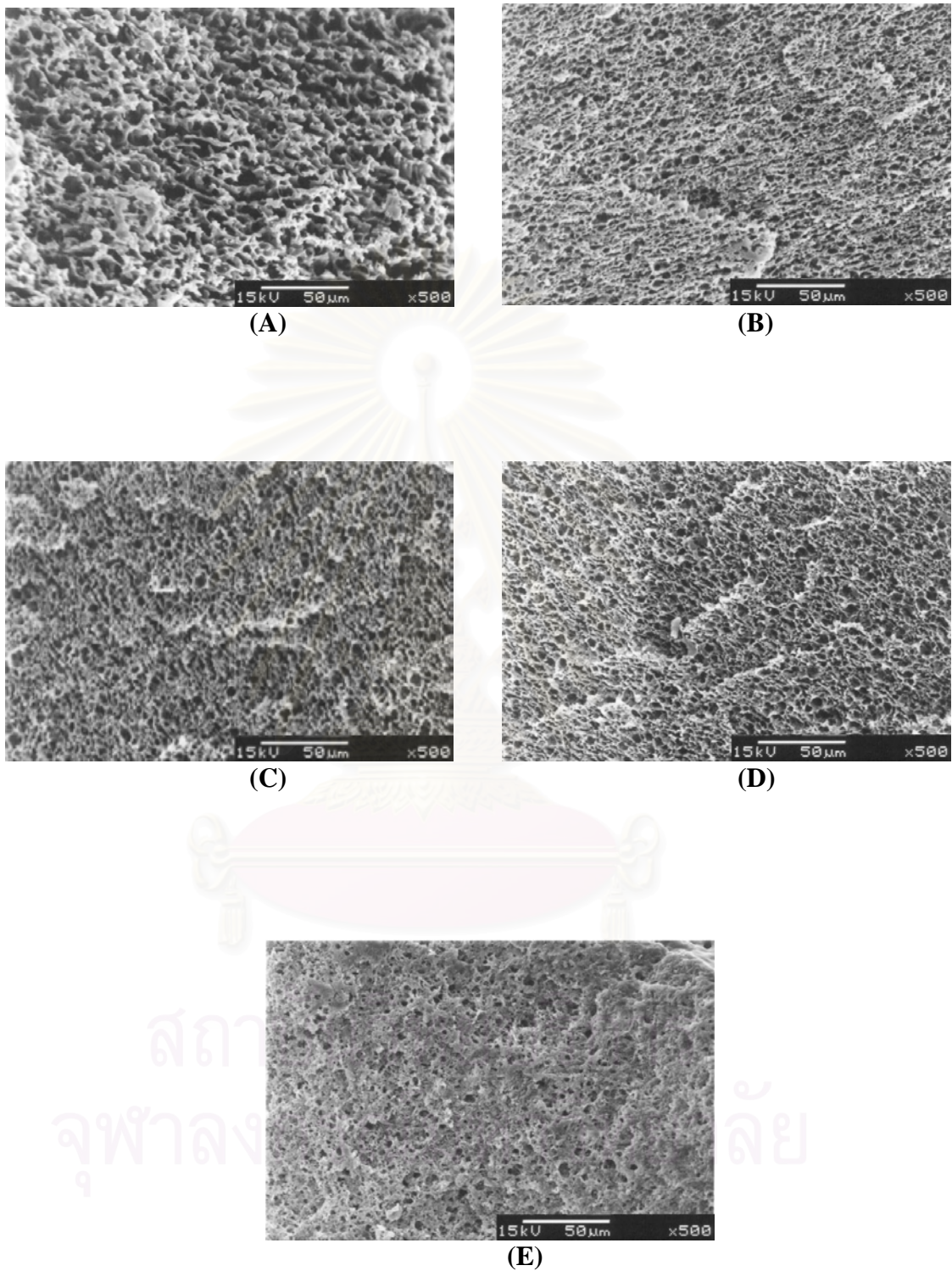


Figure 4.14 Scanning electron micrographs showing etched impact fracture surface of HIPS/HDPE (70/30) blends compatibilized with SEBS as compatibilizer; (A) without SEBS; (B) 5 pphr; (C) 10 pphr; (D) 15 pphr and (E) 20 pphr

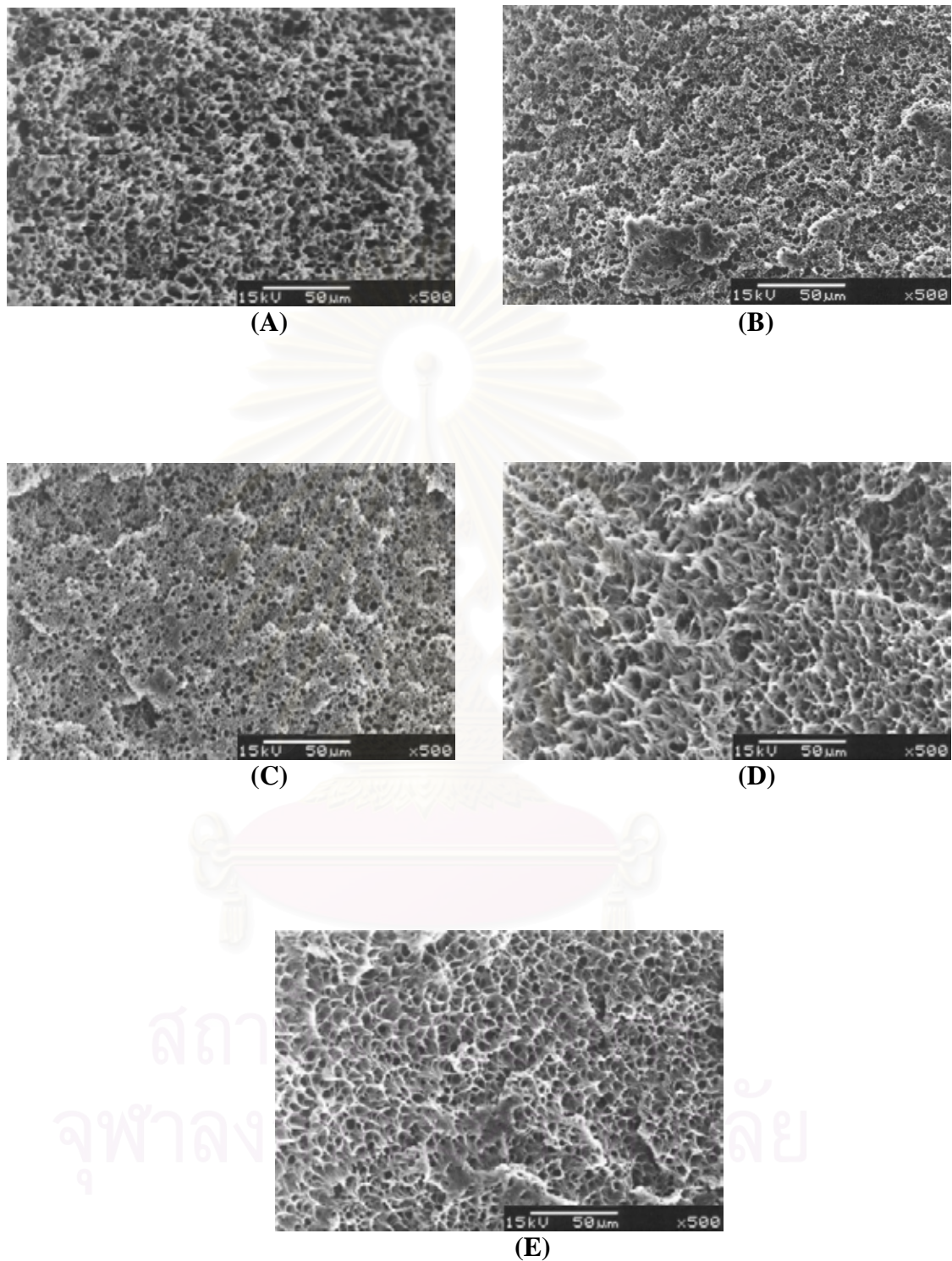


Figure 4.15 Scanning electron micrographs showing etched impact fracture surface of HIPS/HDPE (50/50) blends compatibilized with SEBS as compatibilizer; (A) without SEBS; (B) 5 pphr; (C) 10 pphr; (D) 15 pphr and (E) 20 pphr

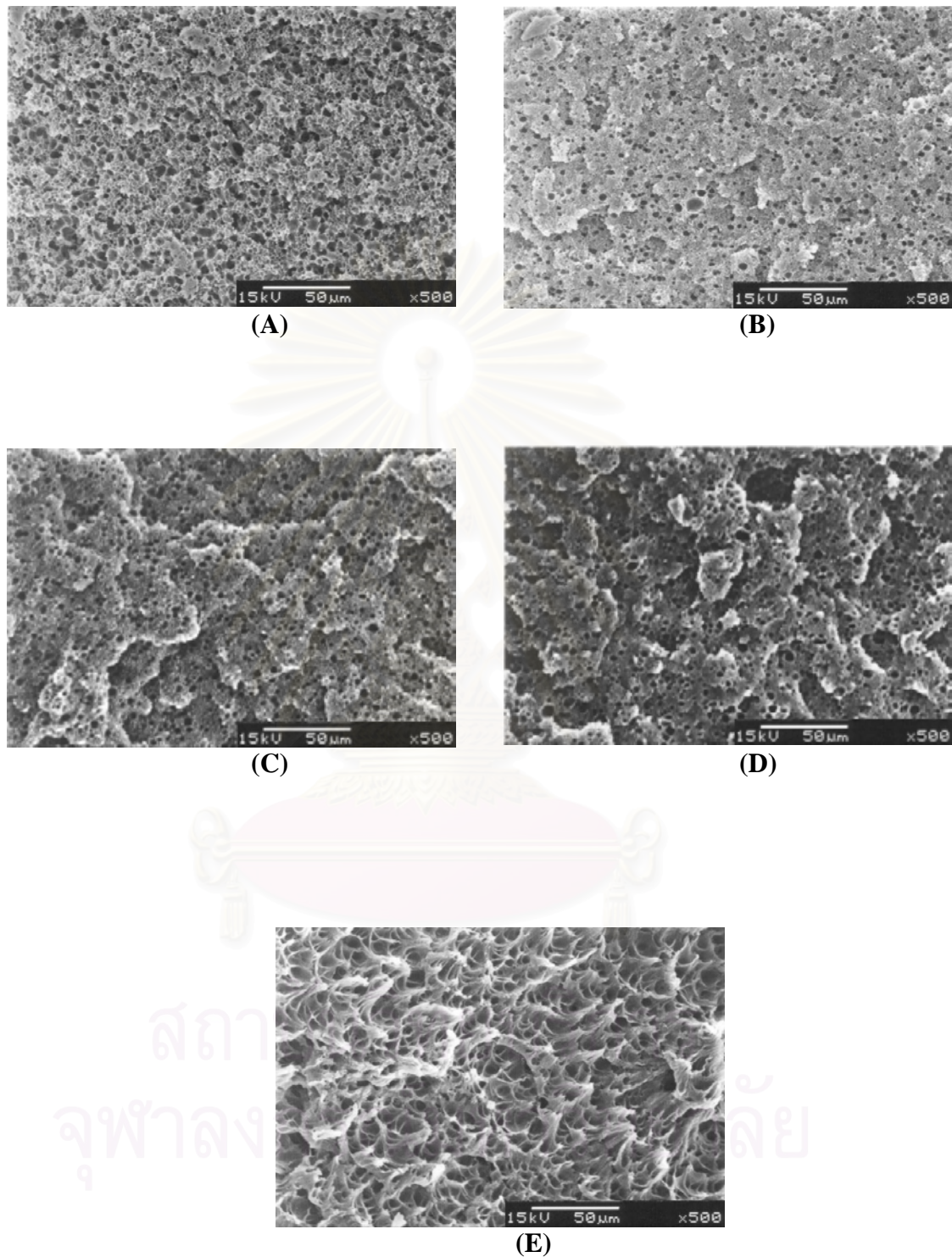


Figure 4.16 Scanning electron micrographs showing etched impact fracture surface of HIPS/HDPE (30/70) blends compatibilized with SEBS as compatibilizer; (A) without SEBS; (B) 5 pphr; (C) 10 pphr; (D) 15 pphr and (E) 20 pphr

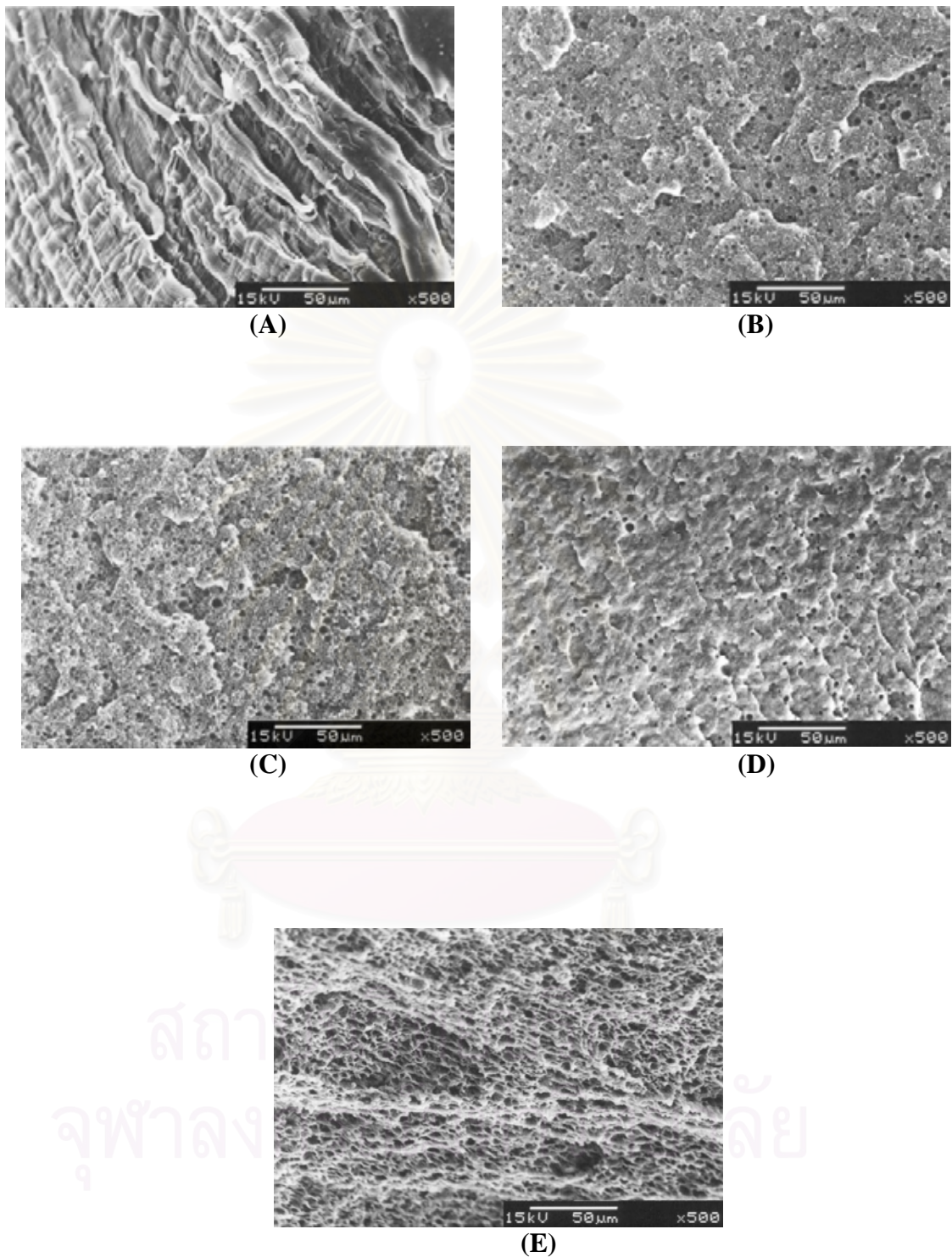


Figure 4.17 Scanning electron micrographs showing etched impact fracture surface of HIPS/HDPE (10/90) blends compatibilized with SEBS as compatibilizer; (A) without SEBS; (B) 5 pphr; (C) 10 pphr; (D) 15 pphr and (E) 20 pphr

For the morphology of the 90/10 HIPS/HDPE blend (Figure 4.13A), the binary blends exhibit coarsely dispersed HDPE domain in the HIPS matrix. After the addition of 5, 10, 15 and 20 pphr of SEBS as a compatibilizer, the blend compositions show a finer and more homogeneous dispersion of HDPE particles in the HIPS matrix as shown in Figures 4.13B to 4.13E, respectively.

The effect of compatibilizer concentration on blend morphology was examined in a 70/30 HIPS/HDPE blend with 0, 5, 10, 15 and 20 pphr of SEBS. Figure 4.14A shows that larger and coarsely dispersed cavities developed and poor interfacial adhesion between phase after toluene extraction of HIPS from the 70/30 HIPS/HDPE blend could take place. A small decrease in particle size was observed with the incorporation of 5 pphr of the compatibilizer. The dispersions of the HIPS/HDPE blends were much finer when the compatibilizer concentration increased because the better interfacial adhesion. Additionally, it is also seen that increasing adhesions between the dispersed and matrix phases are present in the 50/50 HIPS/HDPE blends (Figure 4.15) with SEBS concentrations. Finally it exhibits the co-continuous phase morphology. The size of the dispersed HIPS particles is reduced upon the addition of SEBS triblock copolymer. The reduction is especially evidenced in the 10/90 HIPS/HDPE blend with the SEBS block copolymer as compatibilizer (Figure 4.17). A smaller average interfacial area of HIPS particles compared to that of the blend with 30 wt% of HIPS (Figure 4.16) is the reason for the more efficient interfacial activity of SEBS.

In addition, the melt mixed HIPS/HDPE blend ratios of 90/10 and 10/90 compatibilized with SEBS 15 and 20 pphr, respectively are shown in Figures 4.18 and 4.19. The melt mixing degree in an internal mixer is related to the rotor speed and the

time of mixing. We found that the co-continuous phase morphology in the both of HDPE-rich phase and HIPS-rich phase increased with increasing SEBS concentrations. The better phase morphology of the 90/10 and 10/90 HIPS/HDPE blend ratios is observed because the internal mixer is batch mixing, and can take only a small amount of blend material. The longer the mixing time, the better the dispersibility and lower viscosity of the blend.

Undoubtedly, the mixing time, degree of mixing, dispersibility and viscosity affect the blend morphology. One can see that the HDPE-rich phase (Figure 4.19) is more homogeneous and continuity than HIPS-rich phase (Figure 4.18). One can even foresee its interfacial behavior. Increasing the compatibilizer concentration (20 pphr) increases the interfacial adhesion, reduces the interfacial tension, and the blend has the finer texture and uniform dispersion.

All these results indicate that the role of SEBS concerning the stabilization of the blend morphology is strongly dependent on the blend composition. These results further indicate that the presence of SEBS stabilizes the morphology of the HDPE-rich phase of the blends than the HIPS-rich phase. The location of the block copolymer interacting with the blend ratios of HDPE or HIPS is the key solution revealing the different degrees of dispersibility.

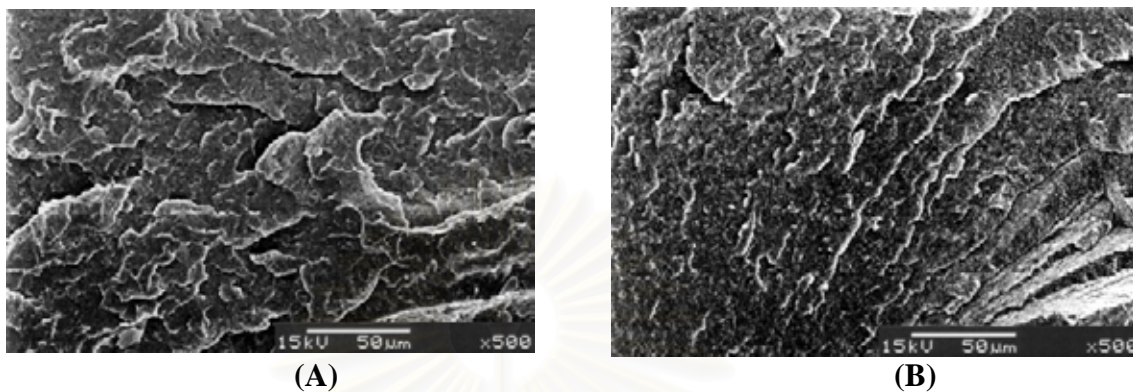


Figure 4.18 Scanning electron micrographs showing unetched cryogenic fracture surface of HIPS/HDPE (90/10) blends compatibilized with SEBS as compatibilizer which prepared by internal mixer; (A) 15 pphr and (B) 20 pphr

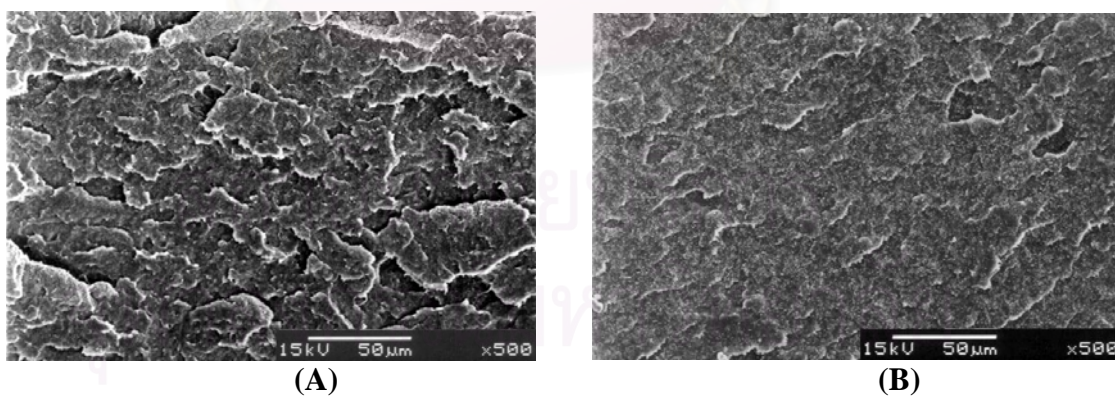


Figure 4.19 Scanning electron micrographs showing unetched cryogenic fracture surface of HIPS/HDPE (10/90) blends compatibilized with SEBS as compatibilizer which prepared by internal mixer; (A) 15 pphr and (B) 20 pphr

4.3 Thermal Analysis of HIPS/HDPE blends

Thermal analysis of the HIPS/HDPE blends is shown in Table 4.2 and Figures 4.20 to 4.24. In general, the glass transition temperature of glassy polystyrene is about 373 K. For the high-impact styrene grade, the mineral oil is added as a plasticizer for adjusting the melt flow index for the injection molding grade. Such an addition of the mineral oil is to increase the free volume of the polymer system, to give more polymeric segmental motion, which leads to reducing in the glass transition temperature. Theoretically, when HIPS is blended with the HDPE portion in the HIPS-rich phase, the HDPE is taking the role of a filler, which reduces the free volume of the system and leads to an increase in T_g of polystyrene chains in the HIPS phase. From DSC thermograms, it can be seen that glass transition temperature (T_g) and the melting temperature (T_m) of the blend remain virtually identical to that of the pure component of HIPS and HDPE, respectively. Thomas and Prud'homme [29] also reported that the DSC and DMTA data of the compatibilizing effect of block copolymers in heterogeneous polystyrene/poly(methyl methacrylate) blends gave two transitions corresponding to PS and PMMA phases. In our case, the low level of HIPS in the blends or the HIPS phase became the dispersed phase, the T_g of HIPS phase is not clearly detected. It was noted that the baseline leading to T_g of HIPS was risen to overlap with the baseline of the melting peak of HDPE matrix in the HDPE-rich phase.

The T_g s from Table 4.2 indicate that calculated T_g s of the mixture of HIPS/HDPE/SEBS by Fox's equation (Equation 2.4) were far different from the experimental values. The glass transition temperatures of the experiment were close to that of HIPS, rather than the calculated values. We could, thus, conclude that the

inclusion of SEBS compatibilizer in HIPS/HDPE did not bring to miscibility of the blends based on Fox's equation.

The compatibilized blends of HIPS/HDPE blends did not show any appreciable shift in T_g values. This indicates that addition of the SEBS as compatibilizer alters the level of miscibility. In the other words, incorporation of compatibilizer promotes some extent of molecular level miscibility. When two polymers are far from being miscible, no copolymer is likely to make a one-phase system (at HIPS/HDPE ratios of 30/70 and 10/90). In a completely immiscible system, the main role of the copolymer is to act as an interfacial agent [30]. By far, the SEBS compatibilizer still does not show any evidence in bringing the two polymer phases to become somewhat miscible. We may then conclude that the SEBS is an interfacial agent.



สถาบันวิทยบริการ
จุฬาลงกรณ์มหาวิทยาลัย

Table 4.2 T_g and T_m of HIPS/HDPE blends with various SEBS concentrations

HIPS/HDPE	SEBS (pphr)	T_g (K)		T_m , (K)
		Measurement	Calculation*	
100/0	0	361.2	-	-
0/100	0	148**	-	410.3
90/10	0	366.1	315.7	399.1
	5	367.0	309.3	399.3
	10	368.1	303.6	399.6
	15	368.5	298.7	399.7
	20	368.5	294.3	399.6
70/30	0	370.7	252.2	402.9
	5	369.4	250.2	402.2
	10	372.5	248.9	402.8
	15	370.4	247.4	403.3
	20	370.4	246.1	403.2
50/50	0	373.5	210.0	404.7
	5	372.1	210.4	404.7
	10	368.8	210.8	404.6
	15	371.0	211.2	404.8
	20	373.7	211.5	405.0
30/70	0	NA	179.8	406.6
	5	NA	181.4	406.7
	10	NA	182.9	406.3
	15	NA	184.2	405.6
	20	NA	185.4	405.2
10/90	0	NA	157.3	408.7
	5	NA	159.4	408.0
	10	NA	161.4	408.6
	15	NA	163.3	408.0
	20	NA	165.1	408.1

* = Based on Fox's equation.

** = Literature value.

NA = No available data.

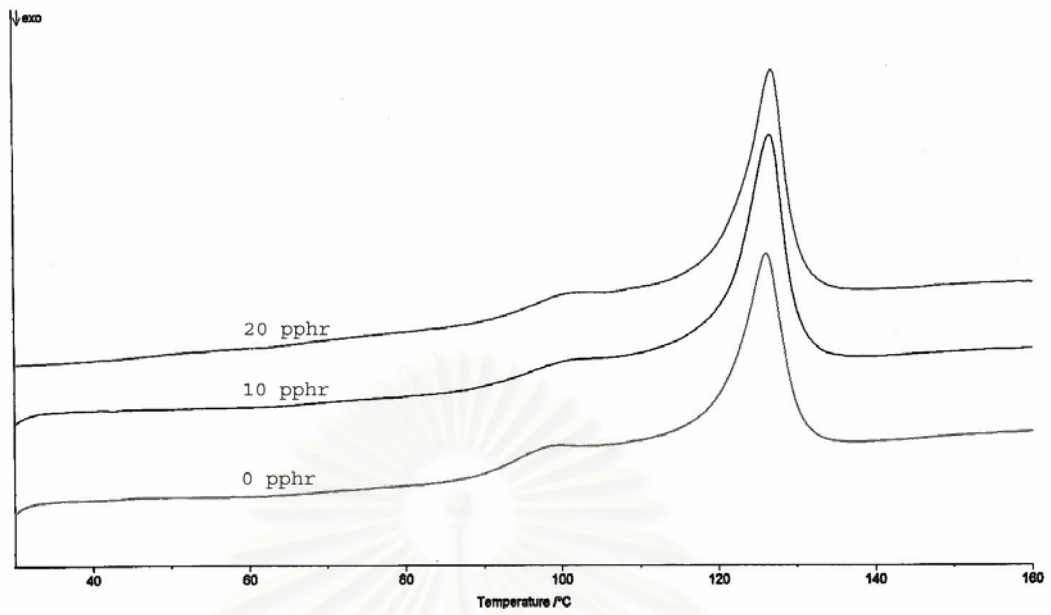


Figure 4.20 DSC thermograms of HIPS/HDPE (90/10) blends uncompatibilized and compatibilized with SEBS as compatibilizer

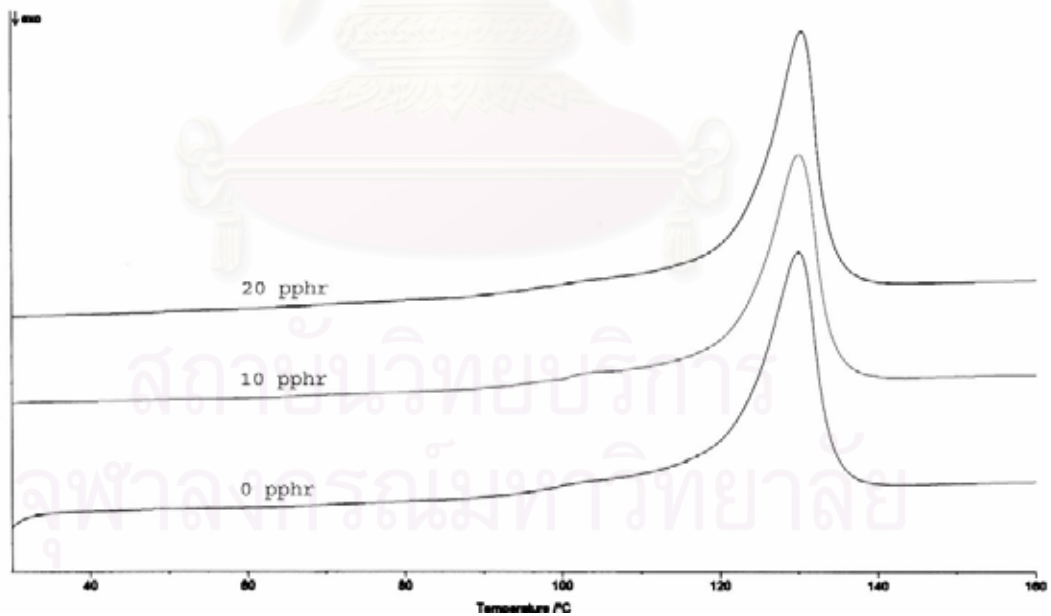


Figure 4.21 DSC thermograms of HIPS/HDPE (70/30) blends uncompatibilized and compatibilized with SEBS as compatibilizer

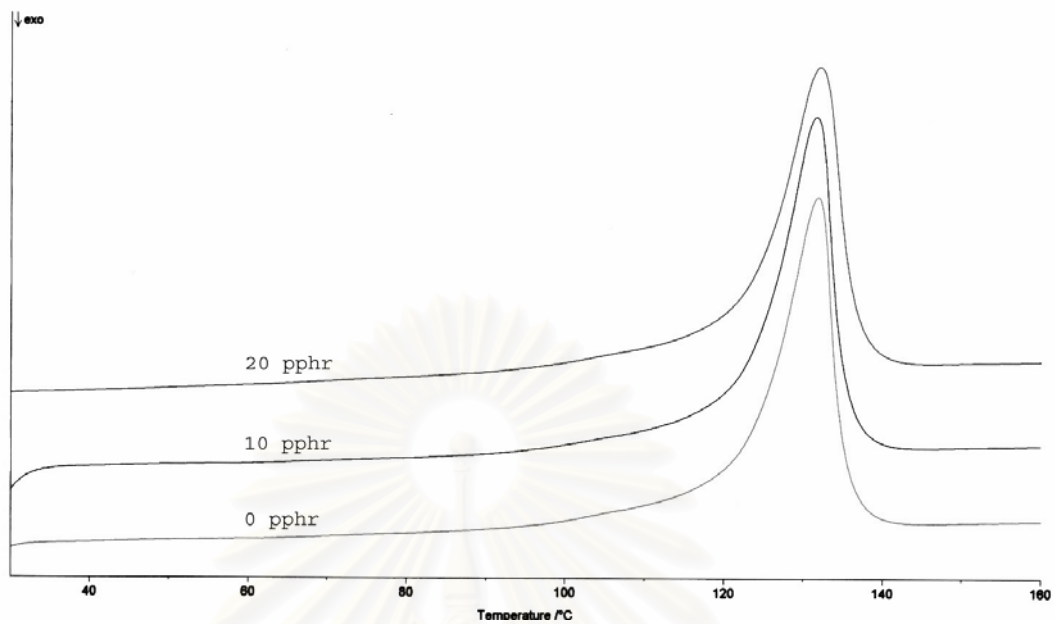


Figure 4.22 DSC thermograms of HIPS/HDPE (50/50) blends uncompatibilized and compatibilized with SEBS as compatibilizer

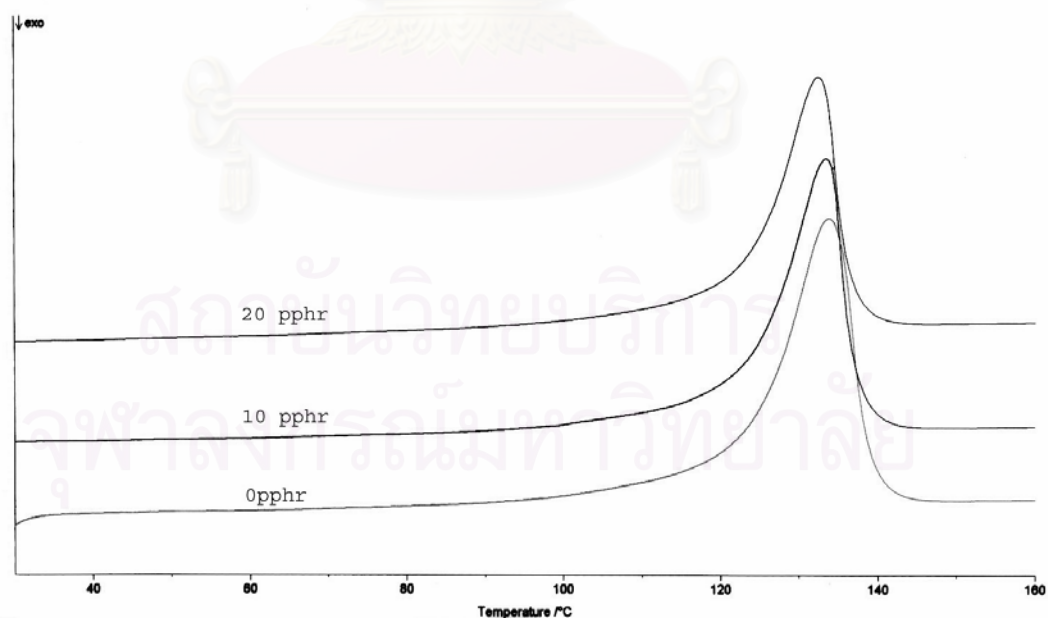


Figure 4.23 DSC thermograms of HIPS/HDPE (30/70) blends uncompatibilized and compatibilized with SEBS as compatibilizer

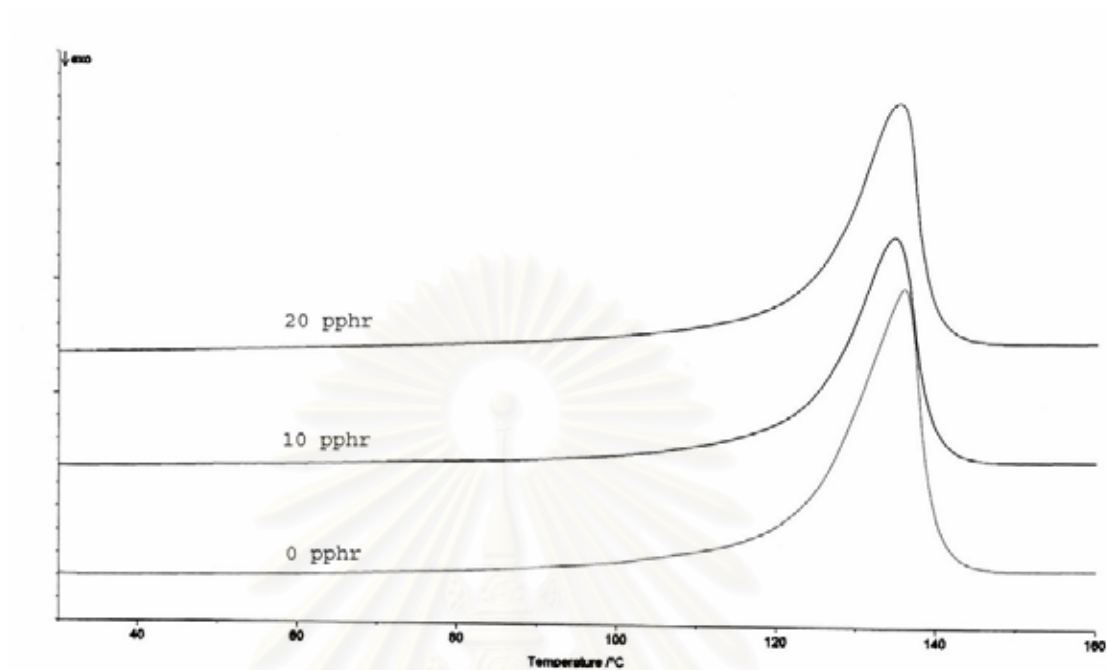


Figure 4.24 DSC thermograms of HIPS/HDPE (10/90) blends uncompatibilized and compatibilized with SEBS as compatibilizer

สถาบันวิทยบริการ
จุฬาลงกรณ์มหาวิทยาลัย

4.4 Mechanical properties of HIPS/HDPE blends

Generally, it has been known for a long time that immiscible polymer blends have inferior mechanical properties due to the existence of weak interfacial adhesion and poor dispersion of the component. In this study, the mechanical properties for the compatibilizing effect of HIPS/HDPE blends by SEBS block copolymer on the impact strength, tensile strength and flexural strength are investigated.

4.4.1 Impact strength of HIPS/HDPE blends

Izod impact strength data of HIPS/HDPE blends of the uncompatibilized and compatibilized with SEBS triblock copolymer are shown in Table 4.3 and Figure 4.25. It can be seen the Izod impact strength of the uncompatibilized blends is poor. This result indicates the poor interfacial adhesion between two phases. When they are compatibilized by SEBS block copolymer, the impact strength was improved and increased with the increasing of SEBS content in the each blend ratio. The poor phase morphology was improved and dispersed phase became much finer and more uniform dispersed (Figures 4.13 to 4.17). Impact strength of the blends of PS/HDPE blends by SEBS copolymer shows a similar trend. Tjong and Xu [21] reported that the impact strength of compatibilized blends increases slowly with HDPE content in the blends are less than 50 wt% when the HDPE became the matrix phase (HDPE content > 50 wt%), the impact strength was sharply increased with increasing HDPE content. These phenomena can be explained similarly as described previously. The HDPE-rich phase (> 50 wt%) is more compatible with SEBS than HIPS-rich phase. In the other words, the HIPS domain in the former can uniformly disperse in HDPE matrix. Unlikewise, the HDPE dispersed phase cannot disperse well in the HIPS matrix.

4.4.2 Tensile strength of HIPS/HDPE blends

It is worthwhile to mention that the uncompatibilized single polymer (HIPS alone or HDPE alone) has higher tensile strength. The single polymer provides its unique property for a particular application. Tensile strength shown in Table 4.3 and their corresponding illustrations in Figure 4.26 indicated clearly that the uncompatibilized and compatibilized blends yield the lower values at all blend ratios and SEBS concentrations. Considering the blends themselves, tensile strength increases and reaches a maximum for the blends (HIPS/HDPE) of 90/10, 70/30, 50/50 and 30/70 at 5 pphr SEBS inclusion. However, the increased tensile strength is not very significant compared with the uncompatibilized blends. It is possibly claimed that the SEBS triblock polymer can, nevertheless, enhance somewhat interfacial adhesion of phase boundaries between two polymers. In 10/90 HIPS/HDPE blend, addition of SEBS shows an inferior property at all SEBS concentrations. The HDPE matrix can hardly accept the SEBS block to compatibilize with HIPS.

The another tensile property of elongation at break yields striking results. For the neat HIPS or HDPE, HDPE gives 300% higher in elongation at break. The uncompatibilized blends (HIPS/HDPE) of 90/10, 70/30 and 50/50 ratios yield the lower values when decreasing the concentrations of HIPS. This observation is inevitable because HIPS is hard, brittle polymer, which cannot miscible in the HDPE matrix. The elongation at break for these blend ratios illustrates the result of poor dispersibility of HIPS domain in the HDPE matrix polymer. When the blend ratios of HIPS/HDPE are 30/70 and 10/90, the elongation at break of the blends shows the effect of the HDPE matrix polymer. Basically, HDPE is a low modulus, ductile material with some degree of crystallinity. These blends, however, still indicate the influence of HIPS since the elongation at break is still lower than that of neat HDPE.

For the compatibilized blends, elongation at break increases with increasing SEBS concentrations. Very interesting results are obtained at high SEBS concentrations, which are incorporated in 30/70 and 10/90 blend ratios of HIPS/HDPE. The blends of 30/70 and 10/90 HIPS/HDPE with 15 to 20 pphr SEBS behave like a rubber-like material, because the elongation at break is as high as 400 – 500%, similar to that of rubber. Our results in elongation at break are similar to work of Tjong and Xu [21] and Chen et al. [23]. Tjong and Xu reported earlier that the aPS/HDPE blends compatibilized with SEBS triblock copolymer showed the major influence of HDPE matrix. Chen et al. gave the same results when sPS/HDPE blends were compatibilized by various types of block copolymer.

4.4.3 Flexural strength of HIPS/HDPE blends

The flexural strength of all HIPS/HDPE blend ratios, either compatibilized or not does not show any improvement in properties. The very striking negative results were observed. Increasing the SEBS concentrations reduced the flexural strength compared with the neat HIPS or HDPE with a compatibilizer of SEBS.

Table 4.3 Mechanical properties of HIPS/HDPE blends with various SEBS block copolymer concentrations

HIPS/HDPE	SEBS pphr	Izod impact Strength (J m ⁻¹)	Tensile strength (MPa)	Elongation at break (%)	Flexural strength (MPa)
100/0	0	95.2 ± 1.37	21.3 ± 0.22	50.0 ± 4.30	36.7 ± 0.24
0/100	0	71.2 ± 1.04	25.5 ± 0.21	161.2 ± 5.07	24.9 ± 0.08
90/10	0	39.0 ± 2.34	18.8 ± 0.23	40.6 ± 1.95	32.7 ± 0.14
	5	93.4 ± 0.82	19.6 ± 0.31	71.2 ± 2.59	35.5 ± 0.20
	10	138.7 ± 1.64	17.5 ± 0.21	98.4 ± 3.05	31.5 ± 0.11
	15	164.4 ± 1.49	16.9 ± 0.21	117.0 ± 2.55	29.0 ± 0.36
	20	204.6 ± 0.88	16.5 ± 0.21	135.0 ± 2.24	27.9 ± 0.09
70/30	0	19.2 ± 0.88	17.4 ± 0.13	12.4 ± 1.14	29.8 ± 0.00
	5	42.2 ± 1.55	18.0 ± 0.05	73.4 ± 2.51	30.3 ± 0.10
	10	70.2 ± 1.12	18.4 ± 0.15	115.4 ± 3.58	28.6 ± 0.13
	15	108.5 ± 3.15	17.8 ± 0.08	141.2 ± 2.59	27.0 ± 0.09
	20	166.6 ± 1.28	17.1 ± 0.05	174.6 ± 1.67	25.3 ± 0.08
50/50	0	14.9 ± 0.44	17.9 ± 0.08	9.80 ± 0.45	27.3 ± 0.18
	5	30.2 ± 1.75	20.4 ± 0.05	88.8 ± 3.03	25.9 ± 0.08
	10	49.1 ± 0.69	19.1 ± 0.10	123.2 ± 2.17	23.5 ± 0.16
	15	94.4 ± 3.06	17.7 ± 0.11	186.2 ± 3.03	21.3 ± 0.27
	20	130.3 ± 3.36	17.1 ± 0.07	254.6 ± 2.79	19.7 ± 0.16
30/70	0	19.4 ± 0.44	18.7 ± 0.16	95.4 ± 3.97	23.9 ± 0.11
	5	40.8 ± 1.49	19.1 ± 0.09	128.4 ± 2.30	21.8 ± 0.07
	10	74.4 ± 1.61	17.2 ± 0.05	198.2 ± 2.86	19.3 ± 0.14
	15	142.3 ± 2.86	15.6 ± 0.11	274.2 ± 3.19	17.5 ± 0.07
	20	518.2 ± 38.48	14.6 ± 0.49	425.4 ± 7.13	15.8 ± 0.11
10/90	0	32.0 ± 0.54	19.5 ± 0.08	105.6 ± 5.73	20.9 ± 0.15
	5	67.7 ± 6.32	18.3 ± 0.04	141.6 ± 3.05	17.9 ± 0.08
	10	254.5 ± 54.41	16.3 ± 0.05	239.6 ± 4.83	15.3 ± 0.18
	15	NA	14.8 ± 0.11	407.0 ± 6.63	13.8 ± 0.05
	20	NA	13.8 ± 0.05	472.0 ± 5.34	12.7 ± 0.07

NA = No available data because the specimens were not broken.

Number of mechanical testing is 5.

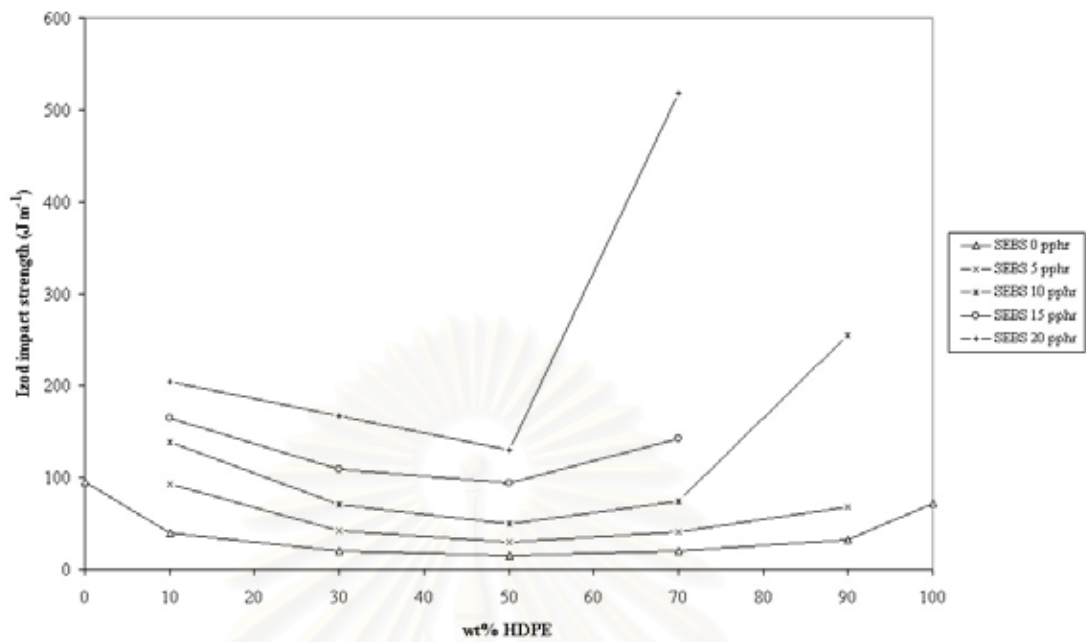


Figure 4.25 Izod impact strength of HIPS/HDPE blends with various SEBS concentrations

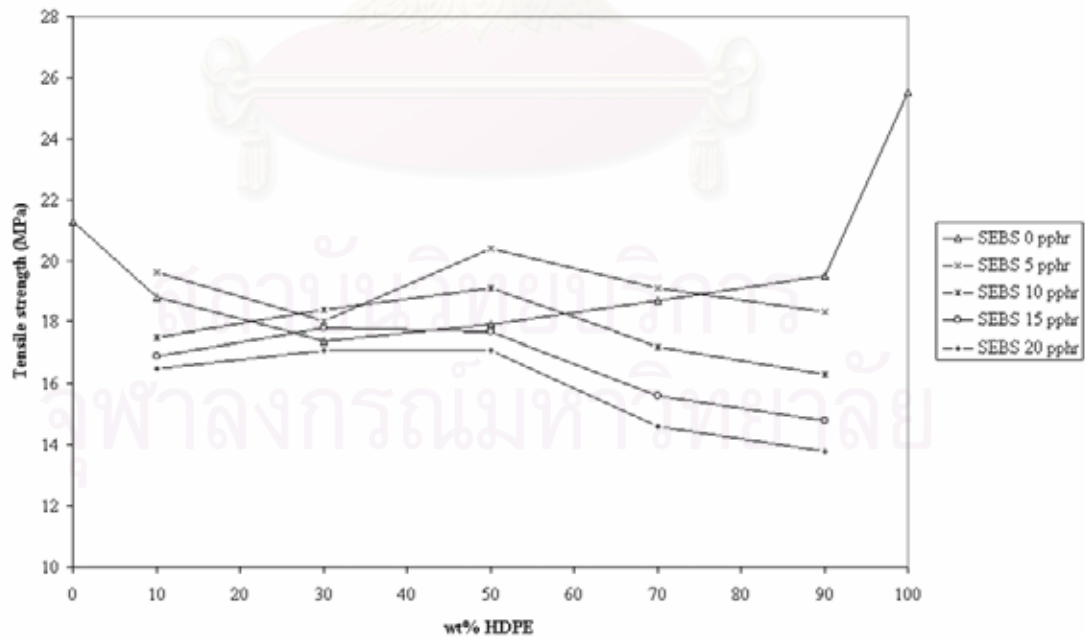


Figure 4.26 Tensile strength of HIPS/HDPE blends with various SEBS concentrations

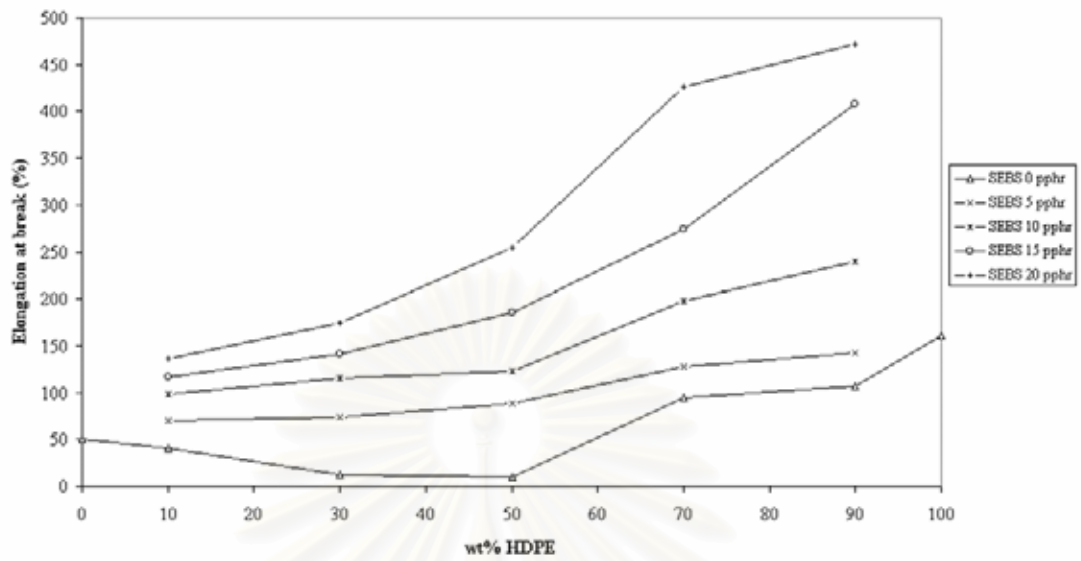


Figure 4.27 Elongation at break of HIPS/HDPE blends with various SEBS concentrations

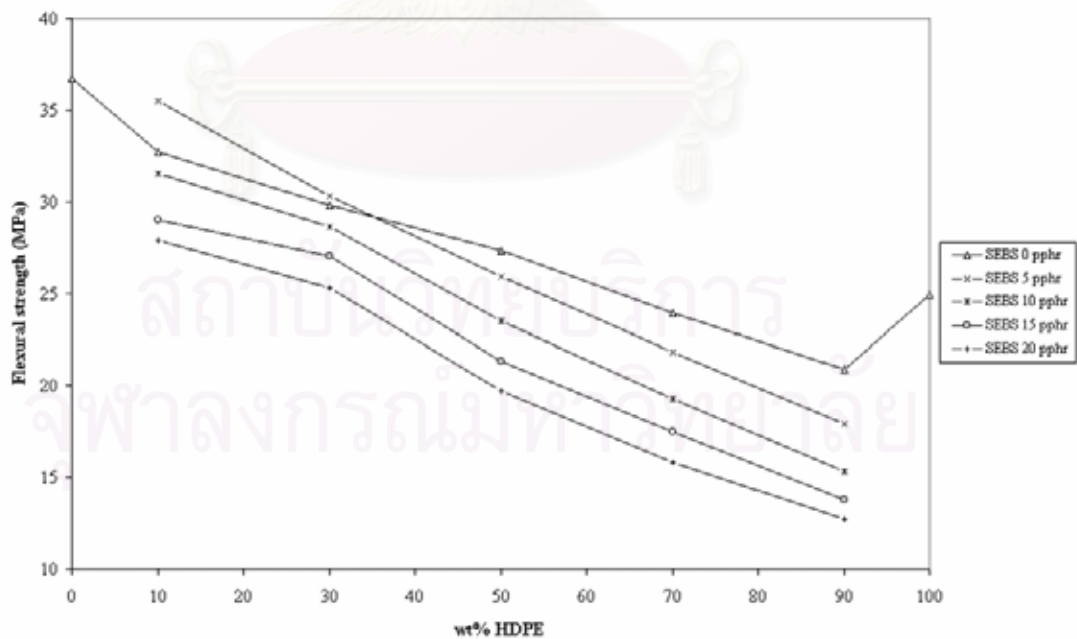


Figure 4.28 Flexural strength of HIPS/HDPE blends with various SEBS concentrations

4.5 Phase separation investigation by pulsed NMR

The spin-spin relaxation time (T_2) is mostly employed to obtain the information on a system where small domains of low molecular mobility are dispersed since spin diffusion often loses the information in the measurements of the spin-lattice relaxation time (T_1) and the spin-lattice relaxation time in the rotating frame ($T_{1\rho}$). In addition, T_2 reflects the mobility of molecules directly and we can get information on the temporal change of mobility from the real-time measurement of T_2 .

Furthermore, we can get information on the degree of heterogeneity from the difference in mobility and the temporal change of the both fraction and T_2 values.

The signals of pulsed NMR for the heterogeneous system of HIPS/HDPE blends, which is compatibilized by SEBS can be obtained from the mobility and fractional amount of each phase by decomposing the NMR signals.

Table 4.4 The results of T_2 and the fractional amount of HIPS/HDPE blends

HIPS/HDPE (wt%/wt%)	SEBS pphr	T_2A_f -	T_2B_f -	T_2A (s)	T_2B (s)
10/90	0	7.17E-01	2.83E-01	7.47E-06	3.34E-05
	5	7.16E-01	2.84E-01	7.46E-06	4.13E-05
	20	7.16E-01	2.84E-01	7.79E-06	6.51E-05
90/10	0	9.00E-01	9.95E-02	1.05E-05	7.47E-05
	5	8.78E-01	1.22E-01	1.07E-05	1.35E-04

Where T_2A_f = fractional amount of HIPS component in the blend

T_2B_f = fractional amount of HDPE component in the blend

T_2A = temporal change of T_2 of HIPS component in the blend

T_2B = temporal change of T_2 of HDPE component in the blend

Table 4.4 and Figures 4.29 - 4.30 are results in terms of the pulsed $^1\text{H-NMR}$ measurement at room temperature and resonance at 20 MHz, temporal change of T_2 and the fractional amount (f) for HIPS (A) and HDPE (B), are shown respectively. There are two T_2 's found in each blend ratio. The shorter T_2 is usually related to glassy or crystalline phase and the longer T_2 is usually related to rubbery phase, in which the crystalline polystyrene phase in HIPS, crystalline phase of HDPE and the hard segment of SEBS correspond to the short T_2 component. In other words, the rubbery phase in HIPS, the amorphous phase in HDPE and the soft segment of SEBS correspond to longer T_2 component [31-33]. The suppression of mobility of crystalline polymer likes HDPE component in the blends is attributed to the perfection of the crystalline structure that crystals with fewer defects inside have lower mobility, and they also suppress the mobility at the interface, which are responded in short T_2 that can be seen in Figures 4.29A to 4.29B, the value of T_{2B} for the HDPE component is almost constant in both acting as the major phase (HIPS/HDPE = 10/90) and the minor phase (HIPS/HDPE = 90/10).

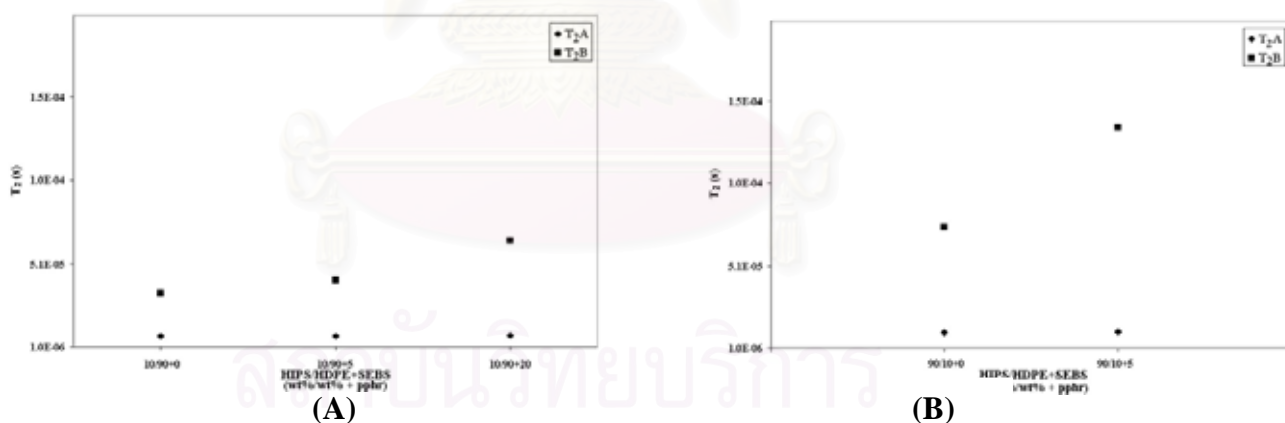


Figure 4.29 Dependence of T_2 of HIPS and HDPE phase in the blends;

(A) HIPS/HDPE = 10/90 and (B) HIPS/HDPE = 90/10

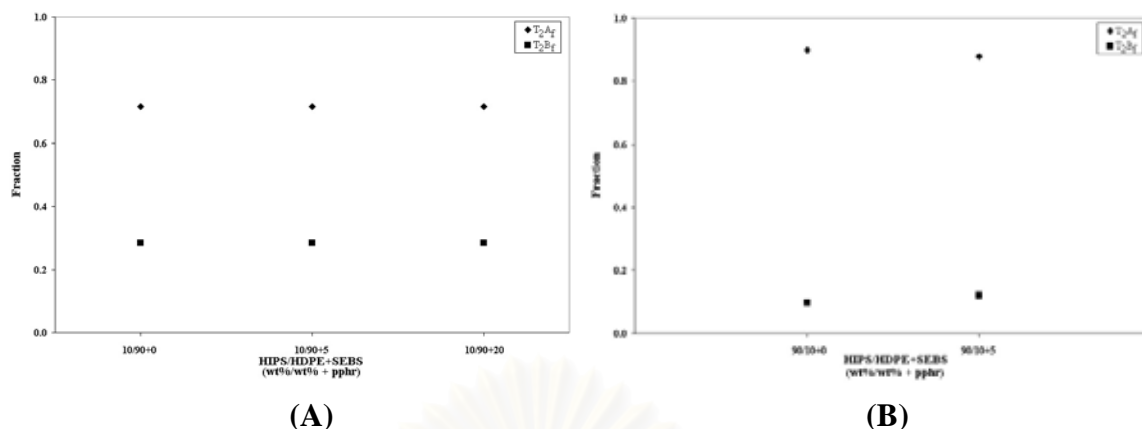


Figure 4.30 Dependence of fractional amount of HIPS and HDPE phase in the blends; (A) HIPS/HDPE = 10/90 and (B) HIPS/HDPE = 90/10

In case of HIPS, HIPS is acting as the amorphous component in the blends that consists of the relatively mobile amorphous domains outside the spherulites and relatively immobile interlamellar amorphous chains constrained by the lamellae [33]. From Figures 4.29A to 4.29B, we found that the T_2A of the amorphous component slightly increases with the SEBS component in the amorphous minor phase and sharply increases when the amorphous component becomes the major phase. There are some changes in molecular structure between two of HIPS and HDPE, which had better interfacial adhesion by the incorporating the segment of SEBS, and lead to increases in T_2A of each blend ratio by increasing the interfacial agent like SEBS. For HDPE-rich phase system (HIPS/HDPE = 10/90) both T_2A_f and T_2B_f stabilized regardless of the increasing amount of SEBS added as shown in Figure 4.30A. The increase in T_2B_f and decrease of T_2A_f take place in HIPS-rich phase (HIPS/HDPE = 90/10) shown in Figure 4.30B when increasing SEBS component is added to give growth of the crystals by incorporating the amorphous chains of SEBS with more interfacial adhesion between two phases.

CHAPTER V

CONCLUSION AND SUGGESTION FOR FURTHER WORK

5.1 Conclusion

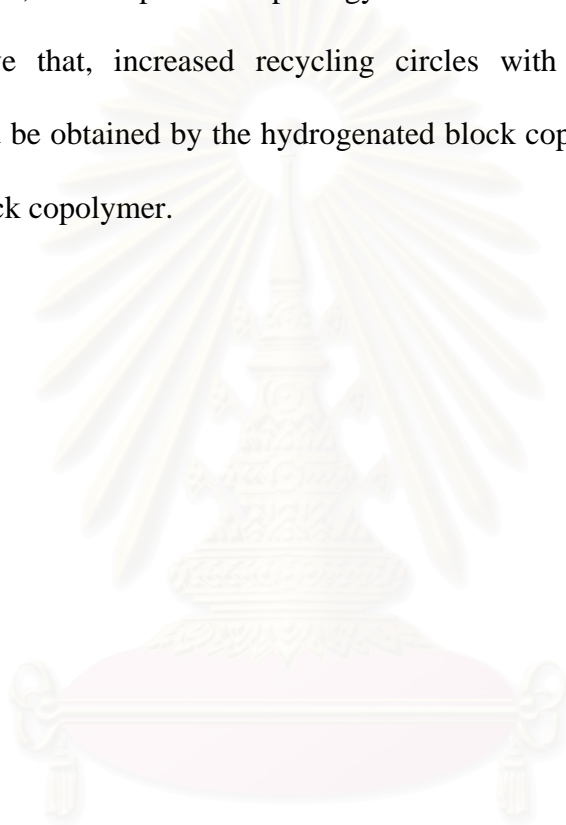
HIPS and HDPE are, basically, the incompatible blend. The SEBS triblock copolymer, which contains 70 wt% of a random copolymer ethylene-butylene, and 30 wt% of styrene, can be used to solve the problem of incompatibility of HIPS/HDPE blends. The role of SEBS triblock copolymer are found, in this work, an interfacial agent and impact modifier to provide the better interfacial adhesion between HIPS and HDPE.

The compatibilizing effect in the industrial applications of HIPS/HDPE blends by SEBS on the mechanical properties was found. The impact strength and elongation at break of the blends were improved by increasing the SEBS content, and sharply increased when HDPE became the major phase or when the HDPE content in the blends were more than 50 wt%. In case of the tensile strength, its values were also improved when the compatibilizer loading was below 5 pphr; if the compatibilizer loading was higher than 5 pphr, its tensile strength decreased and more decrease was found in the HDPE-rich phase. The addition of SEBS compatibilizer could not improve the flexural strength. One has to be in mind that, for a specific piece of properly blended HIPS/HDPE, increases in impact strength is accompanied by the loss of tensile strength and flexural strength.

On evaluation of compatibility, the log additivity rule model is applied to the shear viscosity data from the capillary rheometer for compatibility study of HIPS/HDPE blends by the SEBS block copolymer. The positive deviation behavior was observed at high shear rates for the HIPS-rich phase and at low shear rates for the HDPE-rich phase. At the higher SEBS contents, every blend is more compatible than the uncompatibilized blends. The pseudoplastic behavior (shear-thinning) was observed for every blend ratio. Morphology of the blends was improved by inclusion of the SEBS block copolymer. The SEBS could reduce the dispersed phase particles, which produced more uniform dispersions and finer particles to form the co-continuous phase of the blends. The extent of phase compatibility depends on the blend condition i.e. blend composition, viscosity ratio of blends, mixing time, and compatibilizer loading. Glass transition temperature and melting temperature from DSC measurement were close to those of the base resin. Such a result implied no miscibility at the molecular level of these blends compatibilized by the SEBS block copolymer. Nevertheless, the interfacial adhesion between two phases was improved. The relaxation time by pulsed NMR measurement confirmed the extent of compatibility between HIPS/HDPE blends compatibilized by SEBS. There are two T_2 's found in each blend ratio. The value of T_2 of HDPE component was almost constant in both blends acting as the major phase (HIPS/HDPE = 10/90) and the minor phase (HIPS/HDPE = 10/90). The T_2 of the amorphous component slightly increased with the SEBS component. The better interfacial adhesion achievable by incorporating the SEBS led to increases of T_2 in each blend. We could then conclude that increasing interfacial agent of SEBS provides the better interfacial adhesion between two phases.

5.2 Suggestion for further work

To enhance a better interfacial adhesion, a dual compatibilizer, which is a combination of hydrogenated diblock and hydrogenated triblock copolymers should be pursued. For instance, poly(styrene/ethylene-propylene) or SEP coupled with SEBS could be used to compatibilize HIPS and HDPE blends to improved the impact strength by SEBS, and the phase morphology with finer and more uniform dispersions by SEP. Above that, increased recycling circles with more thermal oxidative resistance could be obtained by the hydrogenated block copolymer rather than by the unsaturated block copolymer.



สถาบันวิทยบริการ
จุฬาลงกรณ์มหาวิทยาลัย

REFERENCES

1. Olabisi, O., Roberson, L.M., Shaw, M.T. Polymer-polymer miscibility. New York: Academic Press, 1979, pp. 1-17.
2. Paul, D.R., Newman, S. Polymer blends. Vol. 2. New York: Academic Press, 1978, pp. 35-62.
3. Folkes, M.J., and Hope, P.S. Polymer blends and alloys. New York: Blackie Academic & Professional, 1993, pp. 46-74.
4. Park, C.P., Clingerman, G.P., Timmers, F.J. and Stevens, J.C. Compatibilized blend of olefinic polymers and monovinylidene aromatic polymers. U.S. Patent 5,460,818, 1995.
5. Utracki, L.A., Polymer alloys and blends: Thermodynamics and rheology. Munich: Hanser, 1989, pp. 147-171.
6. Fayt, R., Hadjiandreou, P. and Teyssie, P. Immiscible polymer blends[Online]. 1998. Available from:
<http://www.psrc.usm.edu/macrog/iblend.htm> [2001, October 25]
7. Paul, D.R., Bucknall, C.B. Polymer blends. Vol. 1. New York: Academic Press, 1999, pp. 461-499.
8. Olabisi, O., Roberson, L.M., Shaw, M.T. Polymer-polymer miscibility. New York: Academic Press, 1979, pp. 277-281.
9. Švec, P., Rosík, L., Horák, R.Z., and Večerka, F. Styrene-based plastics and their modification. West Sussex: Ellis Horwood, 1989, pp. 130-145.
10. Billmeyer, F.W. Textbook of polymer science. 3rd ed. New York: John Wiley & Sons. 1984, pp. 361-368.

11. Shell Chemicals Company. Kraton™ polymers processing guide[Online]. 1998.
Available from: <http://www.shellchemicals.com> [2001, June 25]
12. Sperling, L.H., Introduction to physical polymer science. 2nd ed. New York: John Wiley & Sons. 1992, pp. 437-438.
13. Fayt, R., and Teyssié, P. Molecular design of multicomponent polymer systems. XVIII: Emulsification of high-impact polystyrene and low-density polyethylene blends into high-impact alloys. Polym. Eng. Sci. 30(1990): 937-943.
14. Guo, H.F., Packirisamy, S., Mani, R.S., Aronson, C.L., Gvozdic, N.V., and Meier, D.J. Compatibilizing effects of block copolymers in low-density polyethylene/polystyrene blends. Polym. Eng. Sci. 39(1998): 2495-2505.
15. Taha, M., and Frerejean, V. Morphology development of LDPE-PS blend compatibilization. J. Appl. Polym. Sci. 61(1996): 969-979.
16. Fortelný, I., Michálková, D., Hromádková, J., and Lednický, F. Effect of a styrene-butadiene copolymer on the phase structure and impact strength of polyethylene/high-impact polystyrene blends. J. Appl. Polym. Sci. 81(2001): 570-580.
17. Li, T., Topolkaev, V.A., Hiltner, A., Baer, E., Ji, X.Z., and Quirk, R.P. Block copolymers as compatibilizers for blends of linear low density polyethylene and polystyrene. J. Polym. Sci., Part B: Polym. Phys. 33(1995): 667-683.

18. Harrats, C., Fayt, R., and Jérôme, R. Effect of block copolymers of various molecular architecture on the phase morphology and tensile properties of LDPE rich (LDPE/PS) blends. Polymer. 43(2002): 863-873.
19. Bourry, D., and Favis, B.D. Cocontinuity and phase inversion in HDPE/PS blends: Influence of interfacial modification and elasticity. J. Polym. Sci., Part B: Polym. Phys. 36(1998): 1889-1899.
20. Lindsey, C.R., Paul, D.R., and Barlow, J.W. Mechanical properties of HDPE-PS-SEBS blends. J. Appl. Polym. Sci. 26(1981): 1-8.
21. Tjong, S.C., and Xu, S.A. Impact and tensile properties of SEBS copolymer compatibilized PS/HDPE blends. J. Appl. Polym. Sci. 68(1998): 1099-1108.
22. Bureau, M.N., Kadi, H.E., Denault, J., and Dickson, J.I. Injection and compression molding of polystyrene/high-density polyethylene blends-phase morphology and tensile behavior. Polym. Eng. Sci. 37(1997): 377-390.
23. Chen, B., Li, X., Xu, S., Tang, T., Zhou, B., and Huang, B. Compatibilization effects of block copolymers in high density polyethylene/syndiotactic polystyrene blends. Polymer. 43(2002): 953-961.
24. Oommen, Z., Thomas, S., Premalatha, C.K., and Kuriakose, B. Melt rheological behaviour of natural rubber/poly(methyl methacrylate)/natural rubber-g-poly(methyl methacrylate) blends. Polymer. 38(1997): 5611-5621.

25. George, S., Ramamurthy, K., Anand, J.S., Groeninckx, G., Varughese, K.T., and Thomas, S. Rheological behaviour of thermoplastic elastomers from polypropylene/acrylonitrile-butadiene rubber blends: effect of blend ratio, reactive compatibilization and dynamic vulcanization. Polymer. 40(1999): 4325-4344.
26. George, J., Ramamurthy, K., Varughese, K.T., and Thomas, S. Melt rheology and morphology of thermoplastic elastomers from polyethylene/nitrile-rubber blends: the effect of blend ratio, reactive compatibilization, and dynamic vulcanization. J. Polym. Sci., Part B: Polym. Phys. 38(2000): 1104-1122.
27. Macaúbas, P.H.P. and Demarquette, N.R. Morphologies and interfacial tensions of immiscible polypropylene/polystyrene blends modified with triblock copolymers. Polymer. 42(2001): 2543-2554.
28. Paul, D.R., Bucknall, C.B. Polymer blends. Vol. 1, New York: Academic Press, 1999, p. 509.
29. Thomas, S. and Prud'homme, R.E. Compatibilizing effect of block copolymers in heterogeneous polystyrene/poly(methyl methacrylate) blends. Polymer. 33(1992): 4260-4268.
30. Paul, D.R., Newman, S. Polymer blends. Vol. 2. New York: Academic Press, 1978, p. 48.
31. Tanaka, H. and Nishi, T. Real-time pulsed nuclear magnetic resonance measurement system for the study of nonequilibrium phenomena in polymers. J. Appl. Phys. 60(1986): 1306-1309.

32. Ikehara, T. and Nishi, T. Pre-ordering state in crystallization process of polymer blends detected by pulsed NMR. Acta Polymer. 46(1995): 416-419.
33. Ikehara, T. and Nishi, T. Primary and secondary crystallization process of poly(ϵ -caprolactone)/styrene oligomer blends investigated by pulsed NMR. Polymer. 41(2000): 7855-7864.



สถาบันวิทยบริการ
จุฬาลงกรณ์มหาวิทยาลัย



APPENDICES

สถาบันวิทยบริการ
จุฬาลงกรณ์มหาวิทยาลัย

APPENDIX A

Rheological data of HIPS/HDPE blends with SEBS block copolymer

Table A-1 Rheological data of HIPS, HDPE and SEBS

Shear rate (s ⁻¹)	Shear stress (Pa)			Shear viscosity (Pa s)		
	HIPS	HDPE	SEBS	HIPS	HDPE	SEBS
20	40123	18466	109986	2006.360	923.395	5499.870
50	52868	35496	183969	1057.330	709.915	3679.310
150	81399	77267	319304	542.662	515.114	2128.700
250	97011	98032	386800	388.046	392.128	1547.200
450	115765	145151	454534	257.255	322.559	1010.080
600	126957	172144	499182	211.594	286.906	831.970
800	145227	196732	524362	181.532	245.912	655.444
950	149882	215659	558656	157.769	227.007	588.053
1500	169129	263448	636955	112.753	175.632	424.637
2500	202070	319646	724349	80.829	127.859	289.741
3500	224614	363061	766376	64.174	103.729	218.958
4500	248403	391125	794437	55.201	86.917	176.542
6500	286619	441623	822869	44.095	67.941	126.593
7500	306979	439700	831778	40.931	58.627	110.904
8500	317418	444515	836042	37.344	52.297	98.359
9000	318632	449035	837152	35.404	49.893	93.017

Table A-6 Rheological data of HIPS/HDPE (10/90) blends with SEBS

Shear rate (s ⁻¹)	Shear stress (Pa)					Shear viscosity (Pa s)				
	0 pphr	5 pphr	10 pphr	15 pphr	20 pphr	0 pphr	5 pphr	10 pphr	15 pphr	20 pphr
20	12655	15738	23417	31096	33890	632.799	786.984	1170.957	1554.940	1694.660
50	29932	35644	46846	48977	50284	598.632	712.863	936.896	979.529	1005.670
150	79455	94158	98119	104192	96207	529.702	627.717	654.123	694.616	641.380
250	110630	118198	130389	142168	146490	442.523	472.796	521.557	568.676	585.964
450	151591	154703	176428	178532	179670	336.868	343.786	392.062	396.738	399.267
600	179379	185912	206492	204138	216856	298.965	309.853	344.154	340.229	361.426
800	208731	217907	232615	227476	248299	260.910	272.381	290.765	284.342	310.369
950	220671	233501	251843	250616	264822	232.283	245.788	265.096	263.803	278.758
1500	265075	285337	302093	302159	314995	176.717	190.225	201.395	201.439	209.997
2500	318470	339102	354299	358159	370256	127.388	135.641	141.720	143.264	148.103
3500	362677	380264	391931	399065	415594	103.619	108.644	111.977	114.015	118.738
4500	387595	413448	426338	436620	450693	86.132	91.877	94.742	97.027	100.154
6500	422179	437512	451209	453436	461073	64.950	67.309	69.416	69.758	70.933
7500	423697	444662	453723	456665	468357	56.493	59.288	60.496	60.889	62.448
8500	429226	451612	463031	472644	486616	50.498	53.132	54.475	55.606	57.250
9000	434506	456188	473387	485350	492267	48.278	50.688	52.599	53.928	54.696

Table A-5 Rheological data of HIPS/HDPE (30/70) blends with SEBS

Shear rate (s ⁻¹)	Shear stress (Pa)					Shear viscosity (Pa s)				
	0 pphr	5 pphr	10 pphr	15 pphr	20 pphr	0 pphr	5 pphr	10 pphr	15 pphr	20 pphr
20	15337	18490	23304	28118	32657	766.938	924.597	1165.324	1406.050	1633.010
50	35367	47410	48233	47642	50683	707.330	948.177	964.645	952.820	1013.640
150	82416	82944	84476	85960	98297	549.439	552.960	563.175	573.065	655.312
250	104811	115895	115029	118694	127499	419.245	463.580	460.120	474.779	510.000
450	137747	134480	151006	155199	164277	306.105	298.845	335.569	344.887	365.060
600	157336	169583	178101	182008	184626	262.227	282.638	296.835	303.347	307.711
800	183320	185935	194778	213333	218152	229.147	232.415	243.469	266.663	272.687
950	194941	197891	216721	226405	231543	205.199	208.304	228.125	238.318	243.727
1500	238221	249019	256888	272110	277177	158.814	166.013	171.259	181.407	184.784
2500	284705	301185	317751	323570	330502	113.882	120.475	127.101	129.429	132.201
3500	325747	332549	354758	371562	375840	93.068	95.011	101.356	106.157	107.380
4500	364231	370206	389123	408092	415309	80.940	82.268	86.472	90.687	92.291
6500	418541	426214	453965	466087	481989	64.390	65.570	69.840	71.705	74.151
7500	438181	452062	477460	491080	502840	58.424	60.275	63.661	65.477	67.045
8500	453541	464664	489831	505057	518963	53.358	54.667	57.628	59.419	61.055
9000	462724	477418	501316	517041	523215	51.414	53.046	55.702	57.449	58.135

Table A-4 Rheological data of HIPS/HDPE (50/50) blends with SEBS

Shear rate (s ⁻¹)	Shear stress (Pa)					Shear viscosity (Pa s)				
	0 pphr	5 pphr	10 pphr	15 pphr	20 pphr	0 pphr	5 pphr	10 pphr	15 pphr	20 pphr
20	25742	26652	29758	30086	32014	1287.240	1332.750	1488.050	1504.440	1600.870
50	45248	45605	46117	49666	52639	904.945	912.080	922.313	993.297	1052.760
150	81049	83839	88068	94381	87515	540.327	558.928	587.118	629.207	583.435
250	98761	105695	116610	118167	121102	395.047	422.784	466.444	472.671	484.410
450	127406	137355	148385	149470	153619	283.124	305.233	329.745	332.155	341.376
600	150042	152954	167650	171197	177634	250.069	254.923	279.417	285.329	296.057
800	171026	174529	185612	189541	196242	213.780	218.158	232.013	236.923	245.300
950	178885	184963	196054	201610	213013	188.298	194.696	206.371	212.219	224.222
1500	219917	222467	235602	247721	247963	146.611	148.311	157.068	165.147	165.309
2500	260387	269039	287712	299587	305149	104.155	107.616	115.085	119.835	122.060
3500	293221	314059	327166	338843	344297	83.775	89.729	93.473	96.810	98.368
4500	316997	349851	367812	370151	371561	70.444	77.745	81.736	82.256	82.569
6500	380688	396493	419743	426326	437547	58.567	60.998	64.575	65.588	67.314
7500	398087	419216	444139	454524	456791	53.078	55.895	59.219	60.603	60.906
8500	417398	434499	453531	473743	468444	49.106	51.118	53.357	55.735	55.112
9000	423922	444790	464228	484847	490426	47.102	49.421	51.581	53.872	54.492

Table A-3 Rheological data of HIPS/HDPE (70/30) blends with SEBS

Shear rate (s ⁻¹)	Shear stress (Pa)					Shear viscosity (Pa s)				
	0 pphr	5 pphr	10 pphr	15 pphr	20 pphr	0 pphr	5 pphr	10 pphr	15 pphr	20 pphr
20	27288	30263	30668	35191	35328	1364.556	1513.290	1533.540	1759.710	1766.570
50	48013	49282	47840	49611	52536	960.238	985.628	956.778	992.207	1050.690
150	80336	80129	81760	83338	84419	535.575	534.194	545.065	555.585	562.794
250	98109	95600	103189	106839	112695	392.437	382.402	412.756	427.356	450.782
450	121207	118675	127514	139808	145514	269.348	263.723	283.365	310.684	323.365
600	137420	142998	149679	153305	162154	229.034	238.331	249.465	255.509	270.256
800	155529	153022	167675	171546	182504	194.409	191.276	209.591	214.429	228.128
950	168752	167312	180226	185700	187331	177.632	176.116	189.710	195.472	197.188
1500	195484	197845	213637	219897	227929	130.323	131.897	142.425	146.598	151.953
2500	228034	244452	254181	263635	276484	91.214	97.781	101.673	105.454	110.594
3500	255349	272295	289012	293090	308519	72.955	77.796	82.573	83.738	88.146
4500	290980	305512	314146	322149	338290	64.662	67.892	69.810	71.589	75.176
6500	331003	354616	378683	385086	398810	50.923	54.556	58.258	59.243	61.355
7500	351774	382527	398343	417089	428975	46.903	51.004	53.112	55.612	57.197
8500	368549	388712	416619	434456	445331	43.359	45.731	49.015	51.113	52.393
9000	377286	394639	423096	438614	453574	41.921	43.849	47.011	48.735	50.397

Table A-2 Rheological data of HIPS/HDPE (90/10) blends with SEBS

Shear rate (s ⁻¹)	Shear stress (Pa)					Shear viscosity (Pa s)				
	0 pphr	5 pphr	10 pphr	15 pphr	20 pphr	0 pphr	5 pphr	10 pphr	15 pphr	20 pphr
20	28835	30768	32074	34738	35101	1441.870	1538.530	1603.870	1737.090	1755.240
50	46369	46656	48275	49782	51127	927.361	933.102	965.481	995.627	1022.510
150	75681	76404	81715	83954	80496	504.540	509.358	544.768	559.691	536.643
250	88551	94573	97292	99468	100647	354.206	378.292	389.169	397.874	402.591
450	113459	117518	119738	121866	123622	252.131	261.151	266.084	270.813	274.715
600	123580	130803	139317	146500	147162	205.967	218.005	232.196	244.167	245.269
800	139399	150095	150292	158628	164455	174.247	187.617	187.863	198.282	205.567
950	146169	162663	164656	168755	175211	153.861	171.222	173.320	177.635	184.431
1500	169849	185493	192907	196550	203468	113.233	123.662	128.605	131.034	135.645
2500	198102	219650	231121	237182	243500	79.241	87.860	92.449	94.873	97.400
3500	223069	247087	257621	266255	279131	63.732	70.594	73.604	76.071	79.750
4500	248612	278415	286931	304007	310546	55.247	61.870	63.762	67.557	69.010
6500	297967	322492	349115	351545	360107	45.840	49.613	53.709	54.083	55.400
7500	311148	347861	367250	377337	382016	41.486	46.382	48.967	50.312	50.936
8500	316396	360723	378077	386543	392932	37.224	42.439	44.480	45.476	46.228
9000	324908	365725	387593	390307	398961	36.101	40.636	43.066	43.368	44.329

APPENDIX B

Mechanical properties of HIPS/HDPE blends

Table B-1 Izod impact strength of HIPS/HDPE blends

HIPS/HDPE	SEBS (pphr)	Izod impact strength (J m^{-1})					X	SD	% Variation
		1 st	2 nd	3 rd	4 th	5 th			
100/0	0	94.2	94.2	96.1	94.2	97.1	95.2	1.37	1.44
0/100	0	71.2	72.8	71.5	70.1	70.6	71.2	1.04	1.46
90/10	0	40.2	39.2	42.2	37.3	36.3	39.0	2.34	5.99
	5	93.2	92.2	93.2	94.2	94.2	93.4	0.82	0.88
	10	137.3	138.3	139.3	141.3	137.3	138.7	1.64	1.18
	15	165.8	164.8	164.8	164.8	161.9	164.4	1.49	0.91
	20	204.0	205.0	206.0	204.0	204.0	204.6	0.88	0.43
70/30	0	19.6	19.6	16.9	17.7	19.6	19.2	0.88	4.58
	5	43.2	41.2	42.2	40.2	44.1	42.2	1.55	3.67
	10	71.6	70.6	70.6	68.7	69.7	70.2	1.12	1.59
	15	104.0	108.9	106.9	111.8	110.9	108.5	3.15	2.90
	20	168.7	165.8	165.8	165.8	166.8	166.6	1.28	0.76
50/50	0	14.7	14.7	15.7	14.7	14.7	14.9	0.44	2.95
	5	32.4	31.4	28.4	30.4	28.4	30.2	1.75	5.79
	10	49.1	48.1	49.1	50.0	49.1	49.1	0.69	1.41
	15	97.1	91.2	92.2	98.1	93.2	94.4	3.06	3.24
	20	134.4	127.5	128.5	127.5	133.4	130.3	3.36	2.58

จุฬาลงกรณ์มหาวิทยาลัย

Table B-1 Izod impact strength of HIPS/HDPE blends (continued)

HIPS/HDPE	SEBS (pphr)	Izod impact strength (J m^{-1})					X	SD	% Variation
		1 st	2 nd	3 rd	4 th	5 th			
30/70	0	18.6	19.6	20.6	18.6	19.6	19.4	0.44	4.23
	5	39.2	41.2	42.2	42.2	39.2	40.8	1.49	3.65
	10	72.6	73.6	73.6	76.5	75.5	74.4	1.61	2.16
	15	141.3	143.2	138.3	142.2	146.2	142.3	2.86	2.01
	20	586.6	504.2	499.3	505.2	495.4	518.2	38.48	7.43
10/90	0	31.4	31.4	32.4	32.4	32.4	32.0	0.54	1.69
	5	57.9	71.6	74.6	66.7	67.7	67.7	6.32	9.34
	10	294.3	324.7	215.8	216.8	220.7	254.5	51.41	20.20
	15	NB	NB	NB	NB	NB	-	-	-
	20	NB	NB	NB	NB	NB	-	-	-

NB = *non-break*; an incomplete break where the fracture extends less than 90% of distance between the vertex of notch and the opposite side.

Table B-2 Tensile strength of HIPS/HDPE blends

HIPS/HDPE	SEBS (pphr)	Tensile Strength (MPa)					X	SD	% Variation
		1 st	2 nd	3 rd	4 th	5 th			
100/0	0	21.0	21.2	21.4	21.5	21.5	21.3	0.22	1.03
0/100	0	25.4	25.2	25.7	25.8	25.6	25.5	0.21	0.82
90/10	0	18.7	19.0	18.9	18.4	18.8	18.8	0.23	1.22
	5	19.1	19.9	19.4	19.7	19.7	19.6	0.31	1.58
	10	17.2	17.6	17.8	17.6	17.6	17.5	0.21	1.20
	15	17.3	16.9	16.9	16.9	16.7	16.9	0.21	1.24
	20	16.5	16.7	16.2	16.7	16.7	16.5	0.21	1.27
70/30	0	17.6	17.4	17.3	17.5	17.3	17.4	0.13	0.75
	5	18.0	17.9	17.9	17.9	18.0	18.0	0.05	0.28
	10	18.5	18.4	18.3	18.3	18.1	18.4	0.15	0.82
	15	17.8	17.8	17.8	17.8	17.9	17.8	0.08	0.45
	20	17.2	17.2	17.1	17.2	17.1	17.1	0.05	0.29
50/50	0	17.9	17.8	18.0	17.9	17.8	17.9	0.08	0.45
	5	20.4	20.5	20.5	20.4	20.4	20.4	0.05	0.25
	10	19.2	19.1	19.0	19.0	19.2	19.1	0.10	0.52
	15	17.7	17.7	17.8	17.6	17.7	17.7	0.11	0.62
	20	17.1	17.2	17.0	17.1	17.1	17.1	0.07	0.41
30/70	0	18.8	18.8	18.5	18.5	18.5	18.7	0.16	0.86
	5	19.1	18.9	19.0	19.1	19.1	19.1	0.09	0.47
	10	17.3	17.3	17.3	17.2	17.2	17.2	0.05	0.29
	15	15.6	15.7	15.6	15.8	15.5	15.6	0.11	0.71
	20	15.5	14.4	14.5	14.3	14.4	14.6	0.49	3.36
10/90	0	19.6	19.5	19.4	19.6	19.5	19.5	0.08	0.41
	5	18.2	18.2	18.2	18.2	18.3	18.3	0.04	0.22
	10	16.4	16.3	16.4	16.4	16.3	16.3	0.05	0.31
	15	14.7	14.9	14.9	14.7	14.9	14.8	0.11	0.74
	20	13.7	13.8	13.7	13.7	13.8	13.8	0.05	0.36

Table B-3 Elongation at break of HIPS/HDPE blends

HIPS/HDPE	SEBS (pphr)	Elongation at break (%)					X	SD	% Variation
		1 st	2 nd	3 rd	4 th	5 th			
100/0	0	55	45	52	52	46	50.0	4.30	8.60
0/100	0	165	167	160	156	156	161.2	5.07	3.15
90/10	0	40	40	40	44	39	40.6	1.95	4.80
	5	68	69	73	74	72	71.2	2.59	3.64
	10	102	95	101	98	96	98.4	3.05	3.10
	15	118	117	120	117	113	117.0	2.55	2.18
	20	136	138	135	134	132	135.0	2.24	1.66
70/30	0	12.0	13.0	11.0	12.0	14.0	12.4	1.14	9.19
	5	75	74	69	74	75	73.4	2.51	3.42
	10	112	115	120	118	112	115.4	3.58	3.10
	15	141	145	142	138	140	141.2	2.59	1.83
	20	176	175	172	174	176	174.6	1.67	0.96
50/50	0	9	10	10	10	10	9.8	0.45	4.59
	5	92	88	90	90	84	88.8	3.03	3.41
	10	124	121	126	124	121	123.2	2.17	1.76
	15	190	186	182	188	185	186.2	3.03	1.63
	20	252	258	257	252	254	254.6	2.79	1.10
30/70	0	102	92	96	93	94	95.4	3.97	4.16
	5	130	125	128	128	131	128.4	2.30	1.79
	10	200	196	202	195	198	198.2	2.86	1.44
	15	276	270	275	272	278	274.2	3.19	1.16
	20	433	416	428	430	420	425.4	7.13	1.68
10/90	0	98	106	102	110	112	105.6	5.73	5.43
	5	140	146	138	141	143	141.6	3.05	2.15
	10	243	246	238	237	234	239.6	4.83	2.02
	15	410	402	412	398	413	407.0	6.63	1.63
	20	475	465	468	478	474	472.0	5.34	1.13

Table B-4 Flexural strength of HIPS/HDPE blends

HIPS/HDPE	SEBS (pphr)	Flexural Strength (MPa)					X	SD	% Variation
		1 st	2 nd	3 rd	4 th	5 th			
100/0	0	36.4	36.9	37.0	36.7	36.6	36.7	0.24	0.65
0/100	0	24.9	24.8	24.9	25.0	24.9	24.9	0.08	0.32
90/10	0	32.9	32.5	32.7	32.7	32.7	32.7	0.14	0.43
	5	35.4	35.4	35.8	35.6	35.3	35.5	0.20	0.56
	10	31.5	31.6	31.7	31.5	31.4	31.5	0.11	0.35
	15	29.3	29.2	29.0	29.2	28.4	29.0	0.36	1.24
	20	27.9	27.9	27.8	27.9	27.9	27.9	0.09	0.32
70/30	0	29.8	29.8	29.8	29.8	29.8	29.8	0	0
	5	30.2	30.4	30.4	30.3	30.2	30.3	0.10	0.33
	10	28.4	28.6	28.4	28.5	28.7	28.6	0.13	0.45
	15	27.2	27.0	27.1	27.0	27.0	27.0	0.09	0.33
	20	25.3	25.3	25.4	25.2	25.4	25.3	0.08	0.32
50/50	0	27.5	27.2	27.1	27.5	27.2	27.3	0.18	0.66
	5	25.9	25.8	25.9	26.0	26.0	25.9	0.08	0.31
	10	23.3	23.4	23.4	23.3	23.7	23.5	0.16	0.68
	15	21.7	21.2	21.0	21.2	21.5	21.3	0.27	1.27
	20	19.9	19.6	19.7	19.5	19.5	19.7	0.16	0.81
30/70	0	23.8	23.9	24.0	23.9	23.7	23.9	0.11	0.46
	5	21.9	21.8	21.7	21.8	21.8	21.8	0.07	0.32
	10	19.1	19.3	19.5	19.3	19.3	19.3	0.14	0.73
	15	17.4	17.5	17.6	17.5	17.5	17.5	0.07	0.40
	20	15.8	15.7	15.8	16.0	15.9	15.8	0.11	0.70
10/90	0	20.9	20.9	21.2	21.0	20.8	20.9	0.15	0.72
	5	17.8	17.8	18.0	17.9	17.9	17.9	0.08	0.45
	10	15.2	15.5	15.5	15.1	15.3	15.3	0.18	1.18
	15	13.7	13.8	13.7	13.7	13.8	13.8	0.05	0.36
	20	12.7	12.7	12.6	12.7	12.7	12.7	0.07	0.55

APPENDIX C

DSC thermogram of HIPS/HDPE blends

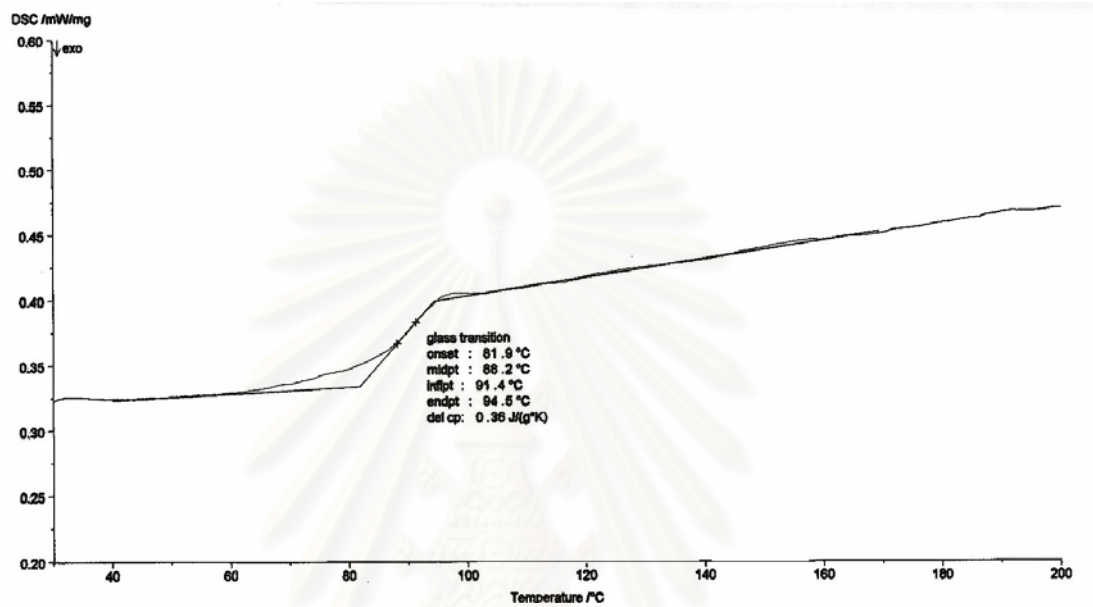


Figure C-1 DSC thermogram of pure HIPS

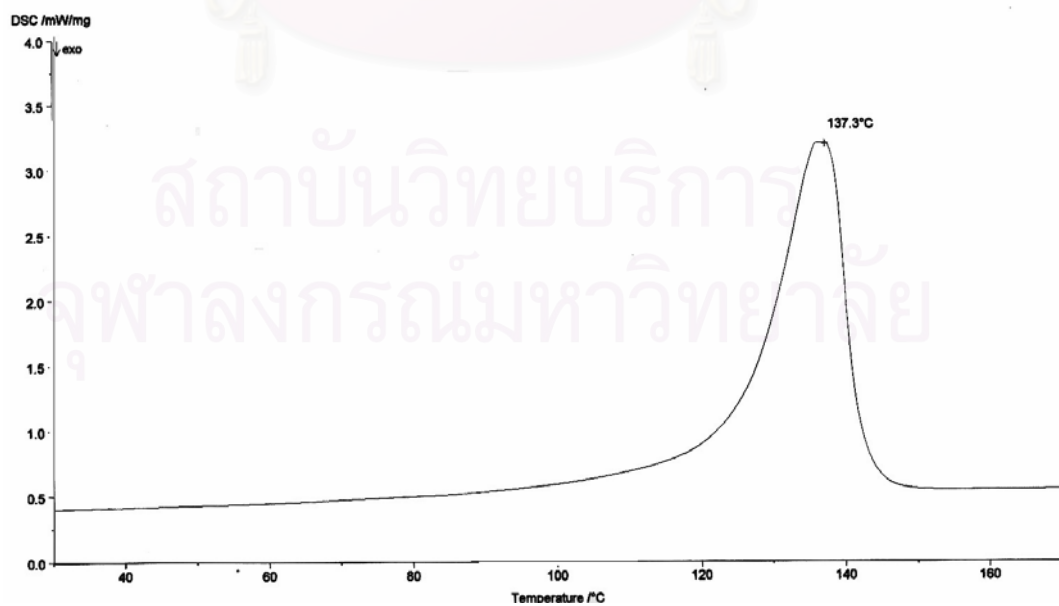


Figure C-2 DSC thermogram of pure HDPE

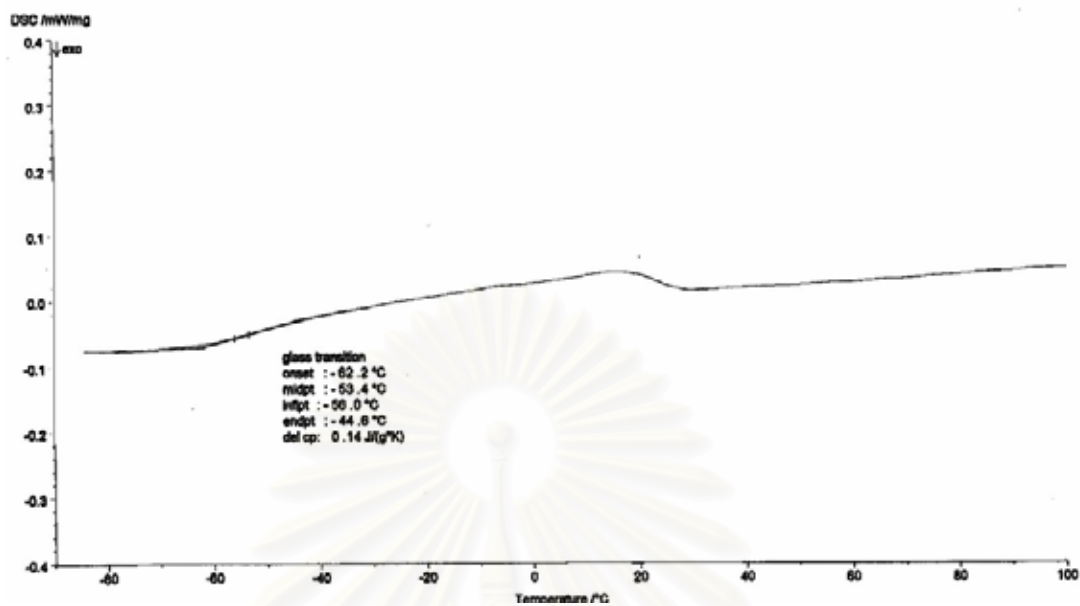


Figure C-3 DSC thermogram of SEBS triblock copolymer

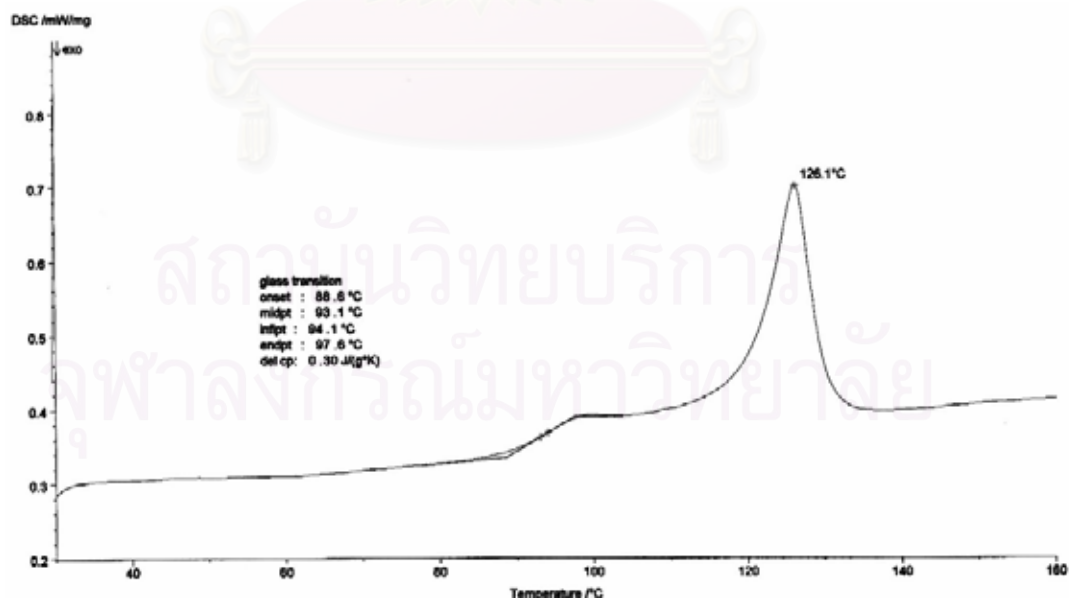


Figure C-4 DSC thermogram of HIPS/HDPE (90/10) blend without SEBS

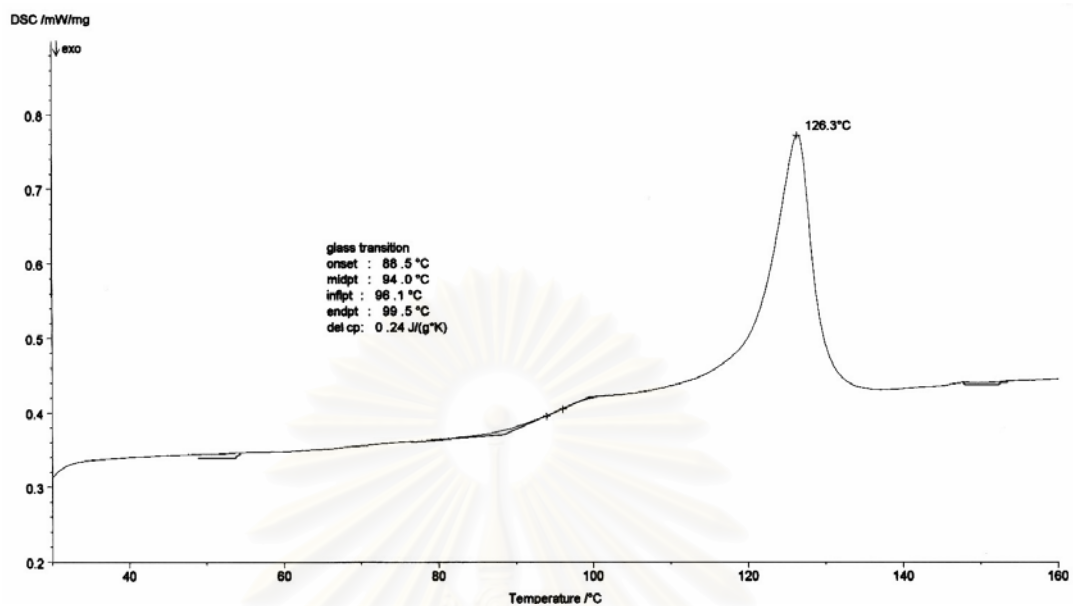


Figure C-5 DSC thermogram of HIPS/HDPE (90/10) blend with SEBS 5 pphr

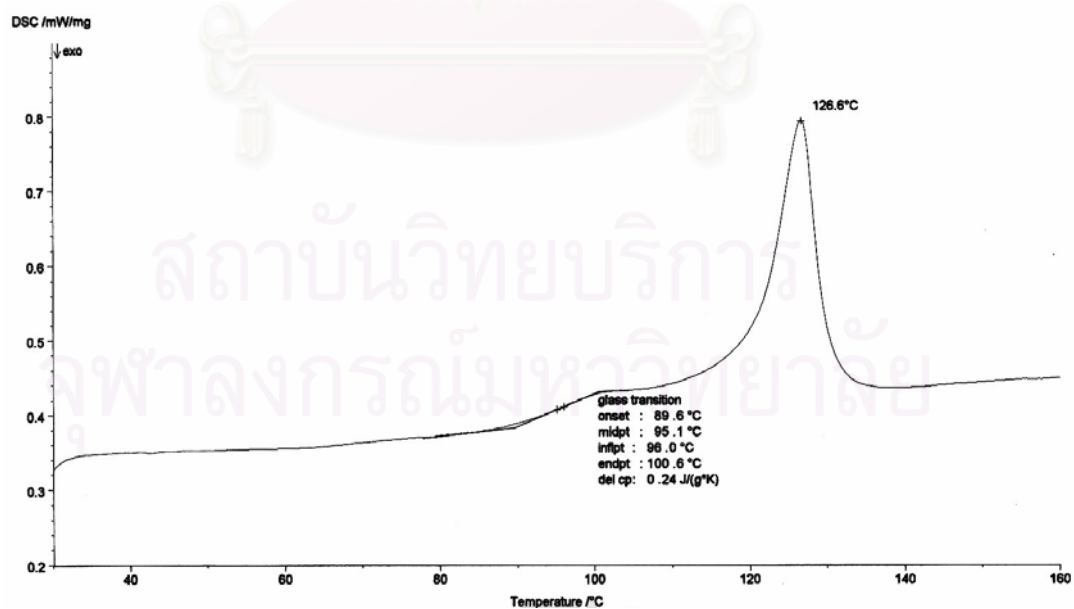


Figure C-6 DSC thermogram of HIPS/HDPE (90/10) blend with SEBS 10 pphr

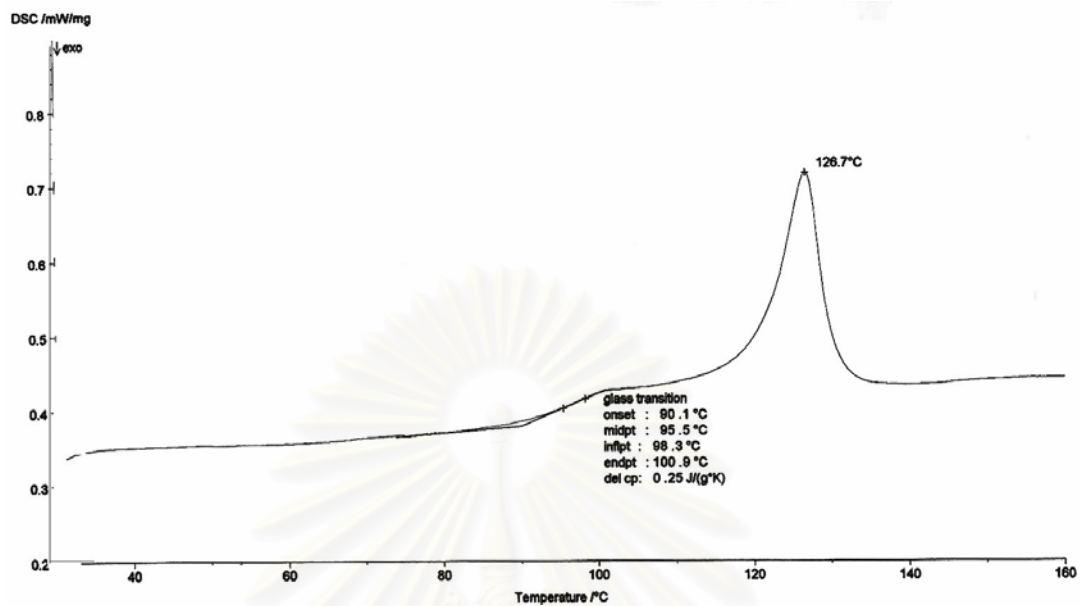


Figure C-7 DSC thermogram of HIPS/HDPE (90/10) blend with SEBS 15 pphr

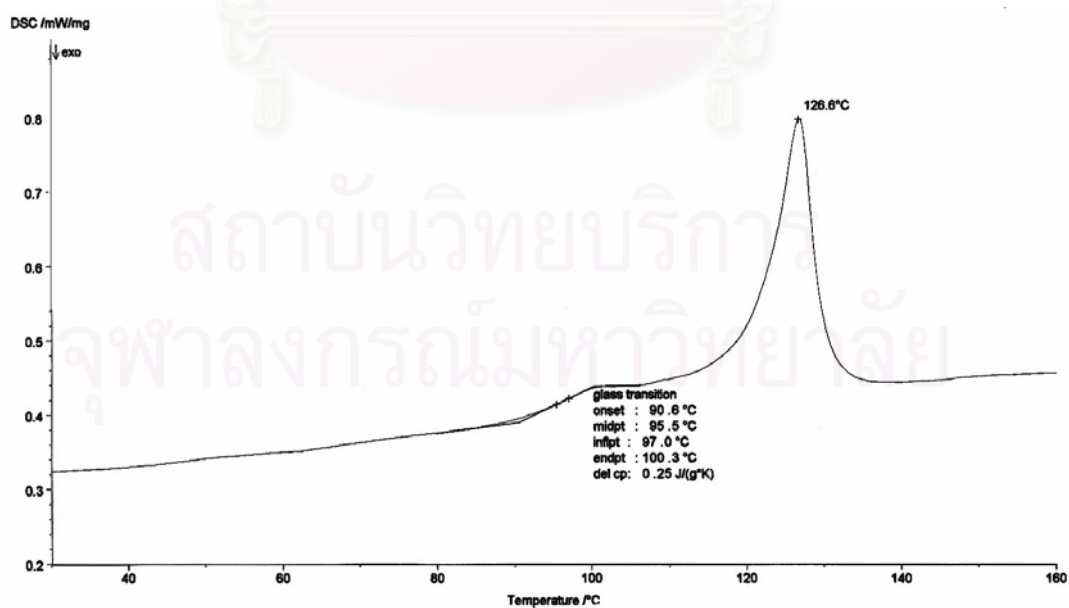


Figure C-8 DSC thermogram of HIPS/HDPE (90/10) blend with SEBS 20 pphr

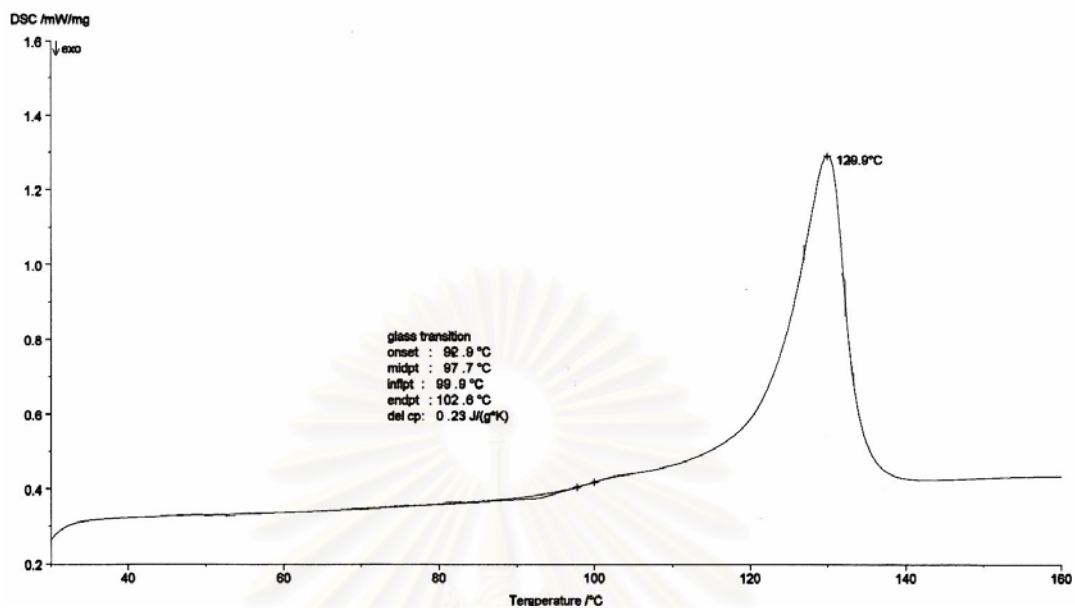


Figure C-9 DSC thermogram of HIPS/HDPE (70/30) blend without SEBS

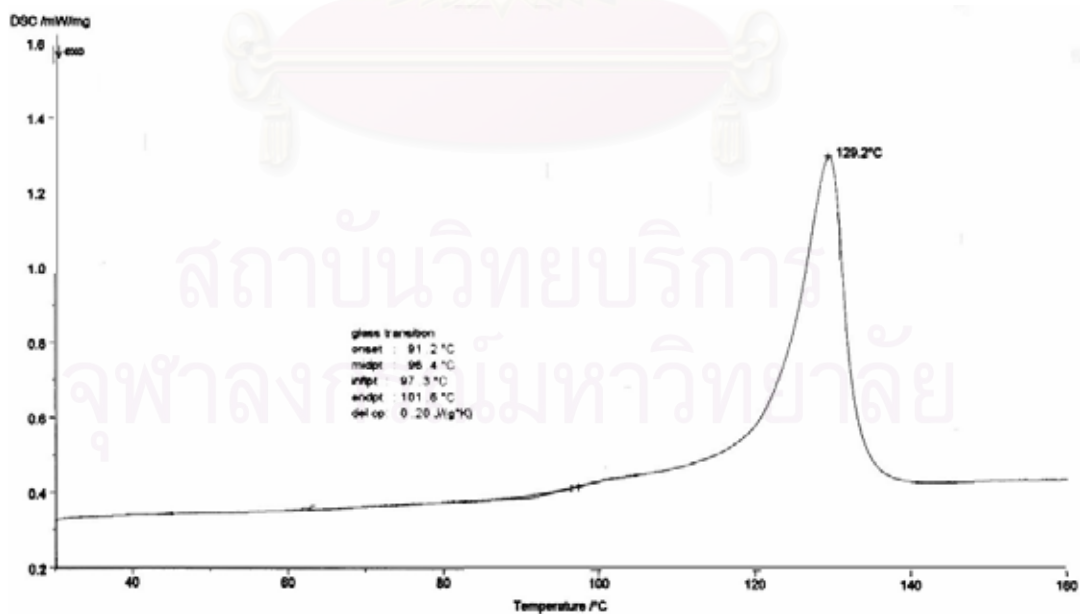


Figure C-10 DSC thermogram of HIPS/HDPE (70/30) blend with SEBS 5 phr

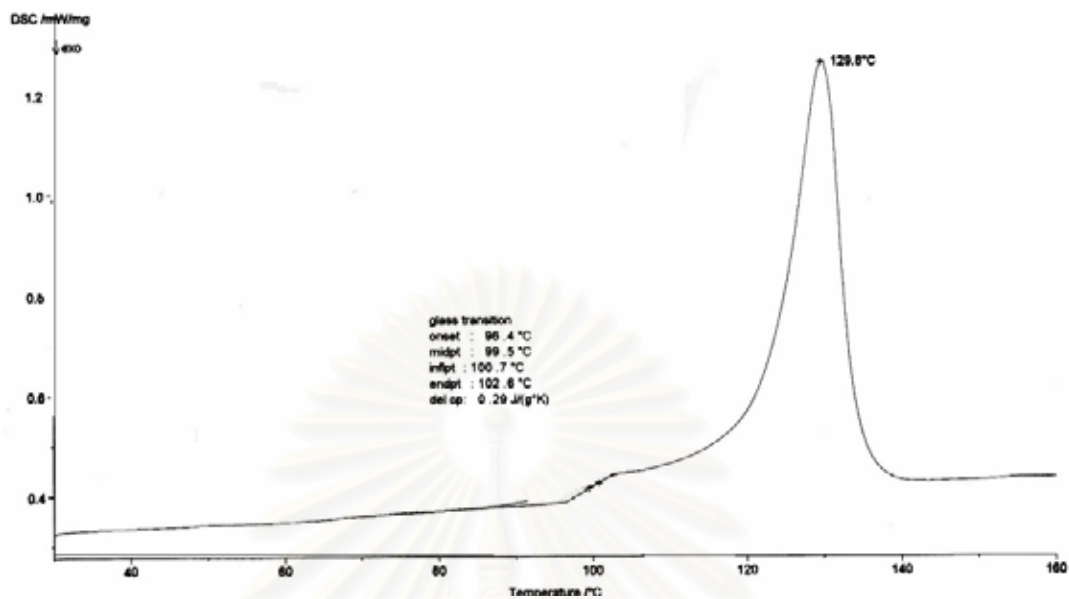


Figure C-11 DSC thermogram of HIPS/HDPE (70/30) blend with SEBS 10 pphr

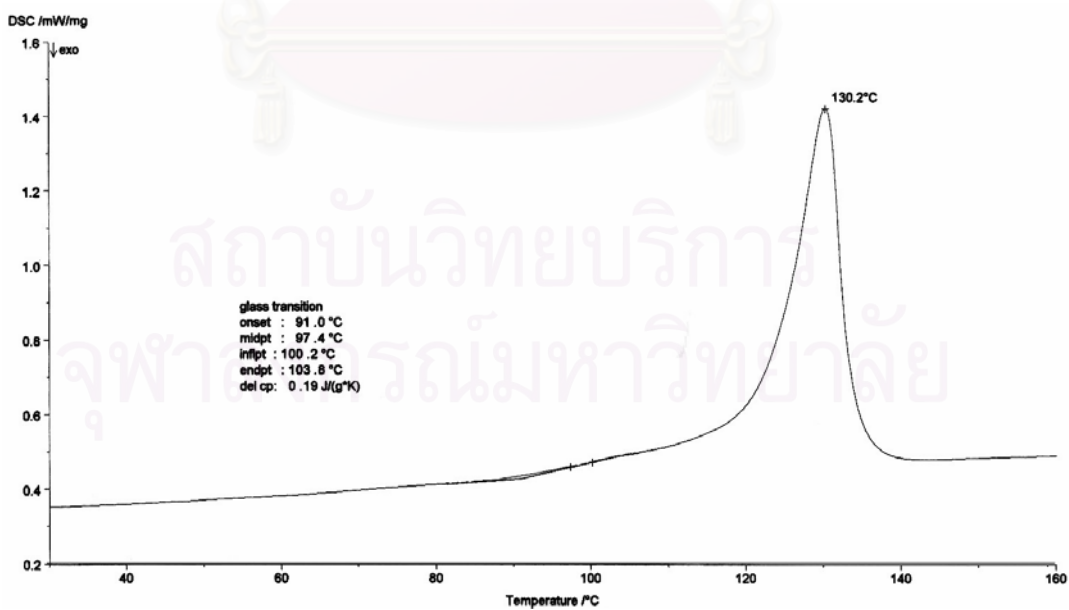


Figure C-12 DSC thermogram of HIPS/HDPE (70/30) blend with SEBS 15 pphr

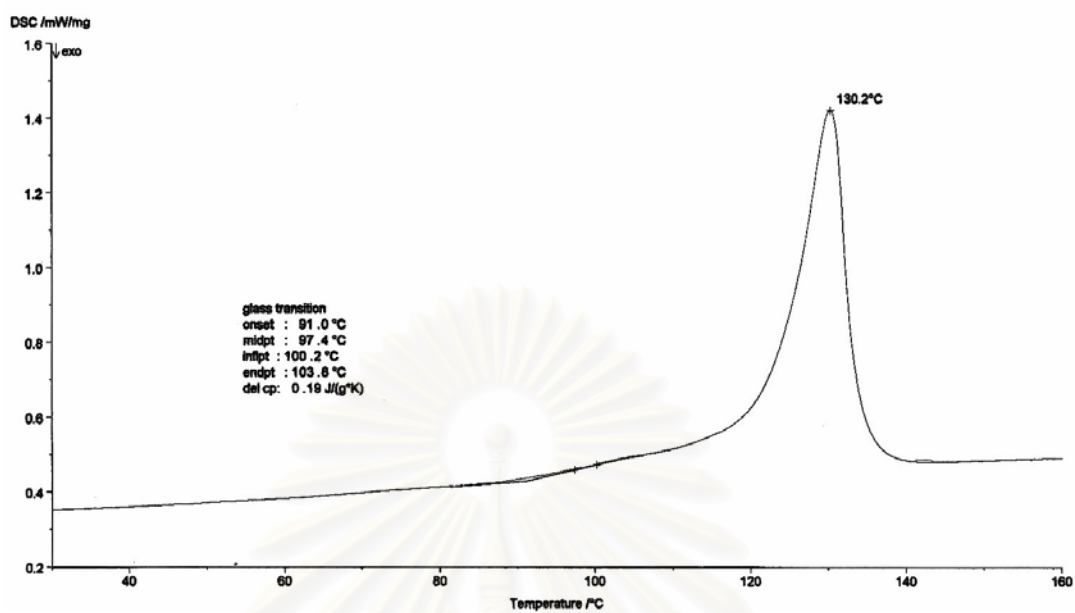


Figure C-13 DSC thermogram of HIPS/HDPE (70/30) blend with SEBS 20 pphr

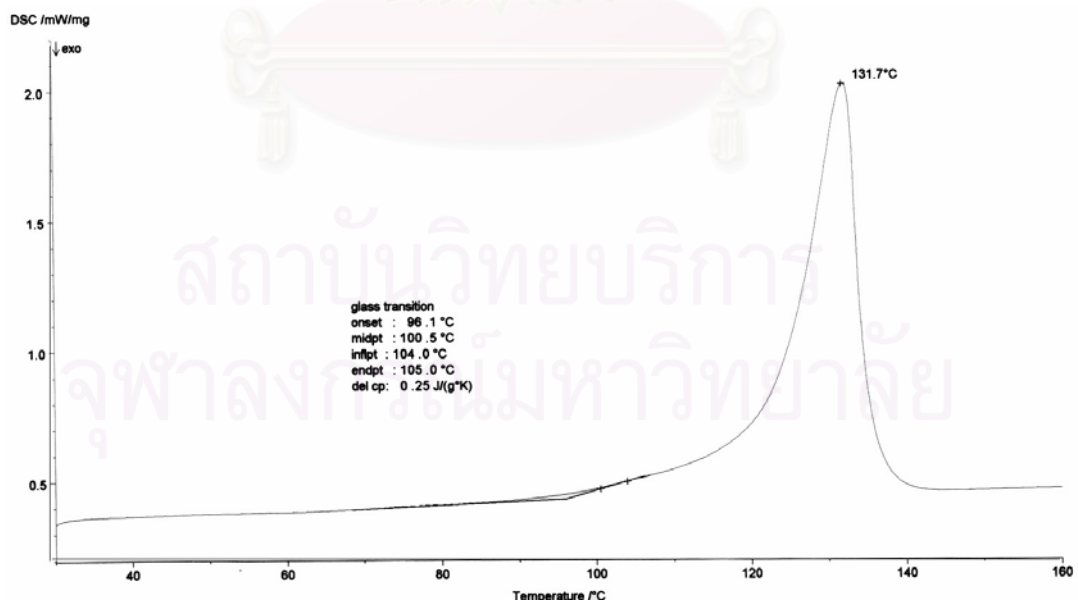


Figure C-14 DSC thermogram of HIPS/HDPE (50/50) blend without SEBS

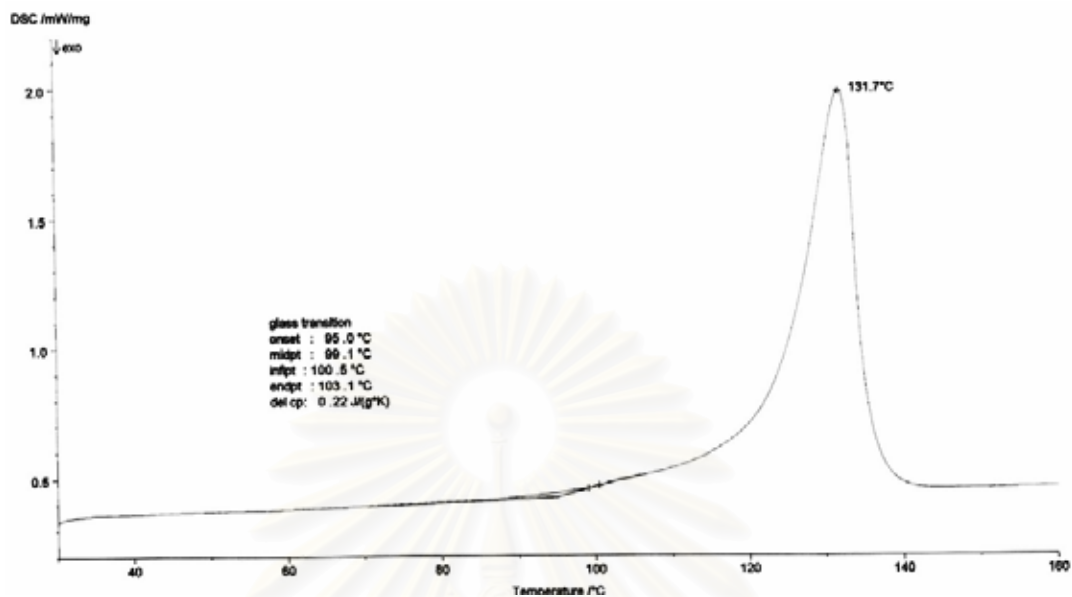


Figure C-15 DSC thermogram of HIPS/HDPE (50/50) blend with SEBS 5 pphr

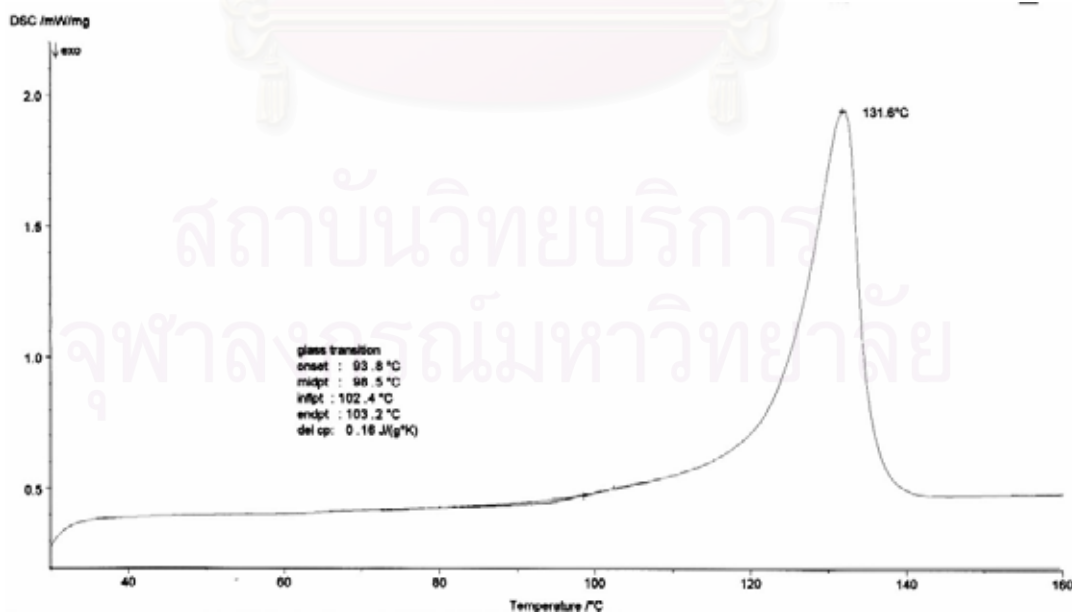


Figure C-16 DSC thermogram of HIPS/HDPE (50/50) blend with SEBS 10 pphr

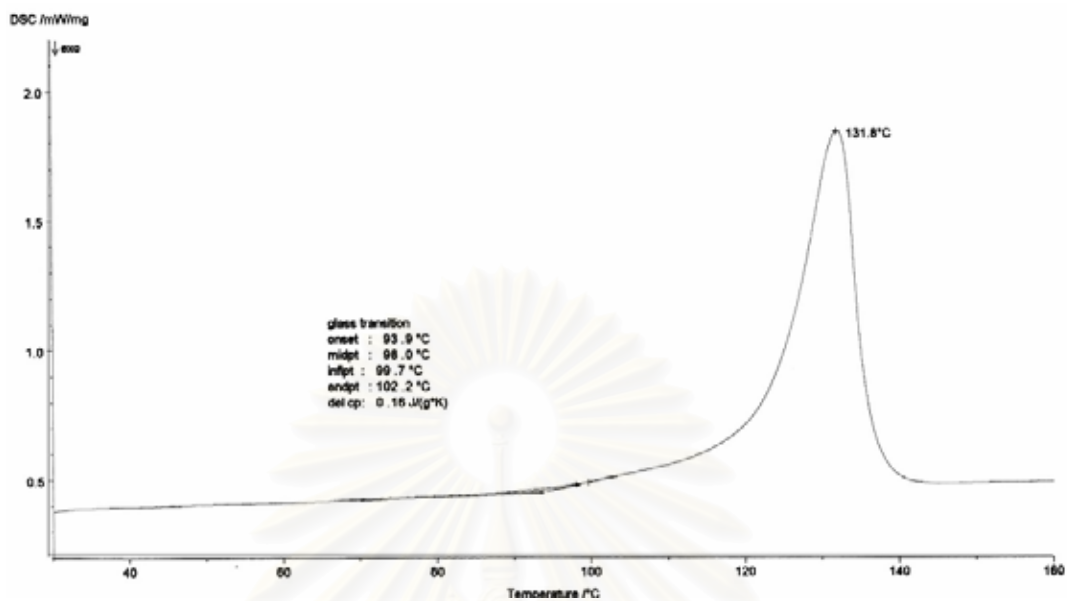


Figure C-17 DSC thermogram of HIPS/HDPE (50/50) blend with SEBS 15 pphr

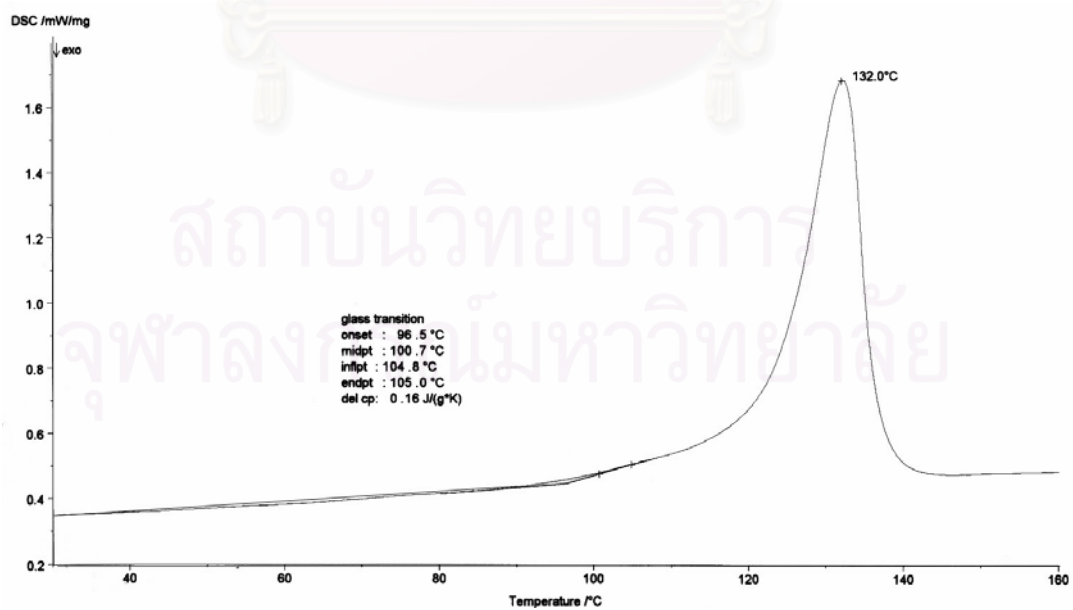


Figure C-18 DSC thermogram of HIPS/HDPE (50/50) blend with SEBS 20 pphr

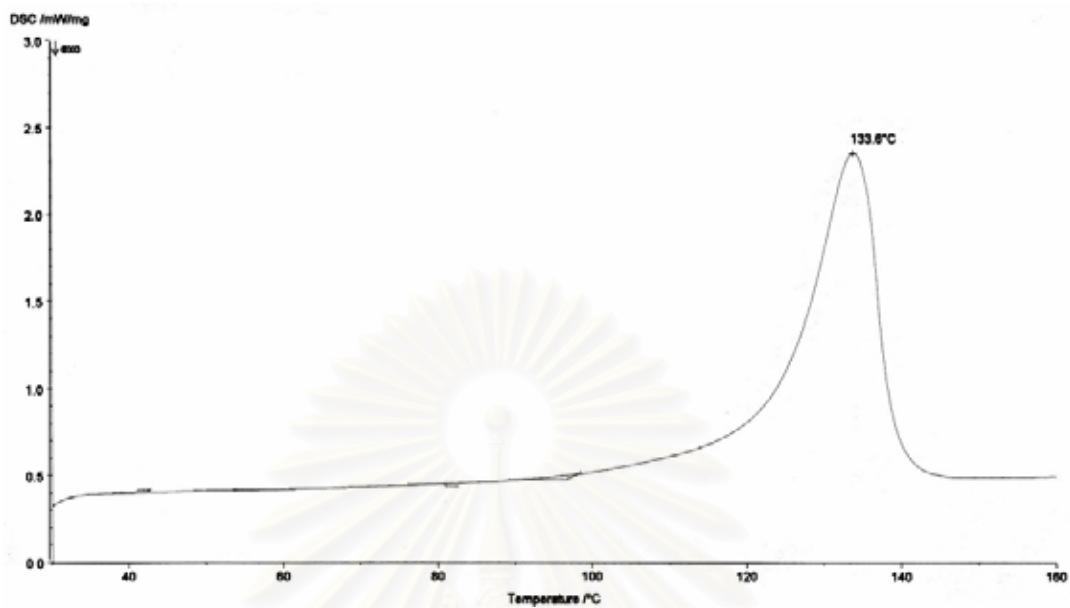


Figure C-19 DSC thermogram of HIPS/HDPE (30/70) blend without SEBS

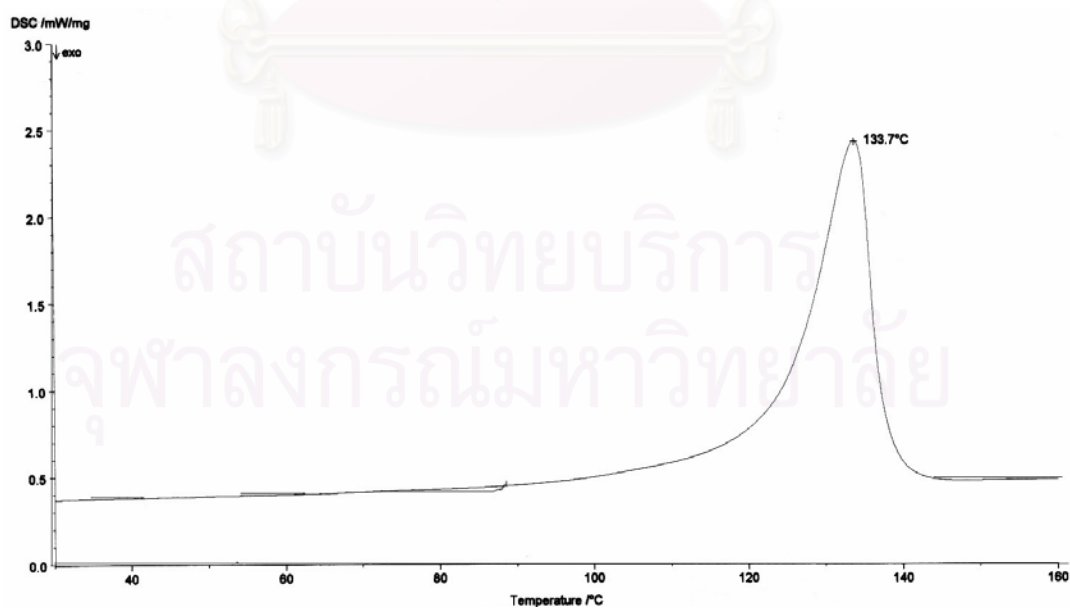


Figure C-20 DSC thermogram of HIPS/HDPE (30/70) blend with SEBS 5 pphr

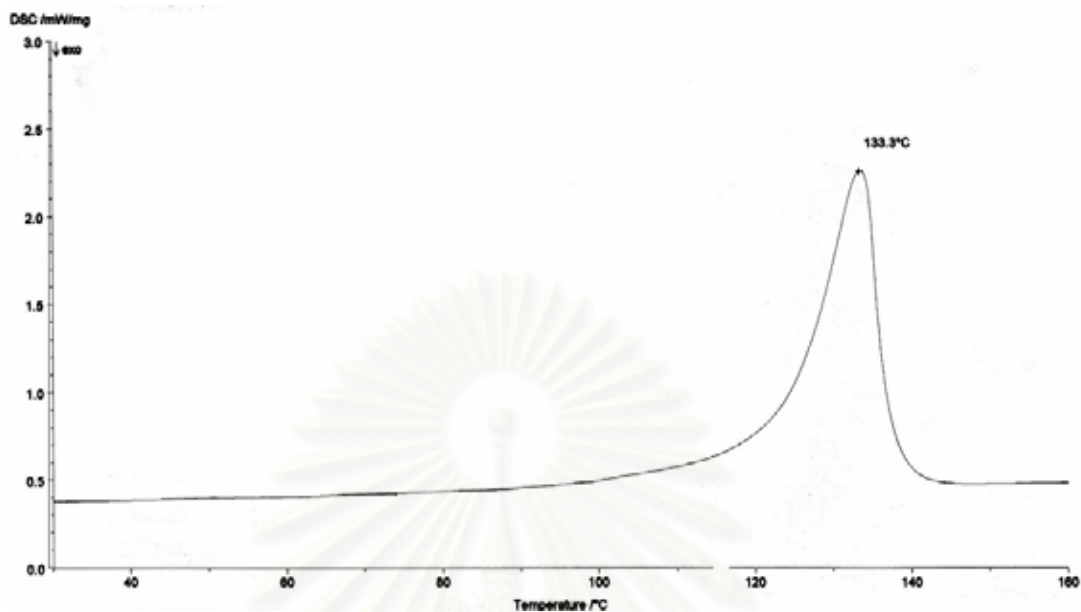


Figure C-21 DSC thermogram of HIPS/HDPE (30/70) blend with SEBS 10 pphr

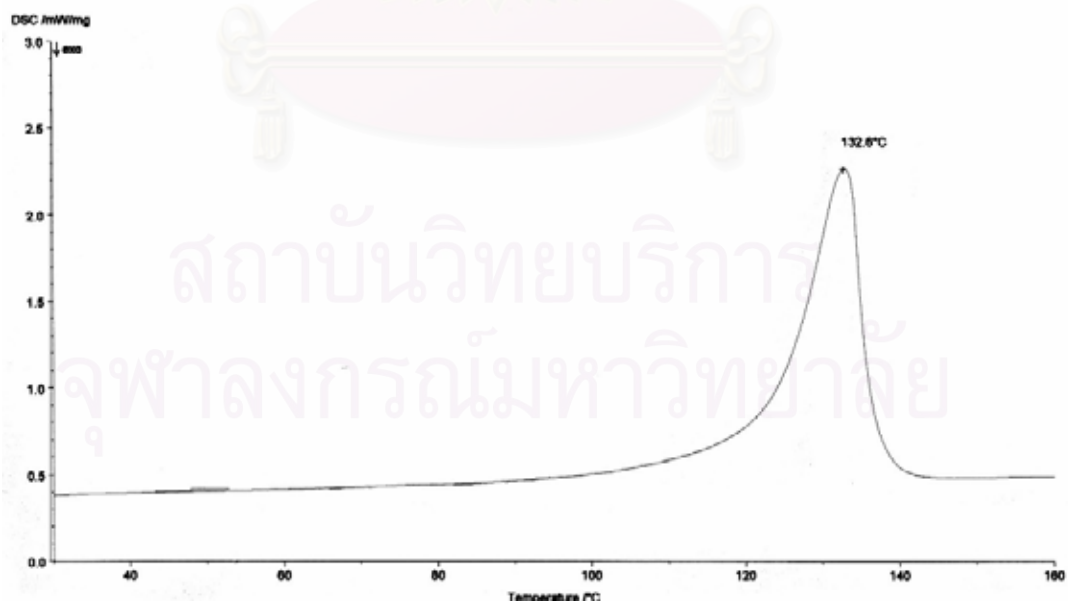


Figure C-22 DSC thermogram of HIPS/HDPE (30/70) blend with SEBS 15 pphr

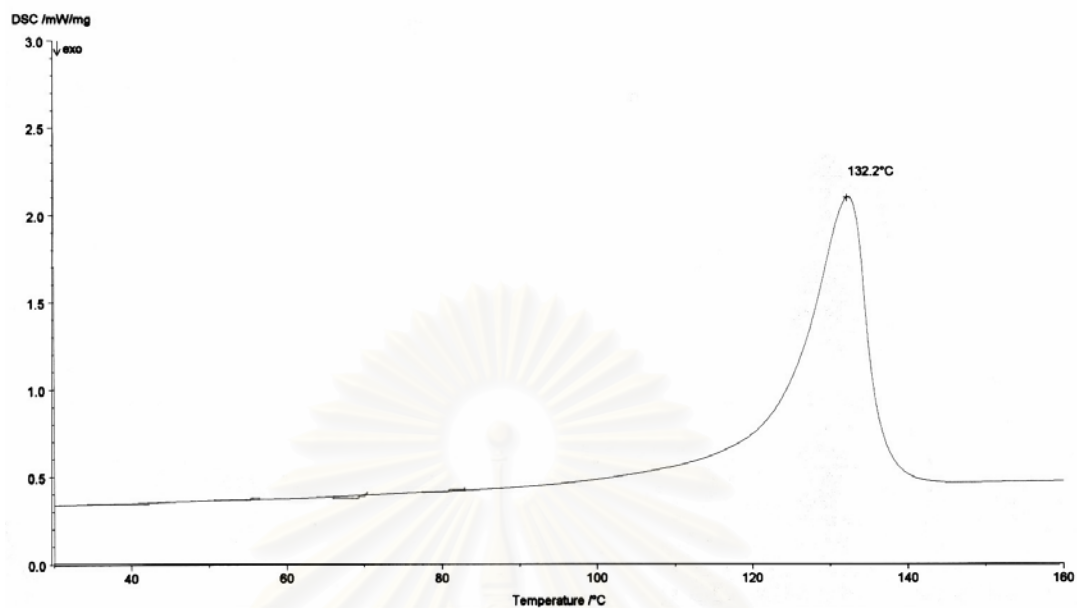


Figure C-23 DSC thermogram of HIPS/HDPE (30/70) blend with SEBS 20 pphr

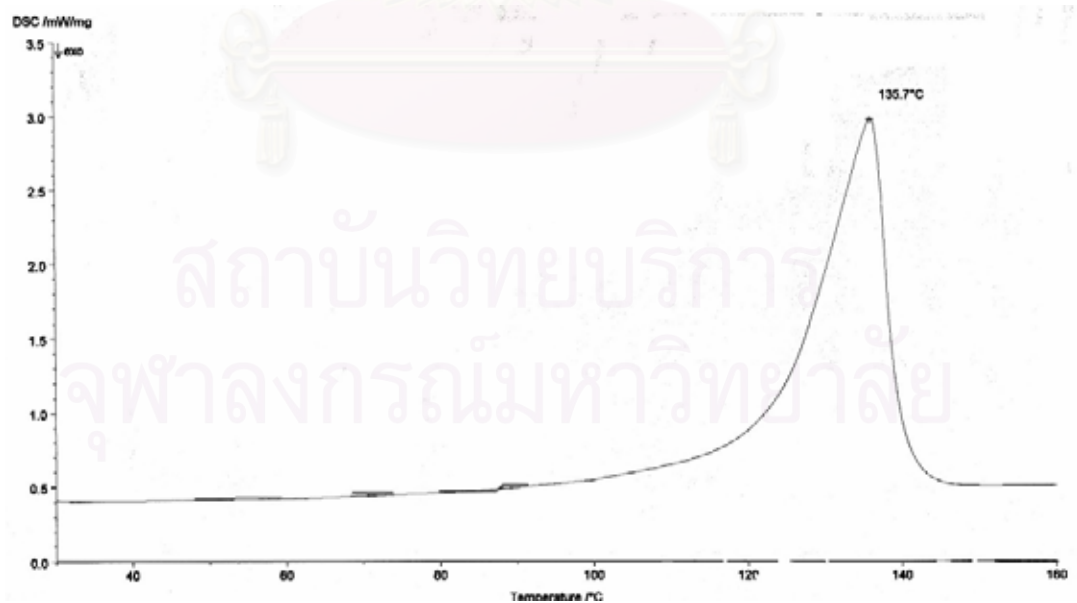


Figure C-24 DSC thermogram of HIPS/HDPE (10/90) blend without SEBS

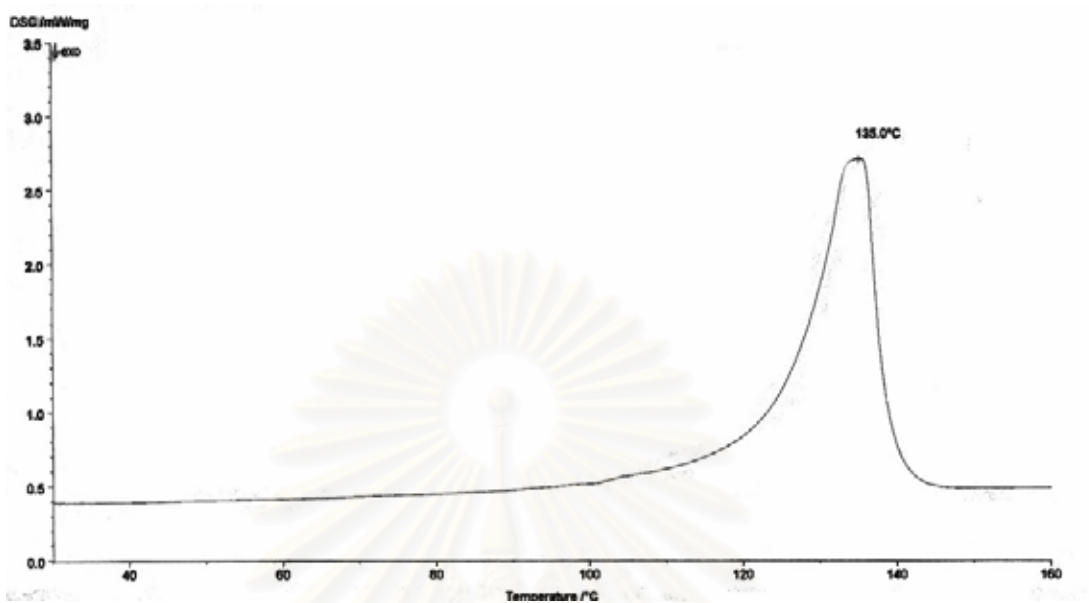


Figure C-25 DSC thermogram of HIPS/HDPE (10/90) blend with SEBS 5 pphr

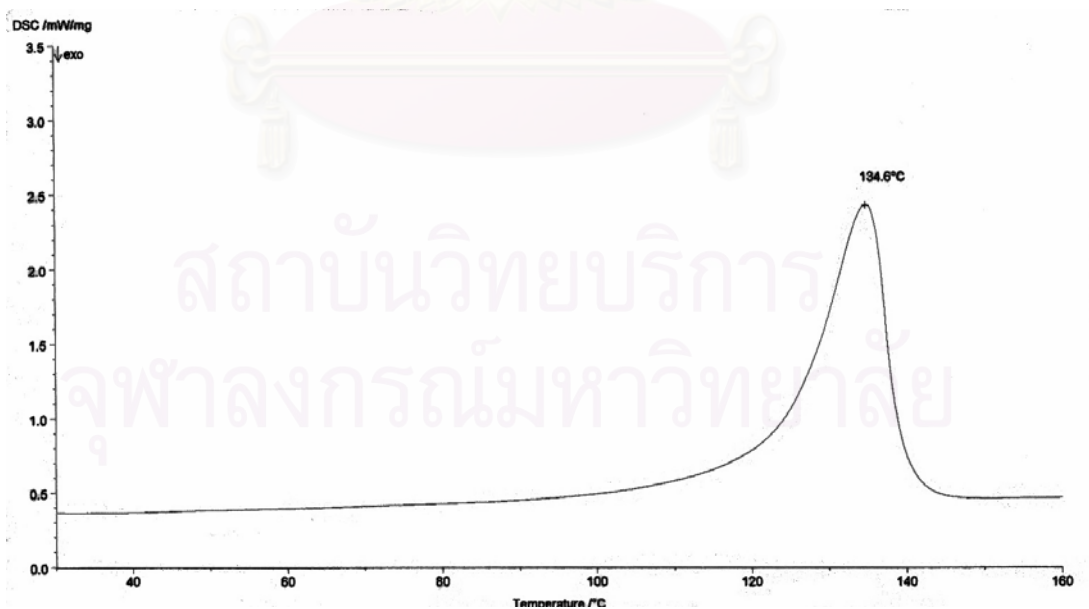


Figure C-26 DSC thermogram of HIPS/HDPE (10/90) blend with SEBS 10 pphr

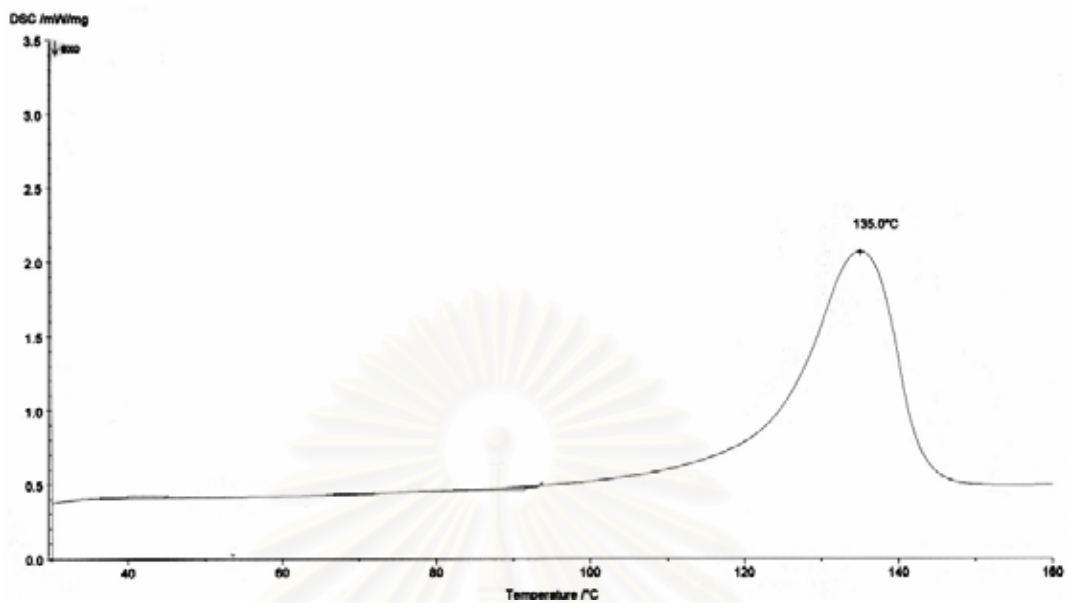


Figure C-27 DSC thermogram of HIPS/HDPE (10/90) blend with SEBS 15 pphr

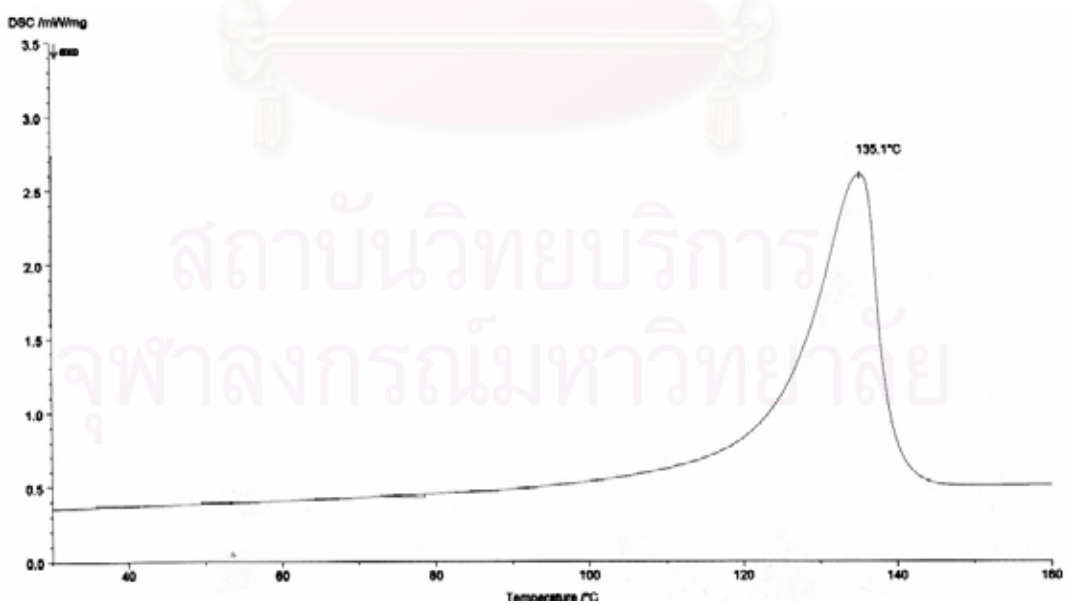


Figure C-28 DSC thermogram of HIPS/HDPE (10/90) blend with SEBS 20 pphr

APPENDIX D

The method for the determination of spin-spin relaxation time

Pulsed NMR is a powerful method to obtain the molecular mobility and the fractional amounts of a heterogeneous phase in a sample for determination of the molecular order miscibility and phase-separated structure in polymer blends. The main quantities obtained by pulsed NMR are the spin-spin relaxation time (T_2), the spin-lattice relaxation time (T_1), and that in the rotating frame ($T_{1\rho}$). The temporal change of the T_2 , which reflects the motional state of protons, can be obtained. When there exists motional heterogeneity in a sample, multiple T_2 components are observed, and the fraction amounts of phases with different molecular mobilities can be obtained by this method.

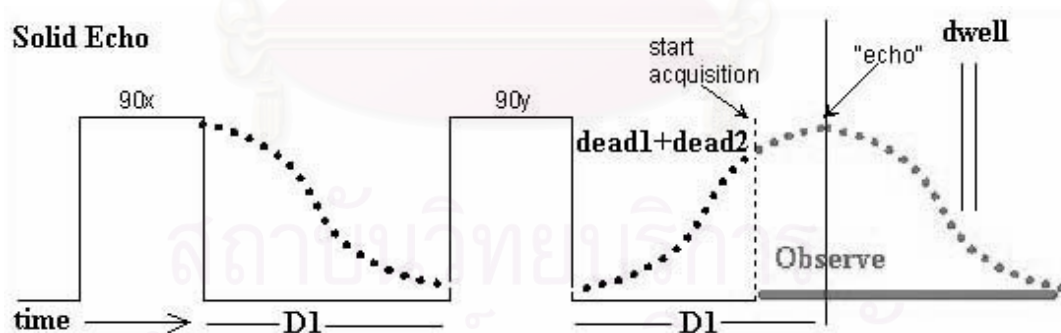


Figure D-1 The solid-echo method diagram

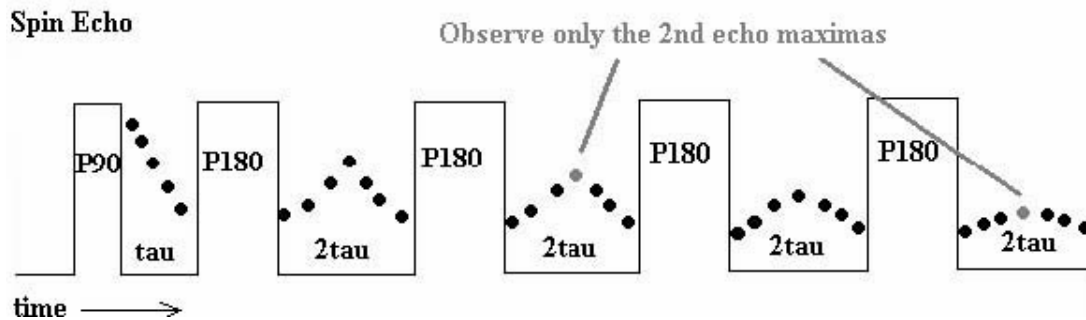


Figure D-2 The spin-echo [Carr-Purcell-Meiboom-Gill (CPMG)] method diagram

The spin-spin relaxation time can be determined by the solid-echo and the spin-echo method. In the case of the solid-echo method ($90^\circ_x \tau 90^\circ_y$) to obtain a rapid free induction decay (FID) without dead effect after the pulse, the signal is digitized by the internal clock of the transient recorder (50 ns). On the other hand, in case of spin-echo [Carr-Purcell-Meiboom-Gill (CPMG)] method ($90^\circ_x \tau (180^\circ_y 2\tau)_n$), n echoes are created to obtain slow FID behavior to avoid the effect of inhomogeneity of the static magnetic field. The spin-spin relaxation time (T_2) describes the decay rate of the magnetization within the xy plane after a $\pi/2$ pulse. T_2 can be estimated by utilizing a standard two-pulse spin-echo sequence: $\pi/2 - \tau - \pi - \tau - \text{echo}$ method. The first $\pi/2$ pulse is used to rotate the magnetization at thermal equilibrium (M_{eq}) from the z -axis to the y -axis. The delay time τ allows the nuclear spins precessing at slightly different frequencies to dephase in the xy plane. The second pulse (π) flips the magnetization across the xy plane. The second delay time allows the spins to refocus together and generate a spin-echo. When set up the pulse sequence, the spin-echo can be observed on the oscilloscope, which is actually a back-to-back FID. With this pulse sequence, T_2 can be determined by systematically varying the interpulse time τ and measuring the maximum amplitude of the spin echo at each time interval (τ). The exponential decay of the magnetization to zero is represented by

$$M(2\tau) = M_{\text{eq}}e^{-2\tau/T_2}, \quad (\text{D-1})$$

Equation D-1 can be transformed to

$$\ln[M(2\tau)] = (-2\tau/T_2) + \ln(M_{\text{eq}}), \quad (\text{D-2})$$

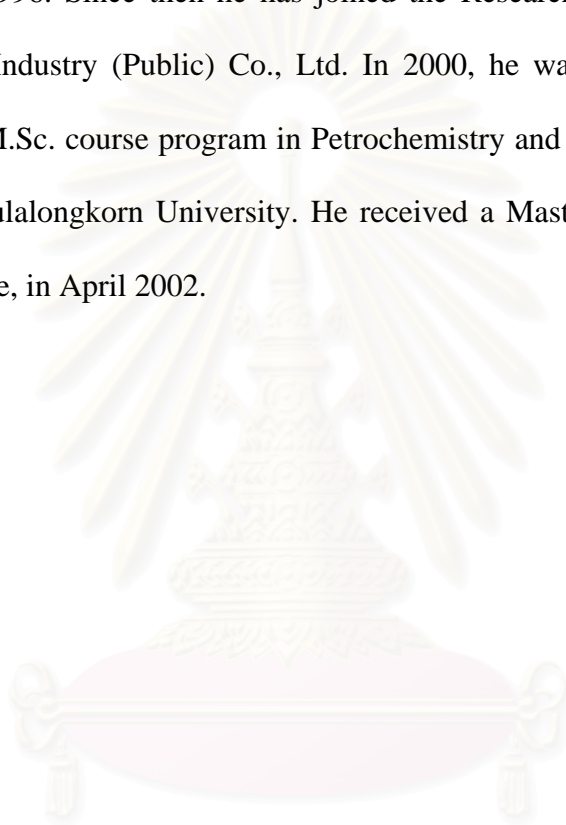
and a plot of the $\ln[M(2\tau)]$ versus 2τ should reveal a straight line with a slope equal to $-1/T_2$. Thus, by performing a linear least squares fit of the experimental data, T_2 can be obtained from the slope.



สถาบันวิทยบริการ
จุฬาลงกรณ์มหาวิทยาลัย

VITA

Mr. Asira Chirawithayaboon was born on January 4, 1975 in Samut Sakhon. He graduated with Bachelor's degree of Science (Chemistry) from Srinakharinwirot University in 1996. Since then he has joined the Research and Development, Thai Petrochemical Industry (Public) Co., Ltd. In 2000, he was accepted as a graduate student in the M.Sc. course program in Petrochemistry and Polymer Science, Faculty of Science, Chulalongkorn University. He received a Master's degree of Science in Polymer Science, in April 2002.



สถาบันวิทยบริการ
จุฬาลงกรณ์มหาวิทยาลัย